Universität Zürich[UZH]

Geographisches Institut

Carbon dynamics in degraded peatland and artificial soils of the Grosses Moos in the Berner Seeland Effects of anthropogenic soil embankment on carbon stabilization

GEO 511 Master's Thesis

Author: Jan Oberholzer, 17-550-989

Supervised by: Prof. Dr. Markus Egli, Ciriaco McMackin

Faculty representative: Prof. Dr. Markus Egli

25.08.2025

Abstract

Drained peatlands used for agriculture are significant sources of atmospheric CO_2 and are subject to severe degradation and land subsidence. The Grosses Moos in the Berner Seeland is a large, drained peatland area that is a key agricultural region in Switzerland. Intensive drainage combined with intensive agriculture over decades has led to peatland degradation in this region. Anthropogenic soil embankments, the application of a mineral cover, is a management strategy used to counteract this degradation. While recent flux-based studies have investigated emissions from these systems, a critical knowledge gap remains concerning the effect of this practice on the quantity, vertical distribution, and functional stability of the underlying SOC. This thesis provides the first analysis of how embankments alter SOC occurrence and investigates whether they can have a stabilizing effect.

Adopting the conceptual framework that separates soil organic matter into POM and MAOM, this study compares original degraded peat profiles with adjacent backfilled profiles. Results show that most likely, embankment creates a geochemically inverted Anthrosol, burying the organic-rich peat horizon under a carbon-poor mineral cover and displacing the SOC maximum downwards from approximately 60 cm to below 100 cm. Paradoxically, this buried carbon is stored primarily in the coarse, POM-like fraction, which is considered biochemically labile. This suggests preservation is not due to chemical recalcitrance but to physical protection afforded by the embankment, which re-establishes anoxic conditions. Concurrently, the new mineral topsoil shows a relative increase in SOC within the fine, MAOM-like fraction, indicating that the added mineral matrix facilitates a new, more stable pathway for carbon stabilization through organo-mineral association.

The study concludes that embankment establishes a dual system: the physical preservation of the old, labile peat stock at depth, coupled with the initiation of new, mineral-associated carbon stabilization in the surface layer. This thesis provides a unifying framework that reconciles the seemingly contradictory findings of flux-based studies. It helps to explain the continued CO_2 emissions observed by other researchers as originating from the new, active topsoil, while simultaneously accounting for the shift in carbon source away from old peat. It thereby offers a more holistic framework for evaluating this land management practice.

The embankments could be a practical and efficient interim solution for agriculture to slow down the progressive degradation of peat, but not to stop it completely.

Acknowledgments

First and foremost, I wish to express my sincere and profound gratitude to Prof. Dr. Markus Egli, who, despite his exceptionally demanding professional commitments, generously provided invaluable expertise and unfailing support throughout all stages of this work. In addition, he responded with sincere understanding to the sometimes-extraordinary circumstances under which the author of this work found himself at that time.

I'm also thankful to Mr. Ciriaco McMackin for his dedicated assistance during the entire sampling process and for his reliable support in the laboratory. Furthermore, I extend my heartfelt thanks to the laboratory team, Ms. Barbara Siegfried and Mr. Yves Brügger, whose tireless commitment and consistently expert guidance on technical matters in the laboratory contributed substantially to the success of this study.

I am especially grateful to my closest family, who have sustained, strengthened, and encouraged me in every possible way throughout the many years of my academic journey. Moreover, I wish to extend my gratitude to my friends, acquaintances, and fellow students, particularly Annette and Philipp, for their advice, encouragement, and steadfast friendship during our studies.

Special thanks to Dominik and his family for their various forms of support throughout the many years of my academic journey, especially during the pandemic.

Table of Contents

List of figures

List of Tables

List of Abbreviations

$CaCl_2$ – calcium chloride

$CaCO_3$ – calcium carbonate

CH_4 – methane

CIA – Chemical Index of Alteration

CO_2 – carbon dioxide, greenhouse gas

$\delta^{13}C$ – carbon-13 isotopic signature (δ13C)

$\delta^{15}N$ – nitrogen-15 isotopic signature (δ15N)

DRIFT – Diffuse Reflectance Infrared Fourier Transform

EA – Elemental Analyzer

GHG – greenhouse gas

IRMS – isotope-ratio mass spectrometer

KBr – potassium bromide

LOI – loss on ignition

MAOM – mineral-associated organic matter

N_2O – nitrous oxide

pH – potential of hydrogen (*potentia hydrogenii*)

POM – particulate organic matter

SOC – soil organic carbon

SOM – soil organic matter

Author's Note

In this paper, the terms embankment and backfilled are used synonymously and refer to the same thing. The term backfilling is used for the presentation of the results and raw data. In the remaining parts of the paper, the term embankment is used predominantly. This decision serves to ensure internal consistency and considers the fact that no uniform nomenclature for this measure has yet been established in the literature.

1 Introduction

1.1 Peatlands and their Importance in the Carbon Cycle

Peatlands represent an essential element of the global climate system due to their significant importance in the global carbon cycle. Often described as global carbon hotspots, they function as the world's largest and most space-efficient natural terrestrial carbon store (United Nations Environment Programme (UNEP), 2022; Z. Yu, 2011). Even though they only cover about 3% of the global land area, peatlands hold an estimated 500 to 600 Gt of carbon (Klingenfuß et al., 2014; J. Leifeld & Menichetti, 2018; Limpens et al., 2008; Liu et al., 2019; Reichstein et al., 2013; Wang et al., 2021; Z. Yu, 2011). This carbon pool constitutes approximately 15–20% of global soil organic carbon. Thus, its conservation is essential for climate-change mitigation and sustainable agricultural land use (Leifeld et al., 2011).

The immense carbon storage in peatlands is a result of their unique, water-logged conditions rather than the presence of inherently non-degradable organic matter. Hydrology represents the key controlling variable in almost all processes within the peatland carbon cycle (Egli et al., 2020a).

However, this highly effective natural carbon sink function is now severely threatened on a global scale by human intervention. Widespread drainage, primarily for agriculture and forestry, is a large driver of peatland destruction and degradation worldwide (United Nations Environment Programme (UNEP), 2022). Extensive peatlands were not only drained and converted for agricultural use; they were also frequently subjected to industrial development, which in turn contributed to the urbanization of these ecosystems. A prominent example in Switzerland is Zurich Airport, which was constructed on former peatland sites (Vincevica-Gaile et al., 2021).

This activity fundamentally alters the hydrology of peatlands. It reverses the ecosystem's function from a carbon sink into a powerful and persistent source of atmospheric CO_2 by initiating a degradation cascade of aeration, oxidation, CO_2 emissions, and land subsidence (United Nations Environment Programme (UNEP), 2022). On a global scale, an estimated 51 million hectares of degraded peatlands, representing about 11% of the total global peatland area, are estimated to emit approximately 1.91 Gt of CO_2-equivalents per year (Leifeld & Menichetti, 2018).

As stated by Jurasinski et al. (2020), a complete assessment of the climate impact from drained peatlands must extend beyond carbon dioxide, since a one-sided focus on CO_2 is inadequate for understanding the full effect on the climate system. These ecosystems also emit significant amounts of the potent greenhouse gases nitrous oxide (N_2O) and methane (CH_4), with fluxes being strongly linked to water level, land use, and the degree of physical soil degradation (Jurasinski et al., 2020; Liu et al., 2019). This situation creates complex management trade-offs, where a measure like rewetting can reduce CO_2 and N_2O emissions but simultaneously increase those of CH_4 (Jurasinski et al., 2020; Zeitz & Velty, 2002). In the Swiss context, agriculturally used organic soils are confirmed as central sources of both CO_2 and N_2O, contributing approximately 0.74 million tonnes of CO_2-equivalents per year (Leifeld et al., 2019).

A changing global climate poses an indirect, but significant, threat to the stability of the remaining peatland carbon sink, putting these vital carbon stores in further jeopardy. The future of these ecosystems is highly uncertain. On one hand, palaeoecological data indicates they could become an even stronger carbon sink in a warmer world. On the other hand, this positive outcome hinges entirely on maintaining the right water balance (Yu, 2011). This potential is severely threatened by climate extremes, which disproportionately impact the terrestrial carbon cycle and can negate the sequestration of many "normal" years (Reichstein et al., 2013). Peatlands are particularly vulnerable to events like drought, which can trigger large-scale carbon losses and cause long-lasting legacy effects that prolong emissions for years after the initial disturbance (Reichstein et al., 2013).

Given their vast carbon stores and their acute vulnerability to both direct and indirect pressures, the stewardship of peatlands represents a critical, yet often overlooked, lever for climate action. According to Leifeld & Menichetti (2018), there is immense potential for avoided emissions, despite being frequently underappreciated as part of global climate strategies**.** Peatland rewetting is an extremely effective and resource-efficient climate mitigation measure, relative to SOC-enhancing measures in mineral soils, it offers significantly greater carbon and nitrogen efficiency (Leifeld & Menichetti, 2018). Without a strategy for protecting peatlands, the climate benefits gained from carbon sequestration in mineral soils would be negated by ongoing emissions from degrading peatlands within 104 to 238 years (Leifeld & Menichetti, 2018).

1.2 SOC, POM and MAOM

Soils are complex, dynamic systems that function as the interface between the Earth's lithosphere, atmosphere, hydrosphere, and biosphere, a concept known as the Pedosphere (Brady & Weil, 2017). Within this system, SOM is a key determinant of soil health and its capacity to regulate global biogeochemical cycles. Organic matter typically constitutes only a small fraction of the soil's dry weight, nevertheless it is central in regulating nutrient cycling, enhances soil structure, improves water retention and support microbial activity (Brady & Weil, 2017). In contrast to mineral soil, organic matter can constitute most of the total volume in peatland soil.

SOM is composed of distinct functional pools, each maintained through stabilization mechanisms and characterized by specific turnover times. Its carbon component plays a crucial role in enhancing nutrient availability, improving soil fertility, and contributing significantly to the global carbon cycle (Gerke, 2022; von Lützow et al., 2007).

This versatility creates a dual, often conflicting, role for SOM, as its decomposition through mineralization is essential for releasing the nutrients, that sustain soil fertility. Simultaneously, its preservation is critical for long-term carbon storage, thereby resulting in a fundamental management trade-off (Gerke, 2022; Yost & Hartemink, 2019). The balance between these functions is governed by stabilization mechanisms that protect SOM from microbial decomposition, primarily through physical stabilization (occlusion within soil aggregates) and chemical stabilization (binding to mineral surfaces). Hence, the persistence of SOM is not simply an intrinsic property of its molecules but manifests as an emergent property of the entire soil ecosystem (von Lützow et al., 2007).

To understand and manage the dual function of SOM, scientific conceptualization has evolved away from the traditional, now outdated, idea of chemically stable humus (Gross & Harrison, 2019). Gross and Harrison (2019) further remark that this concept is being replaced by a model of decomposition continuum. Specifically, the stability of organic matter is conferred by physical and mineralogical protection mechanisms rather than by inherent molecular recalcitrance. Through a robust and measurable framework, this modern understanding is operationalized. It divides SOM into two physically separable and functionally distinct fractions: POM and MAOM (Lavallee et al., 2020; Yu et al., 2022). A soil's ability to store carbon is thus influenced by factors such as soil structure, aggregation, and the clay and silt fractions that provide this protection (von Lützow et al., 2007). The laboratory separation of

SOM into POM and MAOM is typically achieved based on particle size and/or density, and it is proposed that these fractions display distinct biogeochemical properties and decomposition rates (Lavallee et al., 2020; von Lützow et al., 2007; Zimmermann et al., 2007). However, it is important to note that the separation process itself can alter the properties of the isolated fractions depending on the methodology used (Wander, 2004).

The first of these functional fractions, POM, represents the active and more transient component of SOM. POM predominantly consists of plant residues with recognizable cell structures and is composed of structural polymeric organic compounds with relatively short residence times ranging from years to decades (von Lützow et al., 2007; Wander, 2004). This fraction is formed via a plant pathway through the physical fragmentation of litter and its chemical composition still closely resembles the original plant material (Lavallee et al., 2020). POM is a key driver of short-term soil fertility since it represents the primary source of readily available nutrients for both plants and microbes (Gerke, 2022; Wander, 2004). Empirical evidence demonstrates that the accumulation of this fraction is primarily controlled by the quantity and quality of carbon inputs from vegetation (Yu et al., 2022). Consequently, POM exhibits a particularly strong responsiveness to changes in land use, distinguishing it from other soil organic matter fractions (von Lützow et al., 2007; Wander, 2004).

In contrast to the labile POM, the MAOM fraction forms the stable, long-term carbon reservoir in soil. MAOM represents the stable, slow-cycling pool of organic matter, which adheres to mineral surfaces and is thereby protected from rapid decomposition, leading to its extended persistence in the soil (Cotrufo et al., 2019; Lavallee et al., 2020; von Lützow et al., 2007; Yu et al., 2022). This fraction is formed via a microbial pathway, through which soluble organic compounds and microbial byproducts are bound to mineral surfaces (Lavallee et al., 2020). This process of mineral sorption is considered the most important mechanism for the long-term protection of SOC in most mineral soils (Gross & Harrison, 2019).

While the conceptual framework of SOM fractions was developed largely for mineral soils, its principles of stabilization and destabilization are critical for understanding the unique challenges in degraded organic soils. In the specific context of drained Swiss peatlands, the central problem is not merely the balance between fractions, but the progressive and massive loss of the entire organic matter stock through aerobic mineralization, which leads to high greenhouse gas emissions and declining agricultural productivity (Egli et al., 2020a; Guenat, 2022; Paul et al., 2021).

1.3 Carbon and Peatland

To accurately account for the carbon dynamics in these heavily altered soils, a consistent classification system is essential. The classification of peat soils is subject to different definitions. For example, Klingenfuß et al. (2014) refer to the German Soil Classification, which defines soils as having an organic matter content of ≥ 30% and a peat layer thickness of at least 30 cm. Since this definition cannot usually be applied to the sites investigated, a more suitable definition was sought. The Intergovernmental Panel on Climate Change (IPCC) provides a more broadly applied framework with organic soils. The IPCC classification provides a standardized and globally consistent method, defining soil as organic if it has an organic horizon of at least 10 cm with a minimum of 12% organic carbon (Hiraishi et al., 2014). As this thesis investigates degraded peatlands, such as the drained organic soils in the Grosses Moos, stricter national classification categories are no longer met, making the IPCC framework the more appropriate classification for this study. Applying this classification Leifeld et al. (2019) highlights the immense difference in carbon density between Switzerland's organic and mineral soils, underscoring their importance as emission hotspots. Nationwide agriculturally used mineral soils contain approximately 122.6 Mt of organic carbon in the upper 100 cm (Leifeld et al., 2019). In stark contrast, organic soils contain on average 1,366 t of organic carbon per hectare, which is roughly ten times the carbon density of mineral soils (Leifeld et al., 2019). Due to this high concentration of carbon, drained organic soils are disproportionately large sources of agricultural greenhouse gases, responsible for approximately 0.74 million tonnes of CO_2-equivalents per year in Switzerland (Leifeld et al., 2019).

Peat, which contains large amounts of structural molecules such as lignin, cellulose, and hemicellulose from peat-forming plants, is preserved due to inhibited decomposition under water-saturated, anaerobic conditions (Bader et al., 2018; Klingenfuß et al., 2014). However, widespread drainage for agriculture and forestry has exposed this vast carbon store to oxygen, leading to the loss of more than half of Europe's former peatland area (Bader et al., 2018; Wüst-Galley et al., 2020). In these drained Swiss peatlands, the specific composition of the organic matter and the land use type, such as forest or cropland, influence the peat's decomposability and rate of CO_2 release (Bader et al., 2018). The degradation process initiated by drainage is known as secondary humification, which is the oxidative transformation of previously stable organic matter, rendering it more unstable and climate-sensitive (Kalisz & Urbanowicz, 2021).

1.4 SOC in Agricultural Context and Peatland Degradation

SOC is a component of the global carbon cycle as well as a cornerstone of fertile and productive agricultural soils. The storage of SOC is considered a key function of soils and a vital indicator of overall soil quality (Wiesmeier et al., 2019). The preservation of SOC is synergistic with agricultural productivity, as it improves soil structure, enhances water availability, and provides protection against erosion (Wiesmeier et al., 2019).

Despite its critical importance, conventional agricultural practices have historically led to the significant depletion of this vital resource. The conversion of natural ecosystems to cropland leads to a rapid and disproportionate loss of the active SOM fraction, which is the most critical for soil fertility (Tiessen et al., 1994). Intensive tillage accelerates this process by breaking down protective soil aggregates. It exposes previously shielded organic matter to microbial decomposition (Tiessen et al., 1994). Consequently, the loss of this active fraction is directly linked to a decline in natural soil fertility, thereby increasing the dependency on external fertilizers to maintain yields (Tiessen et al., 1994).

The process of peatland degradation and SOC loss is exacerbated by the agricultural activity itself, as the regular input of fresh, labile plant residues from grassland and cropland use can fuel high rates of CO_2 emission in the topsoil (Bader et al., 2018). This highlights that intensive agriculture on these organic soils provides a constant supply of easily decomposable material that accelerates carbon loss from the upper soil profile (Bader et al., 2018).

The drainage of peat soils reverses the soil formation processes and initiates a sequence of physical subsidence mechanisms and oxidative decomposition processes, transforming peatland sites from carbon sinks into net sources of greenhouse gases. The underlying physical mechanisms are described below, before the specific effects in the study area are quantified and classified. It should be emphasized that drainage not only causes physical changes that lead to a reduction in organic matter content but also causes qualitative changes, particularly in chemical composition, as reflected, for example, in altered element ratios (Liu et al., 2019).

According to Götz (1993), the process of peatland subsidence can be divided into four components, although the fourth component, wind erosion, is not relevant to the study area of the Berner Seeland. Firstly, drainage leads to increased suction tension in the root zone and thus to a loss of soil volume, whereby initial shrinkage is partially reversible, but further shrinkage remains irreversible. Secondly, the settlement of the soil, caused by the unstable, fibrous and

water-rich peat structure, causes the pore space to be compressed after water removal, which increases the storage density and decreases the hydraulic conductivity. The pore volume decreases from the original 85-98% to values of approx. 50% (Leifeld et al., 2019). Thirdly, the aerobic environment created by drainage increases the microbial decomposition of organic matter, leading to the mineralization of peat into water, carbon dioxide and minerals (Krüger et al., 2014; Leifeld et al., 2019).

Applying embankments is one of the key strategies researchers are investigating to tackle the challenge of substantial and persistent carbon losses (Paul et al., 2024). The goal is to find management interventions that can mitigate emissions while still preserving agricultural productivity. Such as the application of mineral soil covers. Recent studies in Switzerland demonstrate that this practice has a complex and nuanced impact. However, a four-year study found that applying a mineral soil cover did not lead to a significant reduction in CO_2 emissions or SOC loss compared to an uncovered reference plot (Paul et al., 2024). Furthermore, research using radiocarbon analysis on a similar experimental site in Switzerland revealed that the embankments critically changes the source of the respired CO_2 (Wang et al., 2021). The findings of the study by Wang et al. (2021) indicate that even if total emissions are similar, the mineral layer may offer a physical barrier that provides long-term protection for the bulk of the ancient, underlying peat body.

1.5 Strategies for Stopping the Peatland Degradation

Considering the severe consequences of peatland degradation, stakeholders such as farmers, citizens, authorities and politicians in the study region are confronted with the need to discuss management strategies to slow or halt the ongoing soil and peat loss. These actors must navigate the inherent conflict between maintaining profitable agriculture and achieving conservation goals. The central problem is that continued peat loss simultaneously threatens long-term agricultural productivity through subsidence and soil exhaustion, while also significantly contributing to greenhouse gas emissions at the national level (Ferré et al., 2019; Guenat, 2022). This conflict is reflected in the regional planning for the Berner Seeland, where large-scale projects like the Third Jura Water Correction are discussed and must balance the complex trade-offs between flood protection, agricultural land use, and ecological objectives like reducing emissions from these emission hotspots (Thomet et al., 2018). The urgency of this situation is underscored by projections that, with ongoing degradation, the peat layer in most parts of Berner Seeland will be exhausted within 66 years, making a sustainable reconsideration of land use in these areas a near-term necessity (Ferré et al., 2019).

The most direct scientific approach to halting peat oxidation involves restoring anaerobic conditions through water management. Permanent rewetting is considered the most highly efficient mechanism for peat conservation (Guenat, 2022; Jurasinski et al., 2020; Zeitz & Velty, 2002). However, rewetting does not restore the original peatland ecosystem (Jurasinski et al., 2020; Zeitz & Velty, 2002). Zeitz & Velty (2002) emphasize that the physical degradation resulting from long-term drainage, especially the massive increase in bulk density, is a largely irreversible process. While rewetting successfully stops further oxidation, it creates a new, novel ecosystem on a compacted and physically altered soil body (Zeitz & Velty, 2002). Subsoil Irrigation and Drainage as more moderate water management strategies have also been investigated, but their effectiveness is highly dependent on external factors like weather and local hydrology. Hence, they are not a universally applicable solution (Boonman et al., 2022).

Given the socio-economic barriers and irreversible physical changes associated with rewetting productive agricultural land, alternative land-use models are being explored. Paludiculture, or wet agriculture, like rice, is emerging as an innovative strategy that seeks to reconcile economic land use with climate protection (Egli et al., 2020a). This practice is defined as the cultivation of crops on wet or rewetted peatlands, which allows for the maintenance of the peat body while still generating agricultural products (Guenat, 2022). It is presented as a key pathway that can

combine climate mitigation with continued agricultural value creation. Nonetheless, while paludiculture offers significant climate benefits, it currently faces considerable economic and social barriers, requiring the development of new supply chains, technical knowledge and strong policy support to become a viable alternative.

Furthermore, in addition to water management and land-use change, a third category of strategies has been established that focuses on directly amending the soil itself. However, for the specific goal of long-term peat preservation, the effectiveness of in-situ amendments like biomass and deep plowing is generally regarded as low (Guenat, 2022). Consequently, the application of embankment practice that includes surface covering or the creation of an entirely new soil profile has emerged as a key alternative soil-based strategy (Egli et al., 2020a; Guenat, 2022). Various forms of these practices, which can be broadly termed embankments, have already been applied in the Berner Seeland (Egli et al., 2020a; Ferré et al., 2019; Guenat, 2022; Wallimann, 2023). The long-term effects of such interventions can be profound as demonstrated by Säurich et al. (2019). The study on the application of sand to a temperate bog, found that the practice led to a fundamental and lasting transformation of the ecosystem, including a significant shift in vegetation from Sphagnum mosses to more productive grasses (Säurich et al., 2019).

While the use of embankments represents a potential strategy, each of these management measures faces specific challenges regarding their effectiveness, which represents the central question underlying this study. The practice of adding mineral materials has been shown to have multifaceted and sometimes counter-intuitive effects (Egli et al., 2020a). For instance, in the Grosses Moos, such embankments are being considered as potential measures to maintain fertility, prevent waterlogging, and possibly reduce CO_2 release (Egli et al., 2020a). A 40-year study on sand addition exemplifies the complexity of the outcomes as it found that the practice paradoxically led to a higher net accumulation of carbon and nitrogen (Säurich et al., 2019). The increase in plant productivity, which resulted in a higher carbon input, more than offset the concurrent increase in the rate of decomposition, which led to a higher carbon loss (Säurich et al., 2019). This apparent benefit was accompanied by a negative trade-off in the form of increased N_2O emissions (Säurich et al., 2019). This complexity underscores that significant knowledge gaps remain regarding the effectiveness and quantification of these measures on the overall greenhouse gas balance and the long-term preservation of peat in Switzerland.

2 Study Area

2.1 Introduction to Study Area

The Three Lakes Region in western Switzerland encompasses the lowlands around Lake Neuchâtel, Lake Biel, and Lake Murten (see Figure 1) (Egli et al., 2020a; Mohammadi et al., 2024; Roeoesli & Egli, 2024). Geographically, the region is in the Swiss Plateau, which stretches between the Jura Mountains in the west and the Swiss Alps to the east (Mohammadi et al., 2024). The Grosse Moos, a large, drained lowland peatland area between Lake Neuchâtel and Aarberg, is one of Switzerland's most important agricultural landscapes for vegetable production (Egli et al., 2021; Ferré et al., 2019).

Historically, this area was strongly influenced by the hydrological dynamics of the Aare River, which carved its way through the plain. These periodic shifts in course created a patchwork of lakes, swamps, and peatlands (Egli et al., 2021; Ferré et al., 2019). Later, the extensive marshland was transformed from peatland into agricultural land through the establishment of a system of drainage channels during the Jura water corrections (Egli et al., 2020a).

The Three Lakes Region has benefited greatly from the controlled hydrological conditions and resulting fertile soils, making it one of Switzerland’s most important vegetable-growing area today (Egli et al., 2020a; Ferré et al., 2019). However, decades of intensive farming on peat soils have led to severe degradation, causing subsidence and high carbon emissions (Leifeld et al., 2019; Roeoesli & Egli, 2024).

The following maps provide information about the location and topography of the Grosses Moos study area and the three study sites Lindergut, Rimmerzmatte, and Underi Site. Chapter 2.5 provides a more detailed description of the study sites.

Figure 1: Location Berner Seeland on the LV95 map of Switzerland. Source: (Bundesamt für Landestopographie swisstopo, 2025)

Figure 2: Aerial view of the Seeland region with the three study sites. Source: (Bundesamt für Landestopographie swisstopo, 2025)

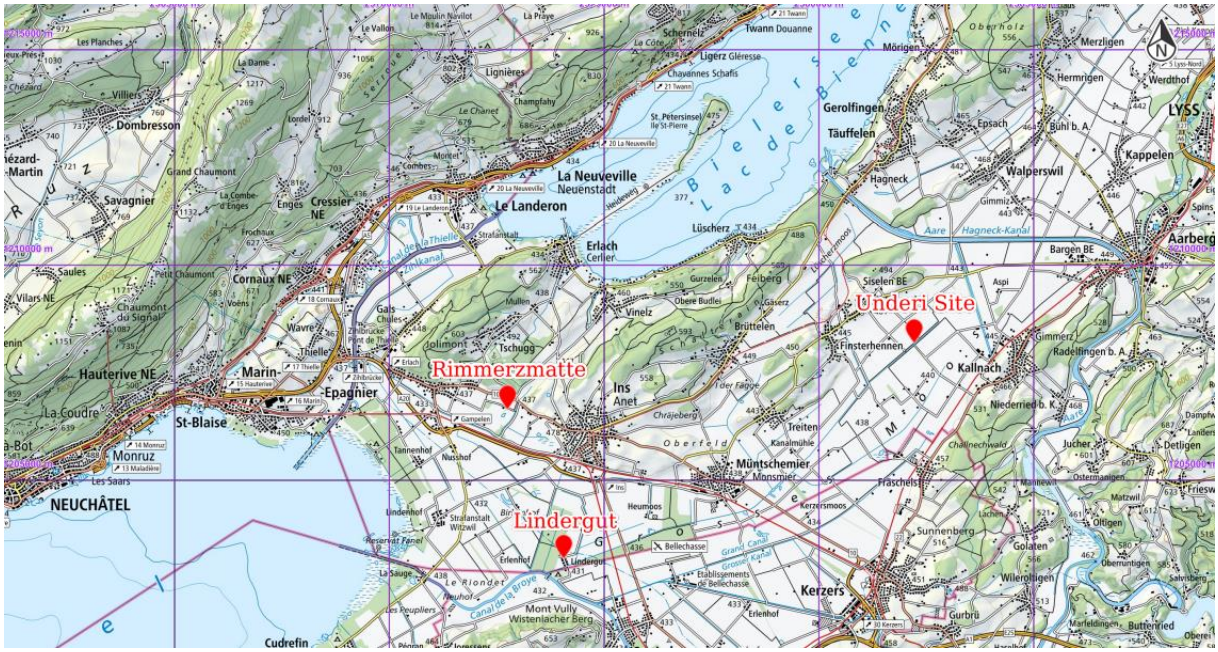

Figure 3: Physical map of the Seeland region with the three study sites. Source: (Bundesamt für Landestopographie swisstopo, 2025)

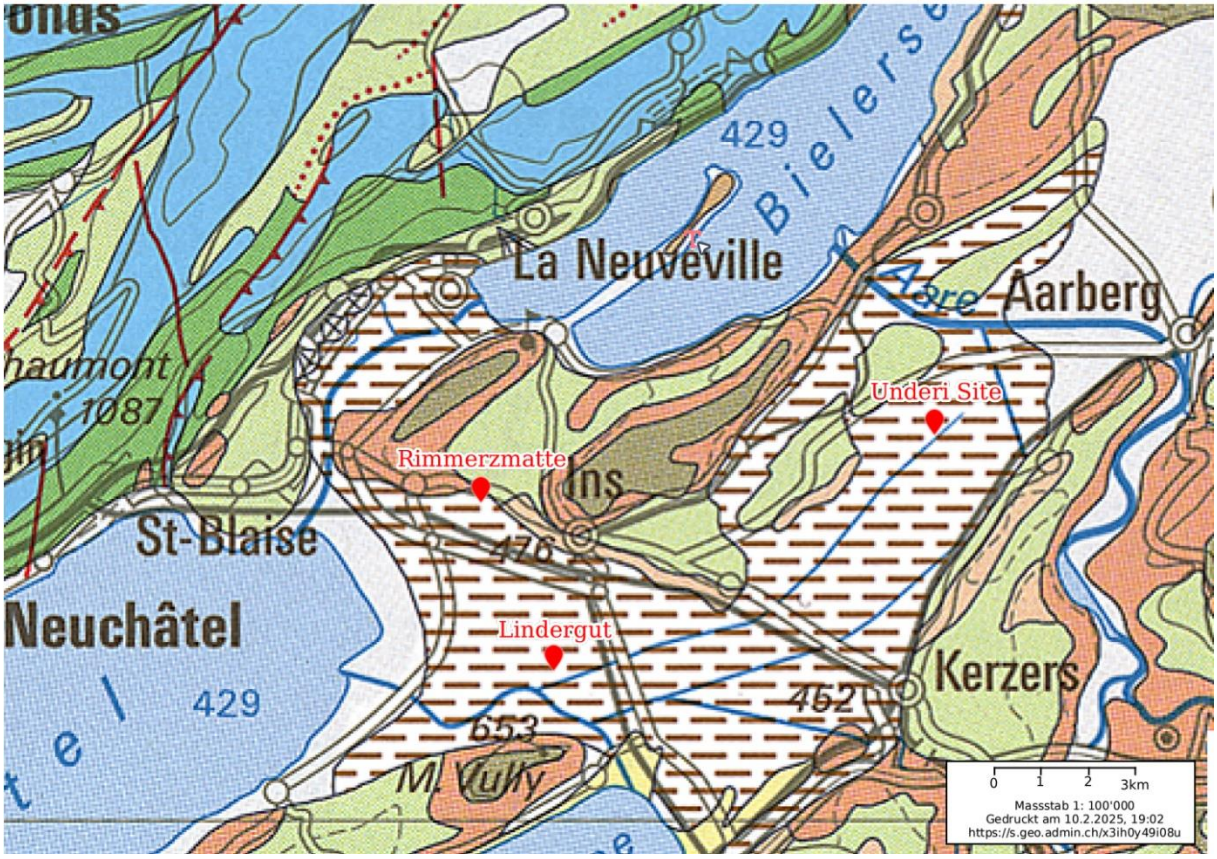

Figure 4: Geologie 500 map of the Seeland region with the three-study site with legends. Source:Bundesamt für Landestopographie swisstopo

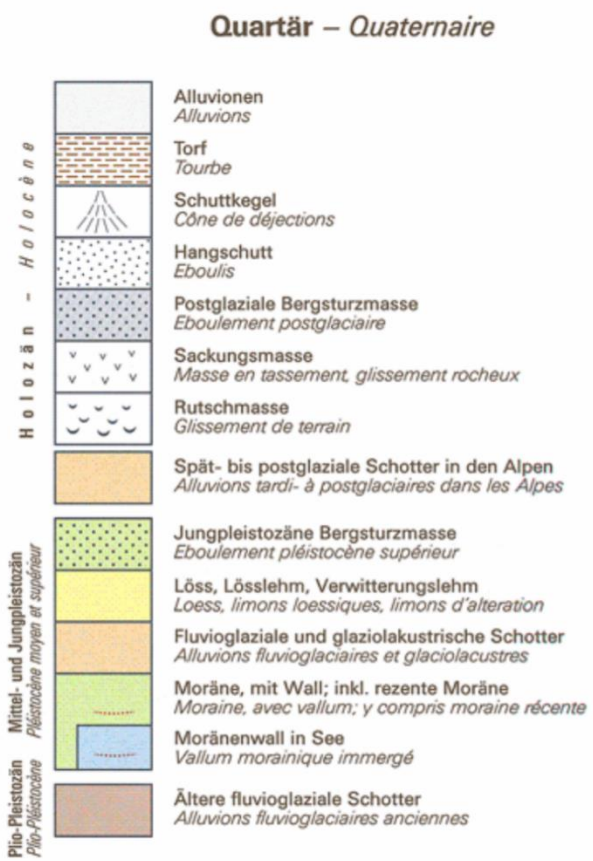

2.2 Historic Background

Over the past century and beyond, the Berner Seeland region has undergone extensive anthropogenic intervention, like the two Jura water correction projects. These actions had a major impact on the ecosystems and agricultural production in the region, which shaped the landscape we see today. Interventions like these have been instrumental in shaping the current perception of the Berner Seeland as Switzerland's vegetable garden (Egli et al., 2021; Egli et al., 2020a; Roeoesli & Egli, 2024). In the early 20th century, the Seeland was severely affected by numerous and periodically recurring floods and associated swamp diseases such as malaria (Egli et al., 2020a). These circumstances created difficult living and economic conditions, which called for a sustainable solution to regulate and stabilize the water level of the lakes. The two Jura water corrections, completed by the end of the 20th century, had a dual impact on the region. While the measures improved agricultural management and reduced the risk of severe flooding, they also initiated significant land subsidence due to the large-scale drainage of the soil (Roeoesli & Egli, 2024). I outline the Jura water corrections below to elucidate their temporary and permanent consequences for the study area.

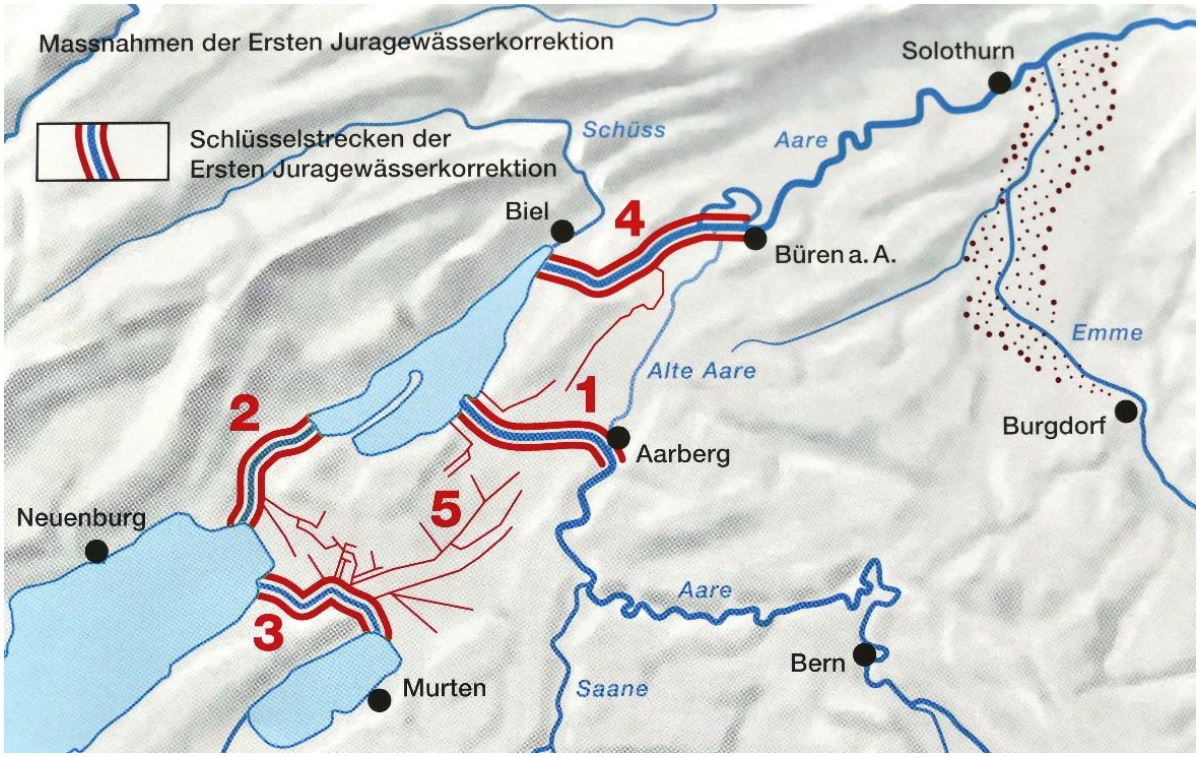

Figure 5: Overview of the measures of the First Jura Water Correction in the Berner Seeland. Source: Amt für Wasser und Abfall des Kantons Bern, 2024

The first Jura water correction project (see Figure 5), carried out between 1868 and 1891, primarily aimed to lower the water levels of Lakes Biel, Neuchâtel, and Murten by an average of 2.5 meters and to increase the drainage capacity of Lake Biel (Amt für Wasser und Abfall des Kantons Bern, 2024; Thomet et al., 2018). In order to achive this lower water level of Lake Biel, the Zihl (2) and Broye (3) canals were built, preceded by the Nidau-Büren canal (4) (Amt für Wasser und Abfall des Kantons Bern, 2024; Egli et al., 2020a).

The Aare was diverted from Aarberg into Lake Biel through the newly built Hagneck Canal (1), which was cut through the Seerücken into Lake Biel (Thomet et al., 2018). The Grosses Moos area was drained by an extensive network of canals (5), an inland correction, up to 80 km in length (Egli et al., 2020a). This first correction resulted in significant gains in cultivated land in peatland areas such as the Grosses Moos and, due to the lowering of the lake level, also on the lake shores (Thomet et al., 2018). Although the first Jura water correction was successful, it led to new problems such as land subsidence and an increased risk of flooding, due to to unexpected side effects. A second measure was initiated to address this issue. This development was followed by the second Jura water correction (1936–1973) with the construction of regulating weirs, bank protection, and canal improvements. This significantly reduced water level fluctuations in the lakes in the Jura region (Amt für Wasser und Abfall des Kantons Bern, 2024).

2.3 Topography and Geology

The geology of the Grosses Moos is not defined by local bedrock but is overwhelmingly dominated by a complex mix of morainic substrates transported from the Alps by glacial action, primarily the Rhône Glacier (Mohammadi et al., 2024). Geochemical fingerprinting shows that the soils are composed of over 75% granitic material and sandstone, sourced from distant locations (Mohammadi et al., 2024). A high contribution from serpentinite (20.8%) was also identified, which is atypical for regions similar to this one (Mohammadi et al., 2024). The local carbonate rock plays only a local role (Mohammadi et al., 2024). This evidence demonstrates the polygenetic nature of the soils, which were formed from a mixture of different parent materials in a glacially reshaped landscape (Mohammadi et al., 2024)

The geological history of glacial deposition in the Grosses Moos directly shapes the region's landforms and their underlying physical properties, which confirms the area to be a glacially altered landscape. The analysis of Mohammadi et al. (2024) reveals a high spatial heterogeneity in the parent material's composition. This heterogeneity is particularly relevant for interpreting physical soil parameters, such as compressibility and water storage capacity, which are closely linked to the landscape's topographical features.

2.4 Climate

Cressier (2571163 / 1210798) is the nearest weather station to the Grosses Moos study area. It is situated at 430 meters above sea level and records a yearly average temperature of 12,8 °C, while the average yearly precipitation lies at approximately 121 millimeters per month, which corresponds to an average annual precipitation of about 1.452 millimeters (Meteoswiss, 2025).

2.5 Sites

The following table shows the three locations examined:

Site	Treament	Municipality	Coordinates	Cover 2024	year of the treatment	material	type of embankment
Lindergut	Original	Ins	46.97976, 7.09825	potato	NA	NA	NA
Lindergut	Backfilled	Ins	46.97957, 7.09827	grassfield	1995	sediments	BC material
Rimmerzmatt	Original	Gampelen	47.01060, 7.08060	wheat	NA	NA	NA
Rimmerzmatt	Backfilled	Gampelen	47.01184, 7.07661	sugar beet	1971	sand	correct setting
Underi Site	Original	Finsterhennen	47.02477, 7.20491	corn	NA	NA	NA
Underi Site	Backfilled	Finsterhennen	47.02520, 7.20556	bare Soil	2013	moraine	BC material

Table 1: Overview of all study sites and their characteristics

Figure 7: Photo of the three study sites showing original soil and embankments. Source: Ciriaco McMackin

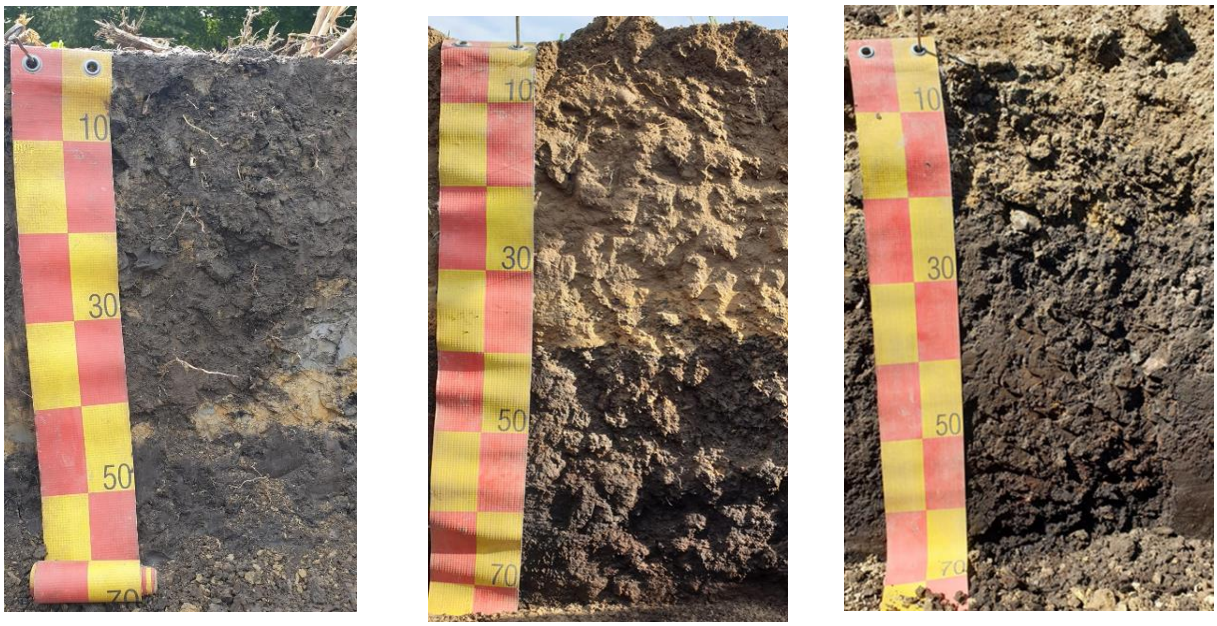

Figure 6: Soil profiles of the sites down to 70 cm depth. From left to right: Lindergut, Rimmerzmatt, and Underi site. Source: Ciriaco McMackin

3. Research Gap and Research Questions

The severe consequences of peatland degradation have led to intensive research on preventive measures for peat protection and their interaction with agriculture. Current research on embankments on agriculturally used peat soils, particularly in Switzerland, has focused primarily on describing and quantifying the effects of these interventions on greenhouse gas fluxes, namely carbon dioxide (CO_2) and nitrous oxide (N_2O). The study by Paul et al. (2024) is a prime example. It carefully measured CO_2 and N_2O fluxes on an embankment and a reference plot, with a focus on the Net Ecosystem Carbon Balance (NECB) and the overall GHG budget. Similarly, the work of Wang et al. (2022) concentrates on a specific flux, analyzing how a mineral top layer alters soil conditions to drastically reduce N_2O emissions. Even broader studies on landscape dynamics in the Grosses Moos evaluate the potential of measures such as embankments mostly from a flux perspective, emphasizing their capacity to reduce CO_2 release (Egli et al., 2020a).

As important as measuring greenhouse gas fluxes is, it provides only an incomplete picture of the long-term soil processes induced by embankments. There remains a substantial knowledge gap regarding the fundamental question of how embankments affect the quantity, quality, and stabilization mechanisms of the remaining carbon inventories within the soil profile. Previous research has largely ignored the underlying changes and distribution of the carbon inventories themselves, instead focusing on the symptoms and emissions (Paul et al., 2024). Since embankments do not stop CO_2 losses, a critical yet unanswered question emerges concerning the underlying carbon inventory and its alternation (Paul et al., 2024). Guenat (2022) likewise highlights in her report the insufficient evidence regarding carbon stocks in peat soils and the consequences of measures such as embankments for the preservation of organic matter. A contrasting study by Otremba et al. (2024) on urban technosols indicated that a protective effect is possible, since a well-preserved carbon-rich peat horizon was found beneath an anthropogenic cover. However, the subject matter was not an agricultural context, and the specific stabilization mechanisms in managed agricultural soils remain unclear (Otremba et al., 2024).

The work of Wang et al. (2021) makes this research gap particularly clear. Using radiocarbon analyses, it indicated that an embankment shifts the source of the respired CO_2. Less carbon originates from old peat. Although this shift is a decisive indication that the stability of the old carbon stock is being influenced, the study did not quantify the resulting changes in the composition and stabilization mechanisms, via physical fractionation into POM and MAOM,

of the remaining carbon (Wang et al., 2021). This master's thesis is part of the research project RESTORE: Rock Heritage, Soil Formation, and Practical Implications for the Three Lakes Region.

Lukas Wallimann (2023) completed an initial study on CO^2 emissions from embankments and original sites in 2023 as part of the same project. Comparative field measurements were carried out in March, May, and June 2022 at ten filled sites and ten reference sites without filling. A total of 360 CO_2 measurements were taken. In addition, relevant weather parameters, soil physical and chemical properties, and agricultural management practices were recorded. The results show that CO_2 emissions are determined primarily by season (higher values in summer than in winter), dew point, and the soil organic carbon content (Wallimann, 2023).

This thesis aims to close the aforementioned research gap by going beyond gas flux measurements to investigate the fundamental effects of embankments on the vertical distribution, functional composition, and biogeochemical stability of carbon inventories in degraded peat soils. This master's thesis examines the processes that control the content and stability of carbon in soils of the Grosses Moos region in the Berner Seeland. In particular, the focus is on the differences in carbon mineralization between original soils (without deposit and not without anthropogenic activity as the all-region was anthropically drained) and anthropogenically embanked soils across the different fractions. Additionally, it investigates potential mechanisms for stabilizing organic matter. The focus lies in the following analytical areas:

Research Question 1:

How do embankments alter the quantitative and vertical distribution of soil organic carbon (SOC) compared to a degraded, uncovered profile?

Working Hypothesis:

Embankments affect the total amount and vertical stratification of SOC within the soil profile relative to degraded, uncovered reference profiles, and if so, at which depths are the largest differences observed?

Research question 2: *How do embankments influence the composition of functional soil carbon fractions, particularly the relationship of labile POM to stable MAOM?*

Working Hypothesis:

The embankments influence the POM/MAOM of carbon stabilization and distribution in soils.

4 Methods

4.1 Fieldwork

Sampling took place on June 4, 2024, in the region of the Grosses Moos. A team of four people, led by Prof. Dr. Markus Egli, conducted soil sampling by drilling at three different locations on a total of six agricultural fields. At the time of sampling, many of the crops were already in advanced phenological stages, significantly influencing the choice of sampling sites. Samples were collected from the field interior, away from boundaries and roads, to avoid edge effects and road-borne contamination while minimizing disturbance to the standing crop. The drilling depths varied, as the goal at each sampling site was to penetrate down to the former lake sediment, thereby obtaining complete soil profiles. The sampling campaign was successfully completed within a single day, resulting in the extraction of 170 samples.

4.2. Sample Preparation and Fractionation

The 170 field samples were subdivided into 10-centimeter increments at the laboratory of the Geographic Institute Zurich, resulting in a total of 141 defined units after applying the new nomenclature. (See Appendix 9.1) Following subdivision, samples were dried in an oven at 75°C for 48 hours. Once dried, samples were manually ground using a mortar to separate the skeletal fraction (>2 mm) from the fine-earth fraction (<2 mm). The separation between these two fractions was accomplished using a 2-mm sieve. The resulting fine-earth fraction (<2 mm) represents the untreated bulk sample. Subsequently, the untreated bulk samples were mechanically ground using a ball mill (Retsch MM400) at 25 rotations per minute for 15 minutes.

For physical fractionation, two replicates of approximately 5 grams each of fine-earth material were processed using water and centrifugation. This procedure yielded two distinct fractions:

- A fraction with a density ≤1 g/cm³ (floating fraction)
- A fraction with a density >1 g/cm³ (sediment at the bottom of the centrifuge tubes)

The fraction ≤1 g/cm³ was carefully decanted into separate beakers and dried at 75°C for several days until complete evaporation of water was achieved. After drying, evaluation showed that there was insufficient material remaining for further analytical procedures. Consequently, the ≤1 g/cm³ fraction was excluded from subsequent analyses due to time constraints and low analytical yield. Following removal of the ≤1 g/cm³ fraction, the residual fraction (>1 g/cm³) remaining in the centrifuge tubes was dried for several days at 75°C. Afterwards, the dried

material was extracted from the tubes and ground manually with a mortar. This material was then sieved through a 63 µm sieve to obtain two additional sub-fractions:

- Fraction >1 g/cm³ with grain size ≥63 µm
- Fraction >1 g/cm³ with grain size <63 µm

The following graphic provides a visual overview of the complete sample preparation procedure:

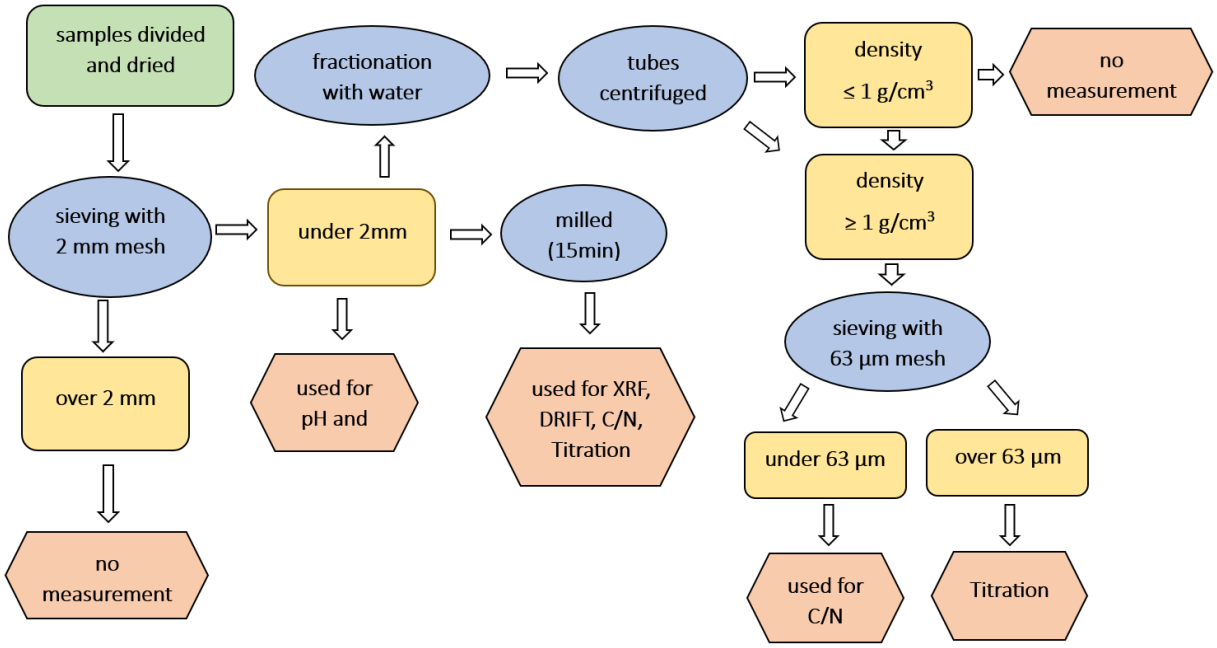

Figure 8: Schematic overview of fractionation and the use of fractions in the laboratory. No measurement means that the sample was not included in the analysis of this thesis.

4.3 Chemical Analysis

The laboratory analysis described in this chapter were conducted at the Laboratory of the Geographic Institute, University of Zurich, according to the laboratory protocol provided by Egli *et al.* (2025).

4.3.1 Quantitative Determination of Total Nitrogen and Total Carbon Content

The quantitative determination of total nitrogen and carbon content was performed using an isotope-ratio mass spectrometer (IRMS) connected to an elemental analyzer (EA). Approximately 2 mg of finely ground material from the bulk fine-earth fraction (<2 mm) and separately from the grain-size fraction <63 µm were weighed into zinc capsules. For each sample, two zinc capsules were prepared. The Analysis was carried out using an elemental analyzer equipped with a thermal conductivity detector, which was connected directly to the mass spectrometer via a dedicated interface. To ensure measurement accuracy and validate analytical results, caffeine (certified according to IAEA-600) and a soil standard based on

Chernozem were employed as reference materials. The measured parameters included total carbon, total nitrogen, $\delta^{13}C$, and $\delta^{15}N$. Additionally, the carbon-to-nitrogen (C/N) ratio was calculated.

4.3.2 X-Ray Fluorescence (XRF)

Precisely 4.0 g of finely ground fine-earth material were weighed into previously prepared sample holders. Subsequently, the sample holders were sealed by closing the lid, taking special care to avoid touching the foil surface to prevent contamination. (See Appendix 9.7)

4.3.3 Diffuse Reflectance Infrared Fourier Transformation (DRIFT)

For the preparation of Eppendorf sample capsules, 270 mg of potassium bromide (KBr), ground manually in an agate mortar, was mixed with 30 mg of the fine-earth sample fraction (<2 mm), which was ground using a vibratory mill. After weighing, the Eppendorf capsules were dried overnight (12 hours) in an oven at 70°C to eliminate residual moisture from the samples. For the actual DRIFT measurement, no precise sample mass is defined, since sample volume and the complete filling of the sample holder are the critical factors. Therefore, a standardized amount of sample material is not applicable in this analytical method. The amount required to fully fill the sample holder typically varies between approximately 20 and 30 mg, depending on the specific characteristics of each sample.

Instrument calibration in the classical sense was not conducted. Instead, samples were analyzed comparatively. Optionally, at the beginning of each measurement series, a standard soil sample (REFESOL 01-A) was measured to verify the functionality and consistency of the instrument. However, no specific target values or limits were established. Instead, the currently measured spectrum was compared to previously recorded spectra of the same standard soil sample to confirm consistency and reproducibility of results. (See Appendix 9.4 and 9.5)

4.3.4 pH Measurement

For the determination of soil pH, exactly 10.0 g of fine-earth material were weighed into a 50 ml glass beaker and mixed with 25 ml of a 0.01 mol/L calcium chloride ($CaCl_2$) solution. A soil-to-solution ratio of approximately 1:2.5 was carefully maintained to ensure that sufficient suspension was available for complete immersion of the electrode (854 iConnect – Metrohm). The suspension was continuously stirred for 30 minutes using a magnetic stirrer, which was followed by a resting period of an additional 30 minutes. Prior to measurement, the pH meter (914 pH/Conductometer – Metrohm) was calibrated using buffer solutions of pH 7.00 and pH

4.00. Subsequently, the electrode was carefully immersed in the suspension to measure pH, gently swirling the beaker to facilitate a rapid stabilization of the reading.

4.3.5 Inorganic Carbon and Carbonate Content

The organic carbon was removed by loss on ignition (LOI), leaving only inorganic carbon in the sample. The inorganic carbon content was calculated from the LOI values and the results of the elemental analysis in accordance with

$$C_{\text{inorg}} = (1 - \text{LOI}) \times C_{\text{total, after ignition}}$$

determined. To determine the organic carbon content, the value obtained was subtracted from the total carbon content of the untreated sample. The carbonate content was determined based on the molar masses of carbon (12 g mol⁻¹) and calcium carbonate (100 g mol⁻¹) as follows:

$$\text{Carbonate content} = \frac{100}{12} \times C_{\text{inorg}}$$

4.3.6 Loss on Ignition (LOI)

To quantify the amount of organic matter and adsorbed water, loss on ignition (LOI) was determined. For this analysis, 2 g of air-dried soil sample material was weighed and subsequently ignited in a muffle furnace (Nabertherm Controller P330) at a temperature of 550 °C for a duration of six hours. After ignition, the amount of organic material was calculated based on the mass difference between the initial and the post-ignition weights. To prevent the thermal decomposition of carbonates during ignition, the furnace temperature was deliberately kept below the critical threshold of 600 °C.

For the calculation of the organic matter content, the following formula was applied:

- $\mathbf{x_1}$: Weight of crucible and sample (before ignition)
- $\mathbf{x_2}$: Weight of crucible and sample (after ignition)

Loss on ignition (LOI)=x1−x2

4.3.7 Chemical Weathering Indices

To analyze chemical weathering of the soil samples, two indices were applied. First, the molar ratio (K + Na)/Ti was used, representing a modified version by (Egli & Fitze, 2000) of the original coefficient (K + Ca)/Ti as proposed by Harrington & Whitney (1987). In both ratios, titanium (Ti) serves as an immobile element relative to the weatherable elements potassium (K)

and calcium (Ca), or in its modified form, potassium (K) and sodium (Na) (Egli et al., 2020b). According to (Egli et al., 2020b) , replacing calcium with sodium in the index increases its precision, as soils from the Berner Seeland contain significant amounts of calcium derived from leaching of carbonate-rich bedrock.

The following indices were applied:

- CIA according to (Nesbit & Young, 1989):

$$CIA = 100\left[\frac{Al_2O_3}{Al_2O_3 + CaO + Na_2O + K_2O}\right]$$

The primitive mantle ratio was calculated based on data from Sun and McDonough (1989).

5 Results

This section breaks down the data on carbon distribution across the three study sites. The following figures and tables illustrate how carbon is partitioned among different soil fractions, highlighting the key differences between the original and backfilled profiles. This analysis begins with the carbon concentrations, followed by a consideration of the mass balance. Additional information can be found in the Appendix 9.2.

5.1 Carbon Concentrations and Carbon Distribution

The following subchapter is structured according to locations (sites) and explains the carbon concentrations, their distribution across the individual fractions, and their contribution to the mass balance. Chapter 5.2 deals with soil composition in greater depth; it also analyzes nitrogen concentrations and their spatial distribution.

5.1.1 Lindergut

Table 2: Concentrations (weight-%) in different fractions and their carbon content: Site Lindergut

Site	Treatment	Depth	Bulk Soil			Fraction <63µm			Fraktion > 63µm		
			Total C	inorg. C	org. C	Total C	inorg. C	org. C	Total C	inorg. C	org. C
		cm	%	%	%	%	%	%	%	%	%
Lindergut	Original	10	10.65	1.38	9.27	12.06	1.46	10.60	10.11	1.35	8.77
Lindergut	Original	20	10.77	1.37	9.40	11.34	1.17	10.17	10.61	1.43	9.18
Lindergut	Original	30	12.54	1.23	11.31	13.21	1.13	12.08	12.22	1.28	10.95
Lindergut	Original	40	12.51	1.24	11.27	14.70	2.03	12.67	11.90	1.02	10.88
Lindergut	Original	50	17.13	0.82	16.31	16.85	1.06	15.79	17.27	0.71	16.56
Lindergut	Original	60	16.83	0.40	16.43	14.44	0.37	14.07	17.78	0.41	17.37
Lindergut	Original	70	10.86	0.22	10.64	8.18	0.26	7.92	12.38	0.20	12.19
Lindergut	Original	77	17.55	0.39	17.16	11.54	0.60	10.94	19.55	0.32	19.23
Lindergut	Backfilled	10	6.26	1.58	4.69	6.26	1.79	4.48	6.26	1.46	4.80
Lindergut	Backfilled	20	5.42	1.63	3.79	5.70	1.83	3.87	5.25	1.50	3.75
Lindergut	Backfilled	30	5.17	1.58	3.59	5.40	1.87	3.54	5.05	1.43	3.61
Lindergut	Backfilled	40	5.51	1.57	3.93	5.70	1.72	3.98	5.39	1.48	3.91
Lindergut	Backfilled	50	5.32	1.80	3.52	5.30	1.93	3.37	5.33	1.73	3.60
Lindergut	Backfilled	60	8.99	1.91	7.08	8.90	1.50	7.40	9.03	2.10	6.93
Lindergut	Backfilled	70	12.47	1.02	11.45	8.37	0.36	8.02	14.23	1.31	12.92
Lindergut	Backfilled	80	12.31	1.13	11.19	12.73	0.84	11.90	12.13	1.25	10.88
Lindergut	Backfilled	90	11.91	1.21	10.70	12.05	1.35	10.69	11.86	1.16	10.70
Lindergut	Backfilled	100	6.49	0.16	6.33	5.65	0.40	5.25	6.67	0.11	6.56
Lindergut	Backfilled	110	13.02	0.23	12.78	7.22	0.52	6.70	15.14	0.13	15.01
Lindergut	Backfilled	120	12.57	0.23	12.34	11.18	0.62	10.56	13.06	0.10	12.96
Lindergut	Backfilled	130	9.68	0.24	9.43	8.92	0.78	8.13	10.00	0.01	9.98
Lindergut	Backfilled	132	8.35	0.15	8.20	8.93	0.47	8.46	8.12	0.03	8.09

5.1.1.1 Carbon Concentration

As Table 2 shows, the total carbon concentration at both sites increases continuously to a corresponding depth in the profiles from the soil surface. The original soil has higher values overall than the backfilled soils, both in the bulk soil and in all fractions. The average organic carbon content in the bulk soil is 12.7% at the original site, while it reaches 7.79% in the backfilled soil. Particularly in the top 40 cm, there is a clear divergence between original and backfilled soils in all fractions. The maximum organic carbon concentration occurs in the original soil between 50 cm and 60 cm depth, regardless of fraction. In the backfilled soils, this maximum shifts to a depth of 70 cm to 80 cm in all fractions. The average organic carbon concentration in the fraction < 63 µm is 11.78% in the original soil and 6.88% in the backfilled soil. Despite these quantitative differences, the concentration pattern at both sites is largely parallel and follows the trend of the total carbon concentration in the bulk soil. However, the fraction < 63 µm has lower organic carbon contents at greater depths than the bulk soil and the fraction > 63 µm. The concentration of inorg anic carbon is very low overall. In general, there is a decreasing trend in inorganic carbon concentration with increasing depth, with the topsoil showing the highest values. The backfilled site exhibits a particularly pronounced decrease with depth.

5.1.1.2 Organic Carbon Mass Balance

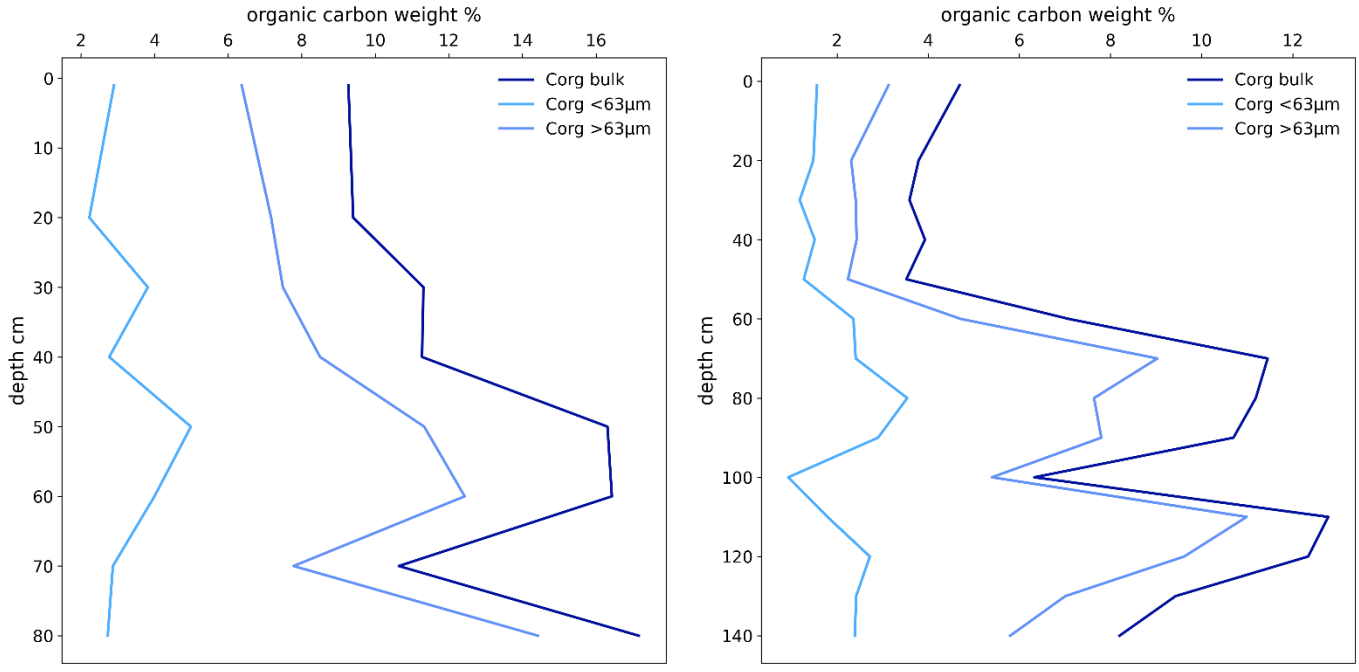

Figure 9: Organic carbon mass balance Lindergut Original (left) and Lindergut backfilled (right)

Figure 9 on the left shows the mass balance of organic carbon in the original soil. The bulk organic carbon content increases continuously with depth and reaches its maximum at 80 cm with 17.16%. The minimum is found in the original bulk at the 0 cm to 10 cm horizon with 9.27%. The organic carbon is mainly concentrated in the coarse fraction (>63 µm), which increases continuously from the surface to a depth of 60 cm. The fine fraction (<63 µm), on the other hand, shows only slight fluctuations and remains fairly constant throughout the original profile. The backfilled profile, Figure 9 on the right, shows a more fragmented distribution pattern in contrast to the original soil. In the upper 50 cm, the bulk values for organic carbon are between 3.5% and 4.7%. This is followed by an abrupt increase in organic carbon content at 60 cm for all fractions, with the coarse fraction and the bulk running similarly parallel. The increase in the fine fraction is also rather moderate here and decreases again after 80 cm. The distribution is not continuous, but discontinuous and organized horizontally. Here, too, the coarse fraction dominates the organic carbon balance and shows a pronounced accumulation with depth. The fine fraction (<63 µm), on the other hand, varies only marginally, analogous to the original profile. In a direct comparison, both profiles, original and backfilled, show an organic carbon distribution dominated by the coarse fraction >63 µm, but the patterns differ in their structure. While Lindergut Original shows a continuous, vertically increasing trend for two fractions, the pattern for Lindergut Backfilled is generally more discontinuous with abrupt enrichment in deeper horizons.

5.1.2 Rimmerzmatt

Table 3: Concentrations (weight-%) in different fractions and their carbon content: Site Rimmerzmatt

Site	Treatment	Depth	Bulk Soil			Fraction <63µm			Fraktion > 63µm		
			Total C	inorg. C	org. C	Total C	inorg. C	org. C	Total C	inorg. C	org. C
		cm	%	%	%	%	%	%	%	%	%
Rimmerzmatt	Original	10	8.09	0.61	7.48	7.84	1.48	6.36	8.12	0.52	7.60
Rimmerzmatt	Original	20	8.04	0.49	7.55	8.84	0.85	7.99	7.92	0.44	7.48
Rimmerzmatt	Original	30	9.15	0.46	8.70	8.21	0.72	7.50	9.27	0.42	8.85
Rimmerzmatt	Original	40	26.38	0.88	25.50	25.55	0.97	24.57	26.46	0.88	25.58
Rimmerzmatt	Original	50	36.15	1.30	34.86	35.87	1.02	34.85	36.17	1.32	34.86
Rimmerzmatt	Original	60	38.33	1.47	36.86	36.89	1.24	35.65	38.45	1.49	36.96
Rimmerzmatt	Original	70	33.16	1.20	31.95	39.25	0.00	39.25	32.87	1.47	31.41
Rimmerzmatt	Original	80	26.14	0.65	25.48	20.97	0.00	20.97	26.77	0.83	25.93
Rimmerzmatt	Original	90	23.40	0.42	22.98	16.42	0.00	16.42	24.33	0.50	23.83
Rimmerzmatt	Original	100	13.15	0.19	12.96	10.19	0.51	9.69	13.73	0.13	13.59
Rimmerzmatt	Original	106	2.94	0.00	2.94	4.64	0.00	4.64	2.77	0.00	2.77
Rimmerzmatt	Backfilled	10	4.41	2.70	1.71	5.47	3.51	1.95	4.26	2.59	1.68
Rimmerzmatt	Backfilled	20	4.15	2.60	1.55	5.34	3.13	2.22	3.97	2.52	1.44
Rimmerzmatt	Backfilled	30	4.48	2.58	1.90	6.17	1.09	5.08	4.31	2.74	1.57
Rimmerzmatt	Backfilled	40	4.99	2.86	2.14	7.13	2.16	4.97	4.71	2.95	1.76
Rimmerzmatt	Backfilled	50	5.10	2.97	2.13	7.29	1.93	5.36	4.85	3.09	1.76
Rimmerzmatt	Backfilled	60	8.03	1.89	6.14	9.05	1.28	7.77	7.93	1.95	5.97
Rimmerzmatt	Backfilled	70	17.93	1.16	16.77	16.90	2.08	14.82	18.00	1.10	16.90
Rimmerzmatt	Backfilled	80	25.83	1.10	24.74	23.28	4.38	18.90	25.92	0.99	24.93
Rimmerzmatt	Backfilled	90	31.51	1.12	30.40	26.08	4.80	21.28	31.68	1.01	30.67
Rimmerzmatt	Backfilled	100+	41.09	1.15	39.94	30.76	11.18	19.59	41.28	0.97	40.31

5.1.2.1 Carbon Concentrations

In an overall comparison with the other investigation sites, the Rimmerzmatt site shows the highest average total carbon concentrations in bulk soil. In the original soil, the average value is 20.45%, and in the backfilled soil, it is 14.75%. In the original profile, the carbon concentration in the bulk soil starts at 8.09% and remains almost constant down to a depth of 30 cm. Between 40 cm and 70 cm depth, there is an abrupt increase, peaking at a maximum of 38.33% at 60 cm. The carbon content then drops, reaching only 2.94% at a depth of 106 cm. In the backfilled profile, the carbon concentration in the bulk soil starts at 4.41% and rises continuously with increasing depth, reaching a maximum of 41.09% at a 100 cm.

A comparison of the two sites reveals clear differences: while the original profile is characterized by a clear peak in total carbon content at 60 cm and higher overall levels, the backfilled profile shows a significantly flatter curve. One common feature is the parallel, low concentration level in the topsoil to a depth of about 50 cm.

With regard to organic carbon concentrations, it can be seen that the distribution in the fraction > 63 µm is almost congruent with the curve of the bulk soil. In contrast, the fraction < 63 µm, especially in the backfilled soil, shows significant deviations from the organic carbon in the bulk soil. Here, the concentration reaches its maximum at 21.28%, after which it begins to decline. In the original soil, the fraction < 63 µm also shows slightly lower concentrations compared to the fraction > 63 µm, but largely follows the trend of the bulk soil.

The first 30 to 40 cm of both profiles show a similar trend, with relatively low concentrations of organic carbon. In the original soil, this is followed by a steep increase in concentration, while the backfilled soil shows a significantly flatter increase and the higher concentrations tend to start at 70 cm.

The pattern of inorganic carbon is the opposite: in the original soil, a continuous decrease in concentration can be seen in all fractions with increasing depth until the values are no longer detectable in the subsoil. In contrast, the backfilled soil shows significantly higher concentrations – with an average value of 2.01%, almost twice as high as in the original soil. Particularly in the <63 µm fraction, an increase in organic and inorganic carbon in the subsoil is visible in the backfilled profile.

5.1.2.2 Organic Carbon Mass Balance

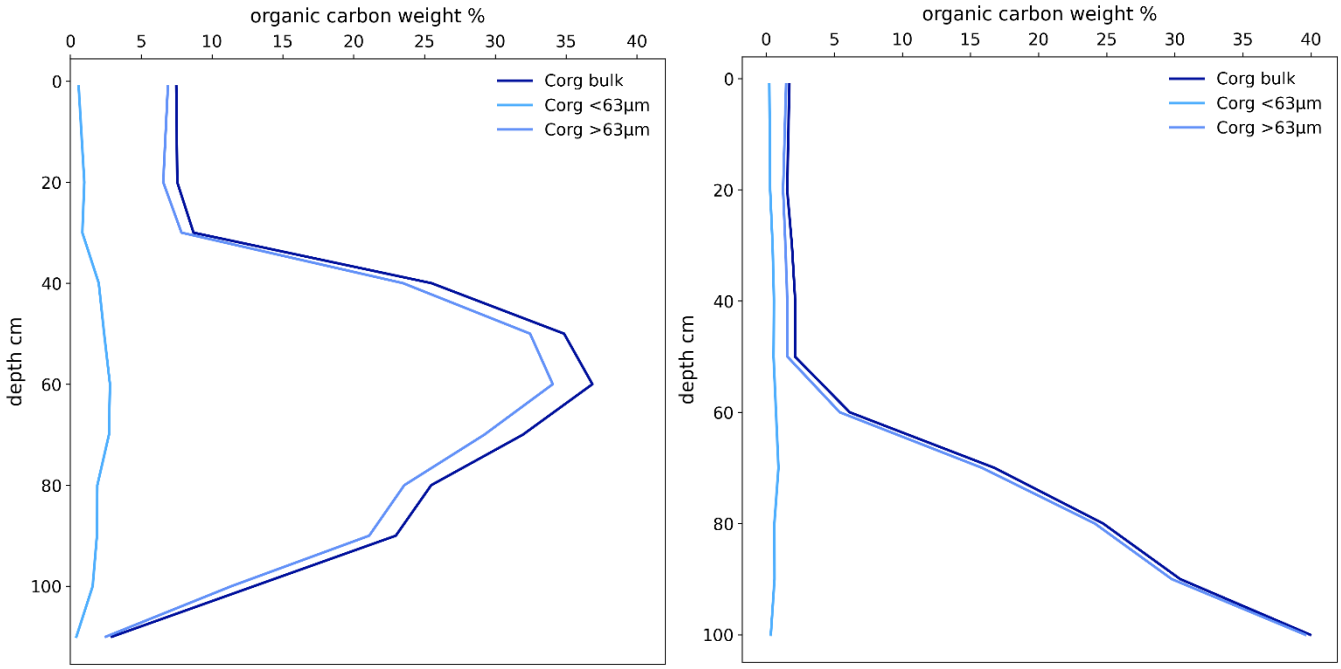

Figure 10: Organic carbon mass balance Rimmerzmatt Original (left) and Rimmerzmatt backfilled (right)

Looking at the distribution patterns in the mass balance (see Figure 10), fundamental differences can be seen in the vertical distribution of organic carbon and in the fractionated composition of organic matter. While the original profile shows a continuous increase in organic carbon content with a maximum in the middle soil horizon at 60 cm, the backfilled profile shows an unnatural, abrupt accumulation of organic matter in the coarse fraction from a depth of 50 cm. In the original profile, the organic carbon content increases from a depth of about 30 cm, reaches its maximum of 36.9% between 50 and 60 cm, and then drops moderately again. This observation was also made regarding concentration. The two peaks of concentration and mass balance are approximately congruent here. In contrast, the organic carbon content in the backfilled profile remains low in the bulk soil and coarse fraction up to 50 cm and shows an almost linear increase from 60 cm to just under 40% at 100 cm. The fraction distribution reinforces this observed difference. In both profiles, the fraction >63 µm clearly dominates the organic carbon content. In the original profile, there is an almost congruent distribution between bulk organic carbon and the coarse-grained fraction, with a consistently high proportion in the >63 µm fraction. The fine-particle fraction (<63 µm) remains rather weak. This distribution pattern can also be observed in the backfilled profile, but with a clear peak: in the backfilled profile, the <63 µm fraction contributes only marginally even to deep horizons, while the entire organic carbon increase is almost exclusively attributable to the >63 µm fraction.

5.1.3 Underi Site

Table 4: Concentrations (weight-%) in different fractions and their carbon content, Site: Underi Site

Site	Treatment	Depth	Bulk Soil			Fraction <63µm			Fraktion > 63µm		
			Total C	inorg. C	org. C	Total C	inorg. C	org. C	Total C	Inorg. C	org. C
		cm	%	%	%	%	%	%	%	%	%
Underi Site	Original	10	14.75	0.10	14.65	12.96	0.65	12.31	15.07	0.00	15.07
Underi Site	Original	20	14.62	0.06	14.57	12.94	0.31	12.63	14.99	0.00	14.99
Underi Site	Original	30	13.99	0.14	13.85	13.05	0.51	12.54	14.36	0.00	14.36
Underi Site	Original	40	14.14	0.17	13.97	12.76	1.11	11.65	14.39	0.00	14.39
Underi Site	Original	50	14.36	0.00	14.36	12.44	0.00	12.44	15.25	0.00	15.25
Underi Site	Original	60	26.43	0.01	26.42	22.71	0.03	22.68	27.89	0.00	27.89
Underi Site	Original	70	12.99	0.00	12.99	11.40	0.00	11.40	13.53	0.00	13.53
Underi Site	Original	80	3.85	0.00	3.85	4.12	0.00	4.12	3.74	0.00	3.74
Underi Site	Original	90	3.56	2.18	1.38	4.35	3.31	1.04	3.21	1.68	1.53
Underi Site	Original	100	4.21	3.48	0.73	5.60	5.30	0.29	3.70	2.80	0.90
Underi Site	Original	106	5.07	3.41	1.66	6.04	5.43	0.61	4.68	2.58	2.09
Underi Site	Backfilled	10	2.77	1.14	1.63	3.14	1.15	1.99	2.56	1.14	1.42
Underi Site	Backfilled	20	2.44	1.28	1.16	3.01	1.56	1.46	2.10	1.11	0.99
Underi Site	Backfilled	30	2.72	1.36	1.36	2.77	1.50	1.26	2.69	1.27	1.42
Underi Site	Backfilled	40	3.15	1.62	1.53	3.37	1.66	1.70	3.06	1.60	1.46
Underi Site	Backfilled	50	5.66	0.87	4.79	6.03	0.97	5.06	5.46	0.82	4.64
Underi Site	Backfilled	60	7.03	0.33	6.70	8.53	-0.28	8.81	6.72	0.46	6.26
Underi Site	Backfilled	70	7.02	0.44	6.58	8.52	0.12	8.40	6.68	0.51	6.17
Underi Site	Backfilled	80	7.12	0.39	6.74	8.23	0.24	7.99	6.61	0.45	6.16
Underi Site	Backfilled	90	7.50	0.10	7.40	8.14	0.10	8.04	7.08	0.10	6.98
Underi Site	Backfilled	100	8.59	0.04	8.55	6.08	0.01	6.07	9.90	0.05	9.85
Underi Site	Backfilled	108.5	11.67	0.00	11.67	8.48	0.00	8.48	12.98	0.00	12.98

5.1.3.1 Carbon Concentrations

In the original soil, the concentration of total carbon in the bulk soil increases continuously until it reaches its maximum at 60 cm with 26.43%. Thereafter, the concentration decreases continuously to 3.56% at a depth of 106 cm. The organic carbon concentration follows this pattern, while the inorganic carbon concentration increases with depth and reaches a maximum of 3.48% at 100 cm. In the fine fraction (< 63 µm), both total and organic carbon concentrations decrease with increasing depth. The inorganic carbon content, on the other hand, increases with depth to 5.43%. The coarse fraction (> 63 µm) shows consistently higher carbon concentrations, but these also follow the general trend of decreasing with depth. The presence of inorganic carbon from 90 cm onwards is striking in the coarse fraction. Up to this depth, no inorganic carbon had been detected in the coarse fraction.

In the backfilled soil, the concentration profiles show a reciprocal depth trend. The total carbon concentration in the bulk soil increases from 2.44% to 11.67%. The same trend is visible in organic carbon concentration. The inorganic concentration decreases from 1.62% to 0%. In the fine fraction (< 63 µm), total and organic C concentrations increase with depth, accompanied by a decrease in inorganic concentration. The coarse fraction (> 63 µm) also shows increasing total and organic C concentrations, while the inorganic fraction decreases to 0% with depth.

In a direct comparison all C concentrations in the top horizons of the original soil are significantly higher than those in the backfilled soil. With increasing depth, the values approach each other or reverse: In the original soil, decreasing concentrations of organic C dominate, while in the backfilled soil, increasing concentrations dominate. Inorganic C increases with depth in the original soil but decreases in the backfilled soil. Common to both treatments is that the organic carbon fraction always accounts for most of the total C and the coarse fraction has higher concentrations than the fine fraction.

5.1.3.2 Organic Carbon Mass Balance

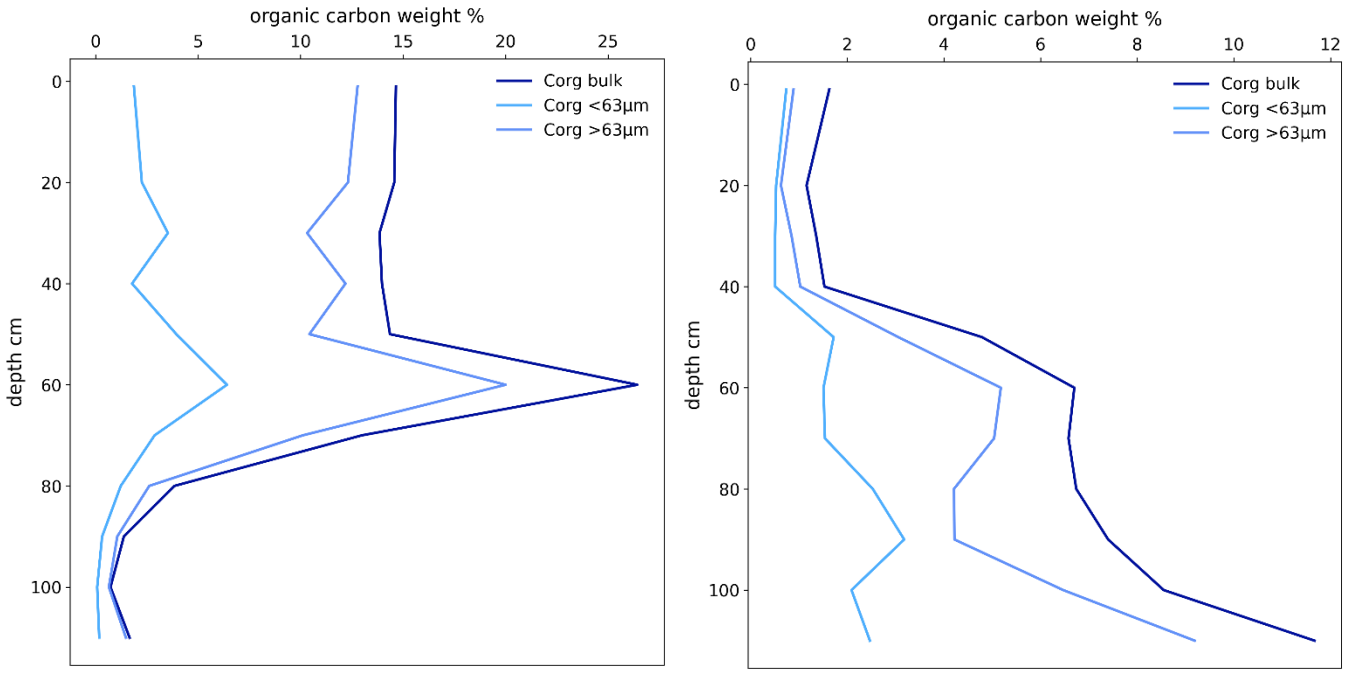

Figure 11: organic carbon mass balance Underi Site Original (left) and Underi Site Backfilled (right)

The organic carbon distributions within the mass balance differ markedly. In the original profile (see Figure 11, left), the bulk content decreases with increasing depth when considering the entire profile. In the uppermost 50 cm, the organic carbon values range between 13.8% and 14.6%, in which the coarse fraction constitutes the dominant share, whereas the fine fraction exhibits significantly lower values.

A conspicuous sharp peak is present at 60 cm, where all three fractions increase significantly (bulk: 26.4%; coarse fraction (> 63 µm): 20.0%; fine fraction (< 63 µm): 6.41%). Below 70 cm, the organic carbon content continuously declines for all parameters, reaching very low values at 100 cm and stagnating at this level. The fractional dominance, however, is maintained: the coarse fraction supplies most of the organic carbon down into deeper horizons.

The backfilled profile (see Figure 11, right) displays a completely inverse distribution of organic carbon. All fractions show rather low values, under 2%, in the topsoil from 0-40 cm. The organic carbon in the bulk fraction is relatively low in the uppermost 40 cm, then increases from a depth of 50 cm up to 11.67% at a depth of 110 cm. The organic carbon contents of the coarse fraction (> 63 µm) rise in parallel with the bulk content, reaching their maximum of 9.19% at 110 cm. The fine fraction exhibits distinctly lower values. However, the values of the fine fraction also increase from 40 cm downwards and rise with depth, although they remain clearly below the level of the bulk and coarse fractions. Here too, a clear dominance of the coarse fraction is evident, but with a lower fractionation intensity than in the original profile.

The vertical structuring and the distribution of organic matter reveal the fundamental differences between the profiles at the Underi Site. In the original profile, the organic carbon distribution is shaped by natural pedogenetic processes, featuring a decrease with depth, layer-specific differentiation, and a clear dominance of the coarse fraction, alongside a high total content in the upper soil matrix. In the backfilled profile, the distribution pattern is controlled by anthropogenic introduction, characterized by an increase with depth, irregular stratification, and likewise a dominance of the coarse fraction, yet at an overall lower level in the upper zone and with high values in deeper layers.

In both profiles, the coarse fraction contributes most of the organic carbon. In the original profile, this dominance is most likely a product of long-term accumulation and soil development; in the backfilled profile, however, it is the result of an unsorted material backfill lacking any structured pedogenetic differentiation.

In summary, the profiles exhibit two opposing systemic states: The original profile reflects a vertical depletion of organic carbon, whereas the backfilled profile documents a vertically inverse carbon distribution.

5.2 Soil Composition : N, Isotopes, LOI ; CaCO3 and C/N

The following figures and tables show the data and distribution patterns of the C/N ratio, nitrogen, and isotopes in the soil profiles of the three investigated sites. The soil profile fractions, and the original and backfilled profiles are compared. First, the carbon concentrations will be described, after which the mass balance will be considered. Supplementary information can be found in Appendix 9.3.

5.2.1 Lindergut

Table 5: Lindergut Nitrogen, d13C, d15N, LOI, CaCO3 and C/N values of the different size fractions

Site	Treatment	Depth	BULK Soil						Fraction <63µm					Fraktion > 63µm		
			N	d13C	d15N	LOI	CaCO3	C/N	N	d13C	d15N	CaCO3	C/N	N	CaCO3	C/N
		cm	%	‰	‰	%	%		%	‰	‰	%		%	%	
Lindergut	Original	10	0.61	-23.94	3.92	22.33	11.50	15.10	0.84	-24.68	4.53	3.34	12.68	0.53	0.98	16.53
Lindergut	Original	20	0.62	-23.82	3.93	22.00	11.42	15.28	0.79	-24.74	4.45	2.13	12.96	0.57	1.11	16.18
Lindergut	Original	30	0.71	-25.00	3.32	25.49	10.25	15.90	0.85	-25.29	3.50	2.98	14.28	0.65	0.87	16.88
Lindergut	Original	40	0.72	-25.44	3.22	36.05	10.33	15.64	0.93	-25.75	3.27	3.69	13.56	0.66	0.80	16.47
Lindergut	Original	50	0.98	-26.53	2.62	35.72	6.83	16.58	1.07	-26.43	3.08	2.79	14.70	0.94	0.49	17.57
Lindergut	Original	60	0.93	-27.34	1.72	28.68	3.33	17.75	0.88	-26.77	2.15	0.87	15.98	0.94	0.30	18.41
Lindergut	Original	70	0.63	-27.48	1.66	25.87	1.83	16.84	0.56	-26.90	2.52	0.78	14.16	0.67	0.13	18.10
Lindergut	Original	77	0.99	-27.32	1.05	37.48	3.25	17.39	0.70	-26.80	1.44	1.25	15.69	1.08	0.24	17.76
Lindergut	Backfilled	10	0.39	-20.16	7.99	12.52	13.14	11.96	0.34	-18.93	3.74	5.17	12.98	0.42	0.96	11.51
Lindergut	Backfilled	20	0.32	-18.91	8.20	10.84	13.56	11.80	0.28	-17.51	3.38	5.85	13.77	0.35	0.92	10.80
Lindergut	Backfilled	30	0.32	-18.65	8.69	10.27	13.15	11.29	0.28	-17.35	4.20	5.18	12.42	0.33	0.96	10.80
Lindergut	Backfilled	40	0.34	-19.11	8.67	11.16	13.10	11.46	0.30	-17.79	4.00	5.45	13.32	0.37	0.92	10.54
Lindergut	Backfilled	50	0.29	-17.49	7.37	10.21	15.02	12.09	0.23	-15.33	3.52	6.07	14.50	0.33	1.07	11.05
Lindergut	Backfilled	60	0.53	-21.71	6.98	17.83	15.92	13.43	0.49	-22.02	2.93	3.99	15.01	0.54	1.43	12.76
Lindergut	Backfilled	70	0.82	-24.88	6.06	25.54	8.52	13.99	0.51	-25.56	2.98	0.89	15.64	0.95	0.92	13.60
Lindergut	Backfilled	80	0.81	-24.82	6.62	26.20	9.38	13.87	0.78	-25.62	3.16	2.08	15.20	0.82	0.88	13.32
Lindergut	Backfilled	90	0.78	-25.13	5.89	25.14	10.08	15.25	0.70	-25.83	2.22	3.05	17.11	0.81	0.84	13.22
Lindergut	Backfilled	100	0.50	-26.81	6.36	18.07	1.34	13.09	0.39	-26.63	1.96	0.59	14.46	0.52	0.09	12.65
Lindergut	Backfilled	110	0.78	-27.20	3.67	27.24	1.96	16.61	0.40	-26.91	0.37	1.17	18.26	0.93	0.09	16.22
Lindergut	Backfilled	120	0.80	-27.29	3.21	28.51	1.93	15.80	0.62	-27.27	-0.01	1.33	17.94	0.86	0.07	15.15
Lindergut	Backfilled	130	0.67	-27.24	3.95	24.27	2.03	14.37	0.58	-26.96	0.61	1.94	15.31	0.71	0.01	14.03
Lindergut	Backfilled	132	0.56	-26.75	4.99	21.78	1.26	14.98	0.51	-26.52	1.00	1.11	17.46	0.58	0.02	14.07

5.2.1.1 Nitrogen Concentration

In the bulk soil of the original profile, an increase is discernible down to a depth of 50 cm. The highest value (0.99% at 77 cm) and the lowest value (0.61% at 10 cm) lie in close proximity. Overall, an increase can be observed down to 50 cm, followed by irregular fluctuations at greater depths.

In the fine fraction (< 63 µm) of the original profile, an increase in nitrogen concentration is apparent down to 50 cm, with a value of 1.07%. From a depth of 60 cm, the nitrogen content decreases significantly, dropping to a minimum of 0.56% (at 70 cm). The distribution pattern shows a uniform increase down to the middle horizon, followed by a distinct decline in the subsoil. For the coarse fraction (> 63 µm) in the original profile, a continuous increase in nitrogen content is observable, with a small dip at 70 cm. The maximum is reached in the lowermost horizon.

In the backfilled profile, the nitrogen content in the bulk soil starts at 0.39% in the uppermost horizon and initially drops to a minimum of 0.29% at a depth of 50 cm. From 60 cm downwards, a continuous increase is observed. Further fluctuations follow at greater depths. The maximum is at 70 cm (0.82%). Down to 50 cm, the nitrogen content remains largely constant and low, after which an increase with fluctuating values occurs.

In the <63 µm fraction, the maximum value is at 80 cm (0.78%), and the minimum is at 50 cm (0.23%). The trend is characterized by an initial decrease down to 50 cm, followed by a subsequent increase and moderate fluctuations.

The >63 µm fraction registers its maximum at 70 cm (0.95%) and its minimum at 50 cm (0.33%). The overall trend is marked by a decrease down to 50 cm, a subsequent increase, and a slight decrease from 120 cm downwards.

The nitrogen distribution differs between the original and backfilled profiles. The original profile displays higher nitrogen contents that consistently increase with depth, reaching up to the 60 cm horizon. In contrast, the backfilled profile initially displays a low nitrogen content, subsequently leading to an increase in deeper layers. The <63 µm fraction contributes the largest share of the total nitrogen in both profiles.

5.2.1.2 Nitrogen Mass Balance

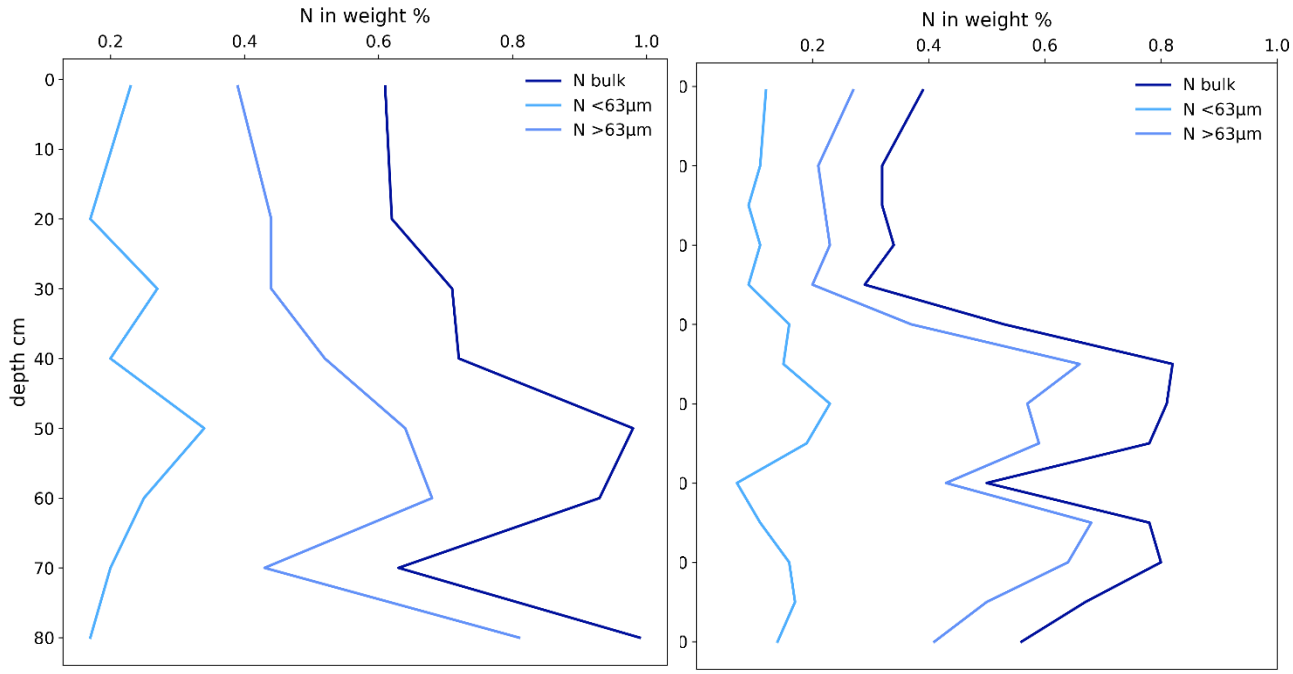

Figure 12: Nitrogen mass balance Lindergut Original (left) and Lindergut Backfilled (right)

The bulk nitrogen in the backfilled profile (see Figure 12, left) ranges from approximately 0.61% to 0.99%, with a maximum at 80 cm. The <63 µm fraction shows values between approximately 0.17% and 0.34%, whereas the >63 µm fraction exhibits higher values between approximately 0.38% and 0.81%. The content of the >63 µm fraction is consistently higher than that of the <63 µm fraction. A sharp increase in the >63 µm values at 60 cm is conspicuous and is also discernible in the bulk value. In general, the coarse fraction follows a trend roughly parallel to that of the bulk soil.

In the original soil (see Figure 12, left), the bulk values range from approximately 0.29% to 0.82%, with lower values in the topsoil. A distinct increase is observed at 60 cm. The <63 µm fraction shows values between approximately 0.07% and 0.23%, while the >63 µm fraction displays values between approximately 0.20% and 0.66%. At all depths, the content of the coarse fraction (>63 µm) is higher than that of the fine fraction (<63 µm). Notably, there are increases across all fractions in the original soil between 50 cm and 70 cm, followed by relatively high values down to 90 cm, before a decline occurs in the bulk and >63 µm fractions at 100 cm.

At all depths, the nitrogen contents of the original samples are higher than those of the backfilled samples, regardless of the fraction. The differences are particularly pronounced in the upper 50 cm, especially in the >63 µm fraction, where comparatively larger deviations occur. Below a depth of 60 cm, the differences are smaller but remain positive in all fractions. The >63 µm fraction consistently shows the highest values and the greatest absolute differences between the original and backfilled soils.

5.2.1.3 C/N

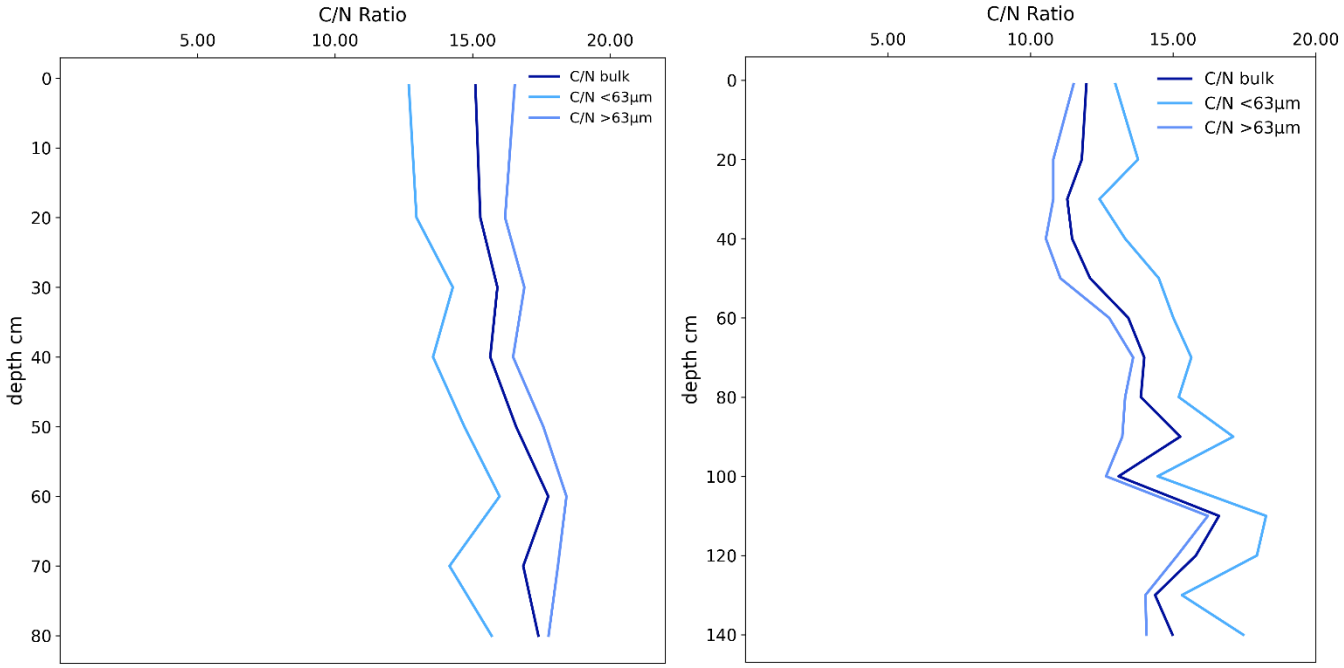

Figure 13: Carbon/Nitrogen Ratios Lindergut Original (left) and Lindergut Backfilled (right)

In the original soil (see Figure 13, left), the C/N ratios for the bulk samples range between 15.10 and 17.75, with a maximum at 60 cm. The <63 µm fraction exhibits values between 12.68 and 15.98, which are consistently below the bulk values. The >63 µm fraction shows values between 16.18 and 18.41 and lies above the bulk and the <63 µm fraction values throughout the entire profile. The spacing between the fractions is consistent across all depths, with the most significant difference between the <63 µm and >63 µm fractions occurring in the topsoil down to 20 cm and after 60 cm. From a depth of 50 cm, the values in all fractions increase slightly, followed by a decrease at 70 cm.

In the backfilled profile (see Figure 13, right), the C/N ratios of the bulk samples range between 11.29 and 15.25. The <63 µm fraction exhibits values between 12.42 and 17.11, while the >63 µm fraction has values between 10.54 and 13.60. Throughout the entire profile, the <63 µm fraction shows higher values than the >63 µm fraction. The 30–40 cm depth range displays the lowest values across all fractions. All fractions intermittently reach their maximum values at 110 cm. From 60 cm downwards, an increase is discernible in all fractions, followed by high values down to 90 cm, before the bulk and >63 µm fractions decrease again at 100 cm.

5.2.1.4 Isotopes

The isotope ratios $\delta^{13}C$ and $\delta^{15}N$ provide information about the origin and the degree of transformation of organic matter in the soil. While $\delta^{13}C$ primarily allows for conclusions about the original carbon source as well as microbial decomposition processes, $\delta^{15}N$ reflects processes within the nitrogen cycle, such as mineralization or nitrogen losses. Together, both parameters enable an assessment of the transformation and stability of organic matter along the soil profile.

5.2.1.5 $\delta^{13}C$

With increasing depth, the profiles show a more pronounced $\delta^{13}C$ depletion. This trend is discernible in both the bulk soil and the fine fraction (<63 µm). The $\delta^{13}C$ values of the <63 µm fraction are below the bulk values in both profiles. In the upper 50 cm, the original profile consistently exhibits more negative $\delta^{13}C$ values than the backfilled profile. From approximately 60 cm downwards, a distinct negative gradient is observed in both profiles, with the decline being slightly more pronounced in the backfilled profile. The original profile shows a shallower decrease with a less pronounced vertical $\delta^{13}C$ gradient. The backfilled profile displays a wider range of $\delta^{13}C$ values, particularly in the fine fraction (<63 µm).

5.2.1.6 $\delta^{15}N$

The $\delta^{15}N$ values decrease with increasing depth in both profiles, in the bulk soil as well as in the <63 µm fraction. In both cases, the lowest $\delta^{15}N$ value is measured in the respective lowermost horizon of the <63 µm fraction. In comparison, however, clear differences in the characteristics are evident: The absolute $\delta^{15}N$ values in the topsoil of the backfilled profile are significantly higher than in the original profile. For instance, the bulk value reaches 8.69‰ at a depth of 30 cm, in contrast to a maximum of 3.93‰ in the original profile. The vertical $\delta^{15}N$ gradient is also markedly more pronounced in the backfilled profile, particularly in the <63 µm fraction. In the original profile, the values decrease continuously but always remain positive. In the backfilled profile, the $\delta^{15}N$ values drop sharply from 60 cm downwards, reaching a negative value in the fine fraction at a depth of 120 cm—a phenomenon that occurs only in this fraction. The difference between the topsoil and subsoil is thus considerably more pronounced in the backfilled material than in the original soil profile.

5.2.2 Rimmerzmatt

Table 6: Rimmerzmatt Nitrogen, d13C, d15N, LOI, CaCO3 and C/N values of the different size fractions

Site	Treatment	Depth	BULK Soil						Fraction <63µm					Fraktion > 63µm		
			Tot_N	d13C	d15N	CaCO3	LOI	C/N	Tot_N	d13C	d15N	CaCO3	C/N	N	CaCO3	C/N
		cm	%	‰	‰	%	%		%	‰	‰	%		%		
Rimmerzmatt	Original	10	0.68	-26.67	5.75	5.11	21.92	11.95	0.65	-27.39	4.65	1.14	12.04	0.68	3.96	11.17
Rimmerzmatt	Original	20	0.60	-27.00	4.37	4.08	21.51	13.42	0.69	-28.41	4.96	0.87	12.89	0.59	3.20	12.75
Rimmerzmatt	Original	30	0.65	-27.35	4.00	3.79	24.49	14.15	0.62	-27.64	4.41	0.68	13.14	0.65	3.11	13.63
Rimmerzmatt	Original	40	1.67	-27.86	3.23	7.37	57.60	15.79	1.49	-28.24	3.03	0.66	17.10	1.69	6.71	15.16
Rimmerzmatt	Original	50	2.15	-27.76	1.85	10.82	74.88	16.83	1.98	-28.14	1.82	0.58	18.08	2.16	10.24	16.13
Rimmerzmatt	Original	60	2.00	-28.13	1.68	12.24	78.46	19.20	1.82	-28.34	1.51	0.81	20.22	2.01	11.43	18.38
Rimmerzmatt	Original	70	1.87	-27.73	1.27	10.02	83.30	17.75	1.99	-28.03	1.17	0.00	19.71	1.86	10.02	16.90
Rimmerzmatt	Original	80	1.26	-27.07	0.55	5.45	58.68	20.78	0.75	-27.63	-0.45	0.00	27.97	1.31	5.45	19.81
Rimmerzmatt	Original	90	0.94	-27.33	-0.45	3.48	48.78	24.95	0.64	-27.85	-0.67	0.00	25.65	0.98	3.48	24.41
Rimmerzmatt	Original	100	0.55	-27.58	0.34	1.62	28.02	23.71	0.47	-27.88	0.22	0.69	21.81	0.57	0.93	23.78
Rimmerzmatt	Original	106	0.15	-27.44	0.33	0.00	7.75	20.22	0.26	-27.63	0.73	0.00	17.96	0.13	0.00	20.67
Rimmerzmatt	Backfilled	10	0.14	-12.26	4.57	22.50	6.06	30.73	0.30	-18.59	4.56	3.62	18.31	0.12	18.88	13.78
Rimmerzmatt	Backfilled	20	0.13	-11.75	4.15	21.71	5.57	31.78	0.28	-18.35	3.86	3.53	19.15	0.11	18.18	13.44
Rimmerzmatt	Backfilled	30	0.13	-11.40	3.98	21.53	5.80	34.17	0.33	-18.62	4.24	0.85	18.47	0.11	20.68	14.24
Rimmerzmatt	Backfilled	40	0.15	-12.09	3.28	23.82	6.18	33.92	0.42	-20.00	3.93	2.09	17.16	0.11	21.73	15.75
Rimmerzmatt	Backfilled	50	0.17	-11.29	4.21	24.78	5.73	30.71	0.42	-20.14	3.81	1.65	17.33	0.14	23.12	12.83
Rimmerzmatt	Backfilled	60	0.45	-21.34	2.88	15.76	15.86	17.94	0.62	-24.00	3.63	1.00	14.62	0.43	14.75	13.89
Rimmerzmatt	Backfilled	70	1.14	-26.36	2.45	9.69	37.45	15.72	1.06	-26.74	2.28	1.06	15.88	1.15	8.63	14.75
Rimmerzmatt	Backfilled	80	1.53	-26.84	1.85	9.15	55.62	16.90	1.26	-27.21	1.77	1.18	18.49	1.54	7.98	16.21
Rimmerzmatt	Backfilled	90	1.93	-26.85	1.44	9.31	59.84	16.34	1.51	-27.28	1.47	1.16	17.26	1.94	8.15	15.80
Rimmerzmatt	Backfilled	100+	2.29	-27.52	0.60	9.60	78.92	17.96	1.58	-27.97	0.17	1.68	19.47	2.30	7.92	17.52

5.2.2.1 Nitrogen Concentration

Overall, the concentrations in the original profile are higher than in the backfilled profile. In the uppermost horizon, the bulk soil in the original profile reaches up to 2.15%, while the maximum value in the backfilled profile is 2.29%. The vertical range is greater in the backfilled profile. In the <63 µm fraction, the nitrogen content is consistently higher in both profiles than in the >63 µm fraction. The nitrogen concentrations in the fine fraction are up to 1.99% in the original profile and reach a maximum of 1.58% in the backfilled profile. The values show a slight decrease with depth, with the decline being less steep in the original profile than in the backfilled profile.

The >63 µm fraction exhibits the lowest nitrogen contents in both profiles. The vertical dispersion is considerably more pronounced in the backfilled profile. Across all sites and fractions, the original profile shows higher mean nitrogen contents and smaller vertical ranges than the backfilled profile. The backfilled profile displays highly variable nitrogen concentrations with distinct maximum and minimum values, particularly in the bulk soil and the coarse fraction (>63 µm).

5.2.2.2 Nitrogen Mass Balance

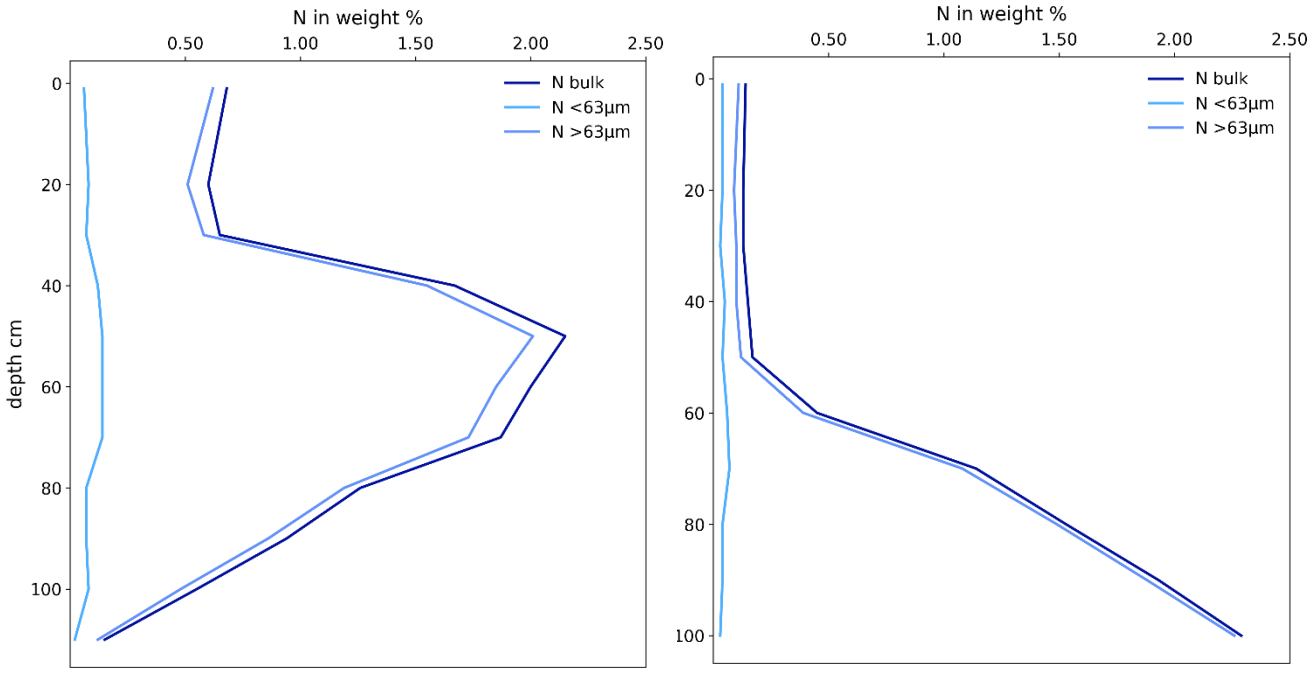

Figure 14: Nitrogen mass balance Rimmerzmatt Original (left) and Rimmerzmatt Backfilled (right)

The nitrogen contents of the bulk samples in the original profile (see Figure 14, left) range between 0.55% and 2.15%. The <63 µm fraction exhibits values between 0.06% and 0.14%. The >63 µm fraction shows values between 0.48% and 2.01%. At all depths, the >63 µm fraction is significantly higher than the <63 µm fraction and dictates the trend of the bulk values. From 40 cm downwards, the nitrogen content increases markedly in all fractions, reaching its maximum at 50 cm, followed by a decrease down to 100 cm. By comparing the bulk and the >63 µm fraction, the <63 µm fraction shows only minor absolute fluctuations. The nitrogen contents of the bulk samples in the backfilled profile (see Figure 14, right) range between 0.13% and 2.29%. The <63 µm fraction shows values between 0.028% and 0.065%, while the >63 µm fraction has values between 0.093% and 2.26%. At all depths, the >63 µm fraction is significantly higher than the <63 µm fraction and shapes the trend of the bulk values. Down to 50 cm, the contents in all fractions remain low, followed by a distinct increase from 60 cm downwards, which reaches the highest value in all fractions at 100 cm. The <63 µm fraction exhibits low absolute values and minor fluctuations throughout the entire profile.

Across the board, the original soil consistently shows a higher nitrogen content than the backfilled profile. This holds true for every depth and every soil fraction analyzed. In the upper section of the profile (1–50 cm), the differences are particularly pronounced, with the bulk and >63 µm values in the original being up to approximately 2% higher. In both datasets, the >63 µm fraction exhibits the highest contents and determines the trend of the bulk values, whereas the <63 µm fraction displays significantly lower values. The depth profiles differ in the original, maxima already occur at 50 cm, followed by a decline down to 100 cm; in the backfilled dataset, the values continuously increase from 60 cm down to 100 cm. The <63 µm fraction shows only minor absolute fluctuations in both profiles but remains lower throughout the entire profile in the backfilled dataset.

5.2.2.3 C/N

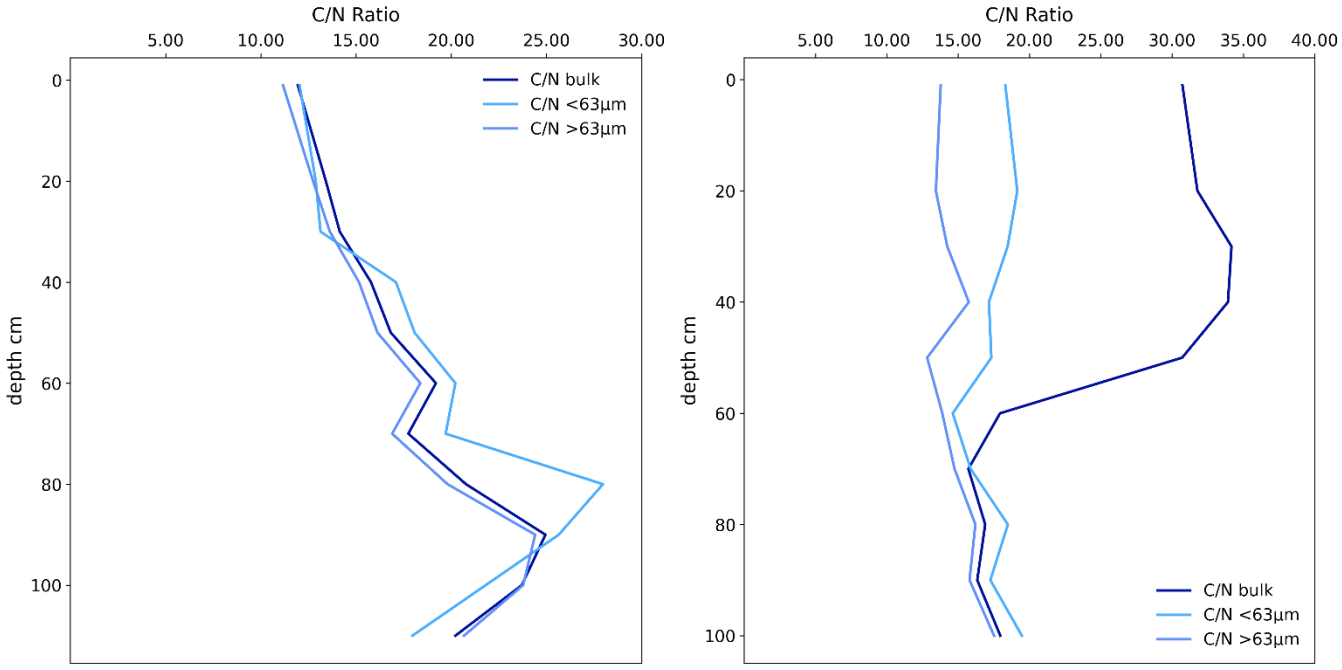

Figure 15: Carbon/Nitrogen Ratio Rimmerzmatt Original (left) and Rimmerzmatt Backfilled (right)

The C/N ratios of the bulk samples in the original profile (see Figure 15, left) range between 11.95 and 24.95. For further information see Appendix 9.2. The <63 µm fraction shows values from 12.04 to 27.97, and the >63 µm fraction from 11.17 to 24.41. From 30 cm downwards, the values in all fractions increase, with a distinct maximum between 80 cm and 90 cm. In the upper 20 cm, the values of the <63 µm fraction are close to or slightly above the bulk values, whereas the >63 µm fraction is lower in that range. From 40 cm downwards, the <63 µm fraction is predominantly the group with the highest values among the fractions, especially with a pronounced peak at 80 cm. The >63 µm fraction runs below the bulk and <63 µm values at all depths.

The C/N ratios of the bulk samples in the backfilled profile range between 15.72 and 34.17. The <63 µm fraction exhibits values between 14.62 and 19.47, while the >63 µm fraction has values between 12.83 and 17.52. In the upper 50 cm, the bulk values are significantly higher than the fraction values, with a pronounced maximum between 20 cm and 40 cm. From 60 cm downwards, the values of the three fractions converge, with the <63 µm fraction remaining predominantly slightly above the >63 µm fraction. A conspicuous feature is the sharp drop in the bulk values from 40 cm to 60 cm, whereas the fine and coarse fractions decrease only moderately. In the lower 40 cm, all three fractions run more closely to one another.

In both datasets, all fractions show an increase in C/N values with depth into the middle to lower regions of the profile. In the upper 50 cm, the values in the backfilled dataset are higher across all fractions than those in the original dataset, with this difference being significantly more pronounced in the bulk and <63 µm fractions than in the >63 µm fraction. Below 60 cm, the values of both datasets run largely parallel, with minor differences. The ranking of the fractions is maintained in both datasets: the <63 µm fraction is predominantly higher than the >63 µm fraction, and the bulk assumes an intermediate position, although it deviates in the upper layers of the backfilled profile due to high absolute values.

5.2.2.4 $\delta^{13}C$

In both profiles, the $\delta^{13}C$ values of the <63 µm fraction are consistently more negative than in the bulk soil. In the original profile, the mean value in the bulk is -27.45‰, while in the fine fraction, it is -27.64‰. In the backfilled profile, the mean $\delta^{13}C$ value in the bulk is -18.77‰, whereas in the <63 µm fraction, it is -19.08‰. The difference between the fractions remains small in both profiles, yet it is systematically negative. The range of the values is significantly wider in the backfilled profile than in the original profile.

In the backfilled profile, the vertical trend shows a pronounced increase in $\delta^{13}C$ values with decreasing depth. In the original profile, the vertical change is more gradual, with a smaller range. The differences between the bulk and the fine fraction remain constant with depth, at a similar, negative level.

5.2.2.5 $\delta^{15}N$

In the backfilled profile, the maximum $\delta^{15}N$ value is 4.56‰ in the fine fraction and 5.86‰ in the bulk. In the original profile, $\delta^{15}N$ reaches a maximum of 4.96‰ in the fine fraction and 4.37‰ in the bulk. In both profiles, the vertical decline of $\delta^{15}N$ values is more pronounced in the <63 µm fraction than in the bulk. The minimum values in both cases occur in the fine fraction: -0.67‰ in the original profile and 0.17‰ in the backfilled profile. The median is higher in the backfilled profile (3.72‰) than in the original profile (1.51‰). The vertical gradient is steeper in the backfilled profile, especially in the fine fraction, whereas the original profile shows more gradual and uniform trends. The difference between the bulk and the <63 µm fraction remains inconsistent with depth and varies between the profiles.

5.2.3 Underi Site

Table 7: Underi Site Nitrogen, d13C, d15N, LOI, CaCO3 and C/N values of the different size fractions

Site	Treatment	Depth	BULK Soil						Fraction <63µm					Fraktion > 63µm		
			N	d13C	d15N	CaCO3	LOI	C/N	N	d13C	d15N	CaCO3	C/N	N	CaCO3	C/N
		cm	%	‰	‰	%	%		%	‰	‰	%		%	%	
Underi Site	Original	10	1.22	-27.43	5.54	0.82	32.03	12.10	0.93	-27.20	2.41	0.82	13.88	1.27	0.00	11.86
Underi Site	Original	20	1.21	-27.35	5.53	0.47	32.41	12.10	0.93	-27.26	2.34	0.47	13.86	1.27	0.00	11.82
Underi Site	Original	30	1.15	-27.37	5.21	1.20	31.18	12.19	0.94	-27.21	2.33	1.20	13.94	1.23	0.00	11.67
Underi Site	Original	40	1.17	-27.40	5.42	1.41	31.59	12.06	0.94	-27.17	2.60	1.41	13.64	1.22	0.00	11.84
Underi Site	Original	50	1.19	-27.68	5.19	0.00	32.26	12.05	0.95	-27.46	2.93	0.00	13.05	1.30	0.00	11.71
Underi Site	Original	60	2.13	-27.61	3.87	0.06	52.82	12.40	1.60	-27.84	1.18	0.06	14.16	2.34	0.00	11.93
Underi Site	Original	70	1.10	-27.60	4.08	0.00	29.82	11.81	0.83	-27.54	0.57	0.00	13.79	1.19	0.00	11.35
Underi Site	Original	80	0.35	-27.80	6.03	0.00	10.40	11.02	0.31	-27.57	1.20	0.00	13.25	0.37	0.00	10.22
Underi Site	Original	90	0.11	-10.14	9.54	18.18	4.49	32.48	0.11	-10.04	1.30	8.53	41.02	0.11	9.65	13.77
Underi Site	Original	100	0.05	-4.68	10.20	28.98	2.77	92.63	0.07	-4.79	1.61	11.97	77.87	0.04	17.01	25.18
Underi Site	Original	106	0.06	-4.90	10.36	28.44	3.18	91.31	0.05	-4.54	1.79	13.19	129.49	0.06	15.25	35.33
Underi Site	Backfilled	10	0.17	-16.63	11.64	9.51	6.17	16.37	0.15	-15.95	4.26	3.58	21.16	0.18	5.92	7.80
Underi Site	Backfilled	20	0.14	-15.80	11.37	10.63	5.98	17.71	0.13	-15.49	3.69	4.76	23.17	0.14	5.87	6.98
Underi Site	Backfilled	30	0.13	-14.18	11.23	11.36	5.56	20.26	0.10	-13.72	4.02	5.06	26.68	0.16	6.30	9.18
Underi Site	Backfilled	40	0.15	-13.82	10.60	13.48	6.10	21.55	0.11	-12.61	3.49	4.14	30.80	0.16	9.33	9.03
Underi Site	Backfilled	50	0.43	-23.41	8.19	7.24	12.74	13.19	0.38	-23.02	3.22	2.75	15.88	0.45	4.50	10.23
Underi Site	Backfilled	60	0.57	-26.00	7.02	2.76	15.85	12.38	0.63	-26.44	3.02	-0.39	13.65	0.56	3.15	11.27
Underi Site	Backfilled	70	0.57	-25.77	7.45	3.66	15.63	12.33	0.63	-26.49	3.09	0.18	13.54	0.56	3.47	11.10
Underi Site	Backfilled	80	0.58	-26.03	6.73	3.21	16.38	12.36	0.60	-26.45	2.94	0.62	13.82	0.57	2.59	10.84
Underi Site	Backfilled	90	0.61	-27.17	5.88	0.82	17.77	12.26	0.61	-27.30	2.65	0.32	13.40	0.61	0.50	11.36
Underi Site	Backfilled	100	0.71	-27.46	5.55	0.30	22.24	12.17	0.48	-27.34	2.63	0.03	12.76	0.83	0.27	11.93
Underi Site	Backfilled	108.5	0.88	-27.78	4.61	0.00	28.21	13.28	0.56	-27.60	1.52	0.00	15.18	1.01	0.00	12.84

5.2.3.1 Nitrogen Concentration

In the original profile, the nitrogen content in the bulk soil decreases with increasing depth, apart from an intermediate peak at 60 cm, and it reaches its lowest value in the subsoil. This vertical decrease in the original soil is also present in both fractions. In the backfilled soil, the opposite trend is observed; here, the nitrogen content in the bulk soil tends to increase with depth, reaching its maximum at 108.5 cm. This trend is also observed in the coarse and fine fractions of the backfilled profile, with rather low contents in the topsoil and higher contents in the subsoil.

Across all fractions, the nitrogen content in the original profile is higher and more dispersed than in the backfilled profile. The vertical range in every fraction of the original profile is wider, particularly in the >63 µm fraction. The backfilled profile, in contrast, shows more homogeneous values with less variation with depth and lower values in the topsoil.

5.2.3.2 Nitrogen Mass Balance

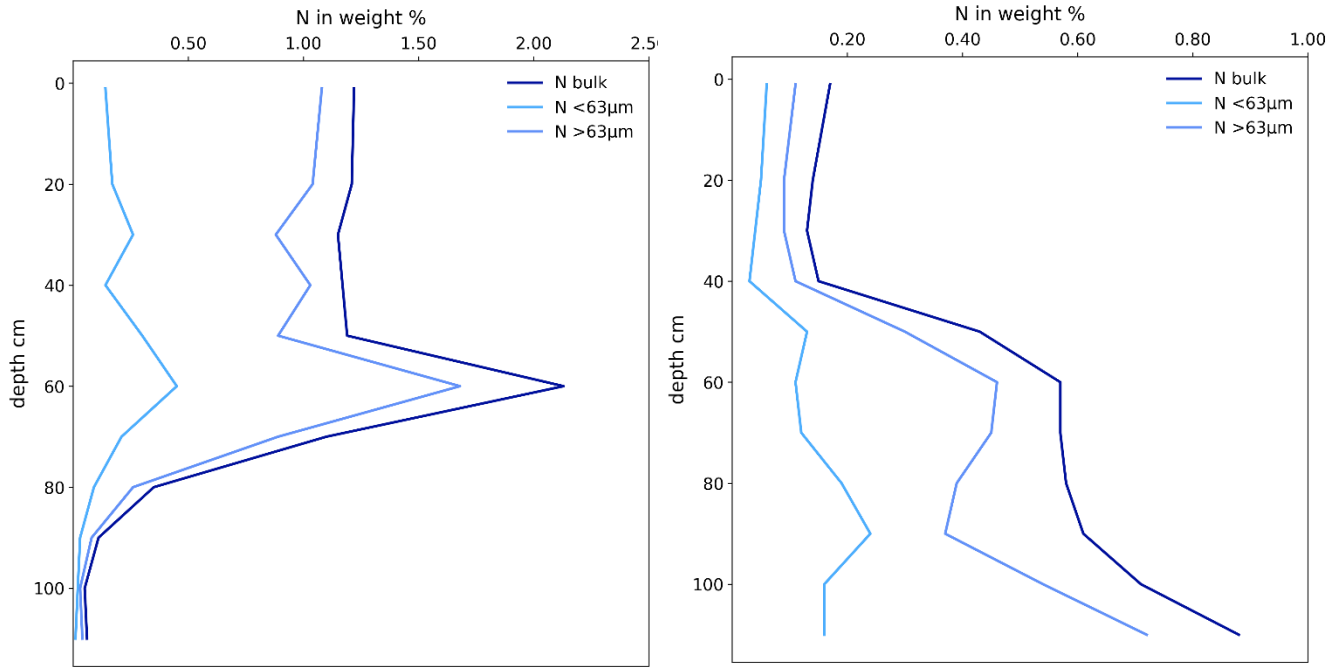

Figure 16: Nitrogen mass balance Underi Site Original (left) and Underi Site Backfilled (right)

The nitrogen contents of the bulk samples in the original soil (see Figure 16, left) range between 0.045% and 2.13%. The <63 µm fraction shows values between 0.019% and 0.454%, while the >63 µm fraction has values between 0.026% and 1.68%. At all depths, the >63 µm fraction exhibits higher values than the <63 µm fraction. Between 1 cm and 50 cm, the bulk values remain relatively constant at around 1.15–1.22%, followed by a distinct increase to the maximum at 60 cm. From 70 cm downwards, the contents in all fractions drop sharply, with very low values below 80 cm. Below 80 cm, almost all lines have congruently converged. Throughout the entire profile, a large numerical discrepancy between the fine and coarse fractions is always discernible.

The nitrogen contents of the bulk samples in the backfilled soil (see Figure 16, left) range between 0.134% and 0.706%. The <63 µm fraction shows values between 0.033% and 0.240%, while the >63 µm fraction has values between 0.090% and 0.542%. At all depths, the values of the >63 µm fraction are higher than those of the <63 µm fraction. Between 1 cm and 40 cm, the contents in all fractions remain low, followed by an increase from 50 cm downwards, which continues to 100 cm in the >63 µm fraction and the bulk. The <63 µm fraction shows its highest value at 90 cm.

Throughout the entire profile, the nitrogen contents in the original profile are higher in all fractions than those of the backfilled profile. The difference is particularly pronounced in the upper profile section (1–50 cm), where the bulk values in the original are above 1%, while in

the backfilled profile, they are below 0.45%. In the original, the bulk maximum of 2.13% is reached at 60 cm, whereas in the backfilled profile, the maximum is 0.71% at 100 cm. In both datasets, the >63 µm fraction shows higher values than the <63 µm fraction at all depths. In the original dataset, the highest values in all fractions occur at 60 cm, followed by a decrease down to 100 cm. In contrast, in the backfilled dataset, the values continuously increase from 50 cm downwards and only reach their maxima at the end of the profile. The <63 µm fraction shows minor absolute fluctuations in both datasets but remains significantly lower across all depths in the backfilled dataset.

5.2.3.3 C/N

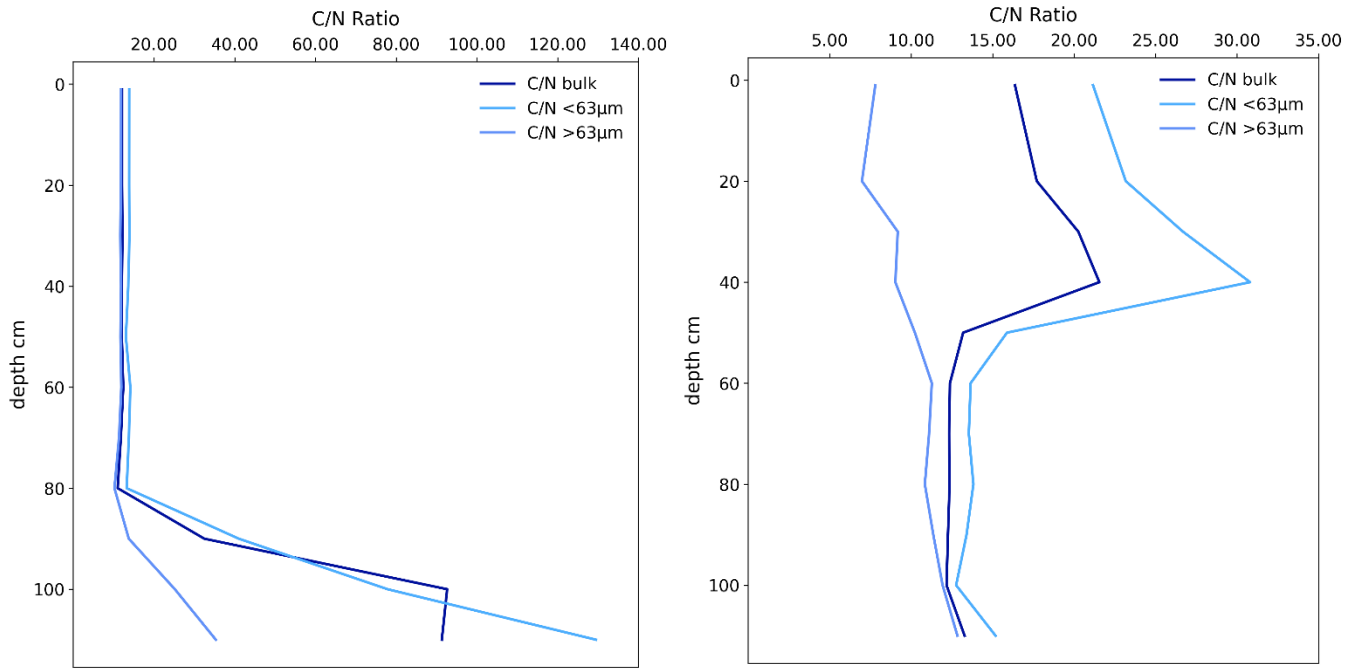

Figure 17: Carbon/Nitrogen Ratio Underi Site Original (left) and Underi Site Backfilled (right)

The C/N ratios of the bulk samples range between 11.02 (at 80 cm) and 92.63 (at 100 cm). The <63 µm fraction shows values between 13.05 (at 50 cm) and 77.87 (at 100 cm), while the >63 µm fraction has values between 10.22 (at 80 cm) and 25.18 (at 100 cm). In the upper 80 cm, the values of the <63 µm fraction are higher at all depths than those of the bulk and the >63 µm fraction, whereas the >63 µm fraction consistently exhibits the lowest values. From 90 cm downwards, very sharp increases occur in all fractions, which are particularly pronounced in the bulk and the <63 µm fraction. Down to 80 cm, the values in all fractions are relatively constant, with minor fluctuations.

The C/N ratios of the bulk samples range between 12.17 (at 100 cm) and 21.55 (at 40 cm). The <63 µm fraction shows values between 12.76 (at 100 cm) and 30.80 (at 40 cm), while the >63

µm fraction has values between 6.98 (at 20 cm) and 11.93 (at 100 cm). At all depths, the <63 µm fraction is higher than the >63 µm fraction, often by a significant margin. In the upper 40 cm, the values in the bulk and the <63 µm fraction are considerably higher than in the deeper sections of the profile. From 50 cm downwards, the values in all fractions remain relatively constant, without pronounced maxima or minima.

In the upper profile section (1–80 cm), the C/N ratios in the backfilled dataset for the bulk and <63 µm fraction are higher than those of the original dataset, whereas the >63 µm fraction consistently shows lower values. From 90 cm downwards, the original dataset exhibits very sharp increases in all fractions, with maxima of 92.63 (bulk) and 77.87 (<63 µm) at 100 cm, which do not occur in the backfilled dataset. In the backfilled dataset, the values from 50 cm downwards run largely constant across all fractions. In contrast, the original dataset shows only minor changes in this range, followed by a sudden increase at the end of the profile.

The ranking of the fractions differs: in the original, the <63 µm values are higher than the bulk and >63 µm values down to 80 cm. In the backfilled profile, the ranking is identical, but the distances between the <63 µm and >63 µm fractions are very close in the upper 40 cm and only begin to diverge after that point. In the original soil, a greater distance between the fractions is already evident in the topsoil.

5.2.3.4 $\delta^{13}C$

In both profiles, the fine (<63 µm) fraction exhibits values and a depth profile that are almost congruent with those of the bulk soil. The vertical range of the $\delta^{13}C$ values is wider in the original profile; particularly in the subsoil, almost positive values are observed, including in the fine fraction. In the backfilled profile, the dispersion is narrower, reaching a minimum of -13.82‰. In general, a trend is discernible where the $\delta^{13}C$ values become more positive with increasing depth in the original profile, while in the backfilled profile, they become more negative with increasing depth.

5.2.3.5 $\delta^{15}N$

In both profiles, the $\delta^{15}N$ values in the <63 µm fraction are consistently below the respective bulk values. In the original profile, the mean value is 6.45‰ in the bulk and 1.84‰ in the fine fraction. In the backfilled profile, the mean value is 8.21‰ in the bulk and 3.14‰ in the fine fraction.

In both profiles, the vertical decrease of $\delta^{15}N$ values with increasing depth is pronounced in the <63 µm fraction. The minimum values are reached in the deepest layers of the <63 µm fraction in each case (Original: 0.57‰; Backfilled: 1.52‰).

The vertical gradient is more pronounced in the backfilled profile, with a higher initial value in the topsoil and a distinct decrease with depth. In the original profile, the decline of $\delta^{15}N$ values in the fine fraction is more gradual and uniform. The absolute range is wider in the backfilled profile. Similarly, the distribution of values differs when comparing the original profile to the backfilled profile. In the original bulk soil, there are low values at the top that increase with depth. In the backfilled bulk soil, the opposite is discernible: high values are present in the topsoil down to a depth of 40 cm, followed by a rapid and sharp decrease to 0‰ in the deepest horizon.

5.3 pH-Values

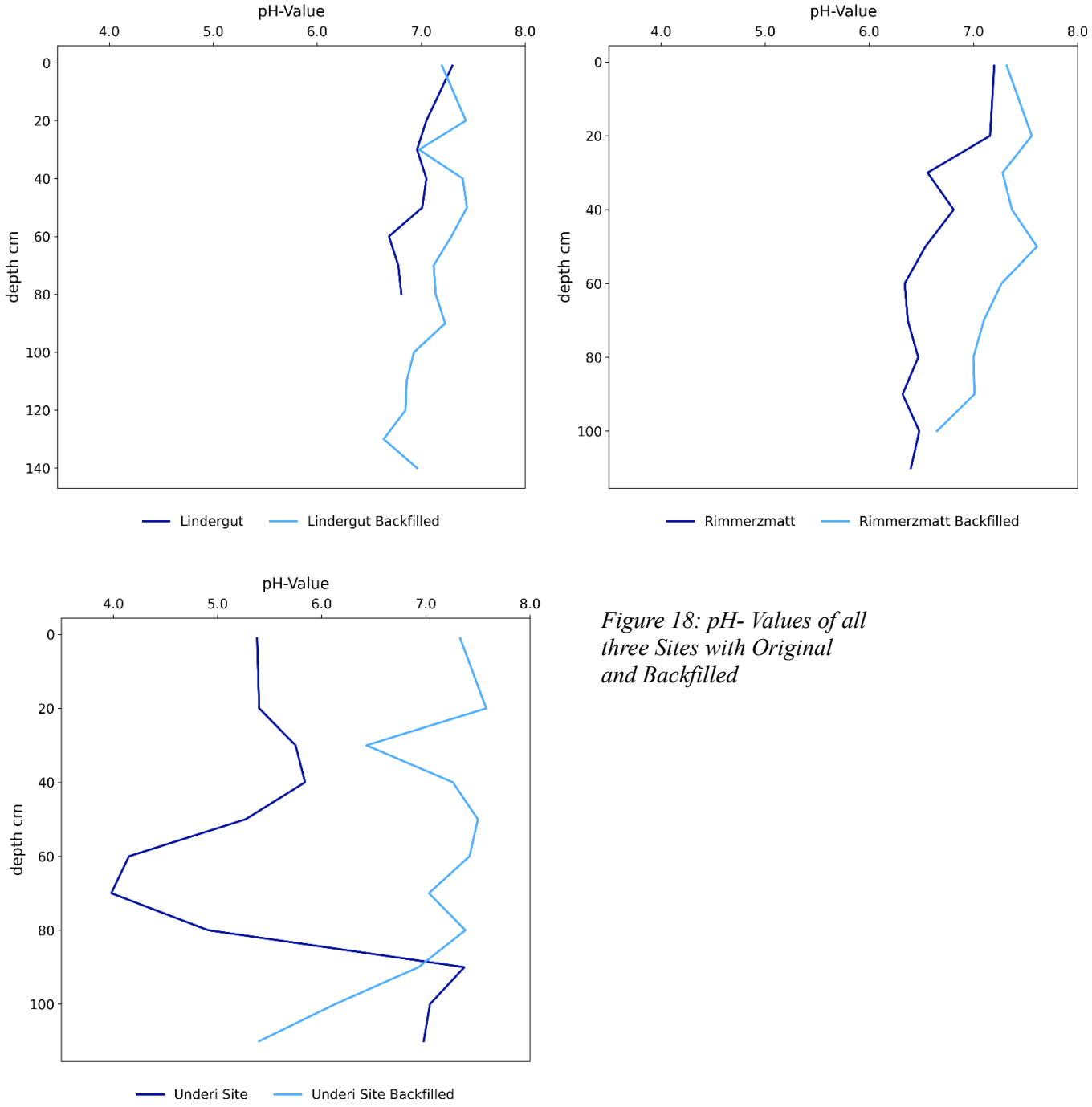

Figure 18: pH- Values of all three Sites with Original and Backfilled

5.3.1 Lindergut

At the Lindergut site (see Figure 18, top left), the pH values in the original soil range between pH 6.69 and pH 7.30, and in the backfilled soil between pH 6.64 and pH 7.44. Both soil profiles thus exhibit predominantly neutral to slightly alkaline conditions. In the vertical profile, both variants show a trend of decreasing pH values with increasing depth, with the values developing from more alkaline ranges in the topsoil towards neutral to slightly alkaline conditions in the subsoil. This pattern suggests a limited depth of acidification and possible buffering by carbonate or base-rich materials in the topsoil.

5.3.2 Rimmerzmatt

At the Rimmerzmatt site (see Figure 18, top right), the pH values in the original soil range from pH 6.32 to pH 7.20, and in the backfilled soil from pH 6.65 to pH 7.61. Both profiles thus exhibit overall neutral to slightly alkaline conditions, with a clear tendency towards alkaline conditions in the topsoil. With increasing depth, both profiles show a decreasing trend in pH values, so that less alkaline or nearly neutral conditions prevail in deeper horizons. This pattern suggests a base-rich surface layer and, concurrently, a decreasing buffer capacity or carbonate content in deeper soil layers.

5.3.3 Underi Site

At the Underi site (see Figure 18, bottom left), the pH values in the original soil show a strongly fluctuating pattern with values between pH 3.98 and pH 7.37, while the backfilled soil exhibits values between pH 5.40 and pH 7.58. In the original soil, the pH in the topsoil is initially in the slightly acidic range around pH 5.5, but it drops with increasing depth to a strongly acidic pH of 3.98 at 70 cm. In the deeper section of the profile, the pH value abruptly rises again, reaching a distinctly alkaline value of pH 7.37 at a depth of approximately 110 cm.

In contrast, the backfilled profile shows a more stable development: down to a depth of about 90 cm, consistently alkaline conditions prevail, followed by a significant decrease to a moderately acidic pH of 5.40 in the lowermost horizons.

Thus, the original profile displays a pronounced pH stratification, whereas the backfilled profile is characterized by a more uniform, generally alkaline pH distribution with an acidic influence that only begins at a greater depth.

5.4 Loss on Ignition (LOI)

The LOI (Loss on Ignition) method is used to determine the organic matter content of a sample. The mass lost between the pre- and post-weighing corresponds to the proportion of organic substance (as a % of the dry mass). Further information can be found in Chapter 4.3.7.

5.4.1 Lindergut

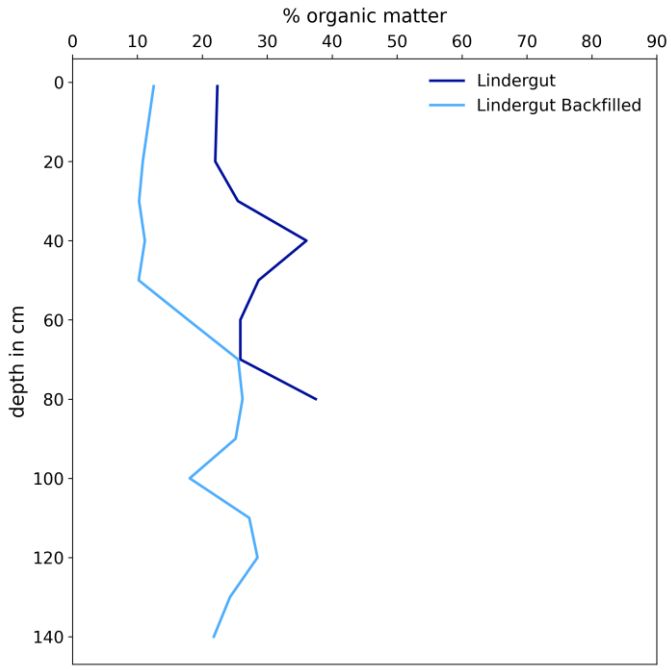

Figure 19: organic matter content % Lindergut

The original profile, as depicted in Figure 19, displays values ranging from 22.00% to 37.48%, with the highest plateau situated between 40 cm and 50 cm. In the original soil, the values range between 22.00% (at 20 cm) and 37.48% (at 80 cm). The upper section of the profile (1–30 cm) shows constant values around 22–25%. From 40 cm downwards, the organic matter content increases significantly, reaching a maximum of over 35% between 40 cm and 50 cm. This is followed by a slight decrease at 60 cm (28.68%) and a renewed increase to the maximum at 80 cm.

In the backfilled profile, the values range between 10.21% and 28.51%. The uppermost 50 cm show little variation, with values around 10–12%. From 60 cm downwards, a distinct increase is discernible, which reaches its maximum of around 25–26% at 70–80 cm. Subsequently, the values fluctuate in the range of 18–28% without a clear depth maximum.

When comparing the two profiles, the original soil consistently contains significantly more organic matter at all depths. This difference is especially pronounced in the topsoil (0–50 cm), where the original soil's organic matter content exceeds that of the backfilled profile by as much as 25 percentage points. The original profile is characterized by a clear increase and a high plateau in the middle section, whereas the backfilled profile exhibits a more gradual, delayed increase with an overall lower maximum value.

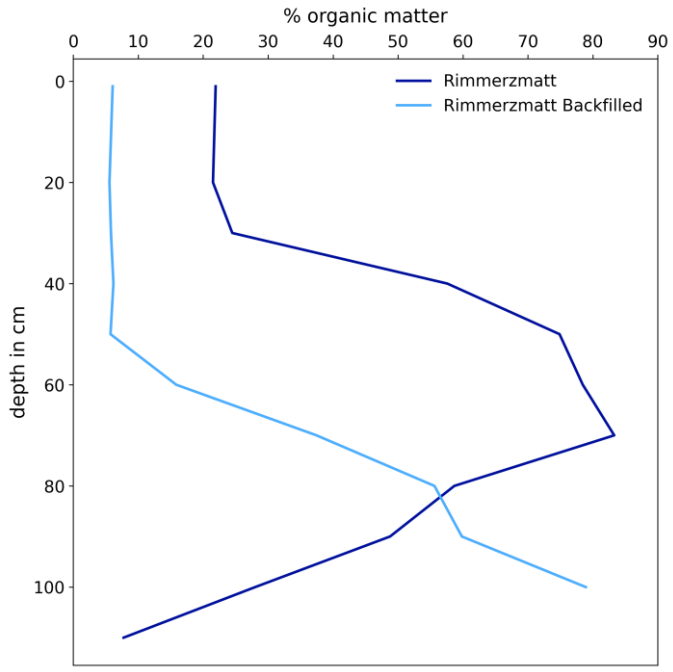

Figure 20: organic matter content % Rimmerzmatt

5.4.2 Rimmerzmatt

Original profile (see Figure 20): Values range from 21.51% to 83.30%, showing a distinct increase starting at 40 cm, peaking in the 60–70 cm range, and maintaining a high level down to a depth of 90 cm. Backfilled profile: Shows values between 5.57% and 78.92%, with a sharply pronounced increase from 50 cm; from 70 cm downwards, the values are similarly high as in the original. Comparison: In the upper section of the profile, there are substantial differences (up to ~52 percentage points); from 70 cm downwards, the values converge.

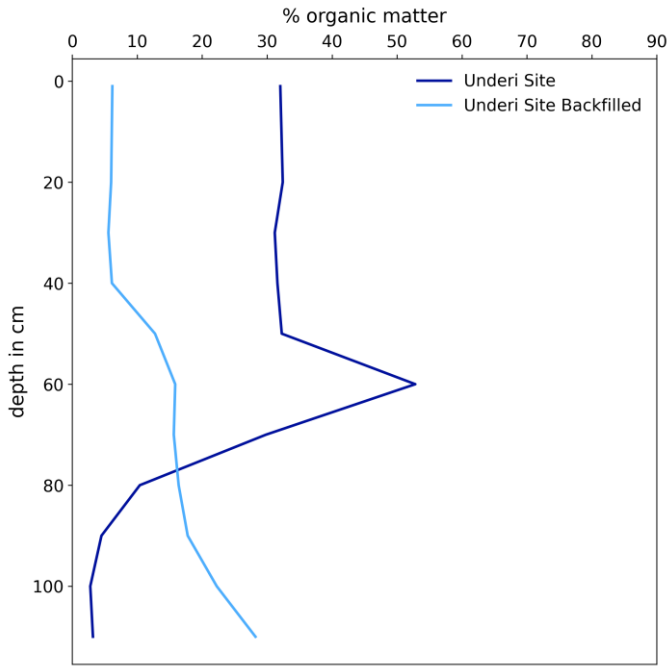

Figure 21: organic matter content % Underi Site

5.4.3 Underi Site

In the original profile (see Figure 21), values range between 2.77% and 52.82%, with high values down to 60 cm, followed by a distinct drop towards the end of the profile. In the backfilled profile, values range between 5.56% and 28.21%; the organic matter content is consistently lower than in the original profile, with the smallest differences found in the lower section of the profile (Lal et al., 1995). The values for the original soil are significantly higher down to a depth of 60 cm. The backfilled profile shows a lower overall proportion of organic matter but, in turn, less variation with depth.

When comparing the results from all sites, Rimmerzmatt exhibits the highest organic matter values in the entire profile, particularly in the middle section. Lindergut is in the middle range, showing a strong contrast between its original and backfilled profiles. The Underi Site displays the lowest maxima in its backfilled dataset and the sharpest relative decline in values in the lower profile. At all sites, the values from the original profiles are higher than those from the backfilled profiles, with the largest absolute differences occurring in the upper sections of the profiles.

.

5.5 Weathering Indices

5.5.1 (Na+K)/Ti

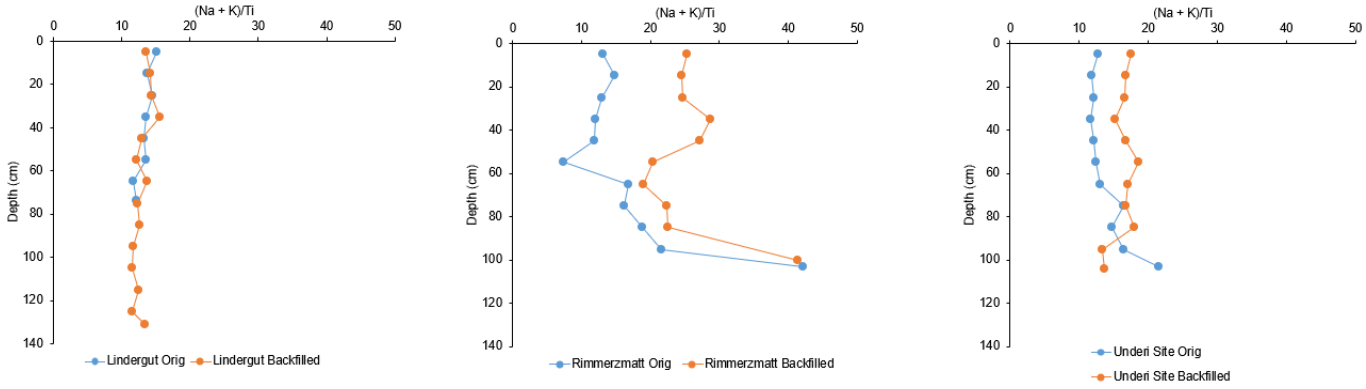

Figure 22: (Na+K)/Ti Index: Lindergut, Rimmerzmatt, Underi Site

When comparing the Na+K/Ti ratios of the three study sites, clear differences in the distribution patterns become apparent.

The Lindergut site (see Figure 22, left) is characterized by generally low values that exhibit only minor fluctuations down to a depth of 130 cm. Furthermore, it is notable that the values for the original and backfilled profiles run almost congruently throughout the entire profile.

In contrast, the Rimmerzmatte site (see Figure 22, middle) shows a distinctly contrasting pattern: On the one hand, clear differences between the original and the backfilled data are discernible, particularly in the topsoil. Interestingly, the pattern shifts below about 60 cm, where the Na+K/Ti ratios for both profiles begin to run parallel and increase. This rise in the ratio is a clear indicator of less intense chemical weathering in the deeper soil horizons.

The profile of the Underi Site (see Figure 22, right) also shows clear differences between the original and backfilled values down to a depth of 80 cm. Below this depth, however, the trends of the profiles diverge significantly, with the original data exhibiting higher Na+K/Ti values than the backfilled data.

5.5.2 Chemical Index of Alteration (CIA)

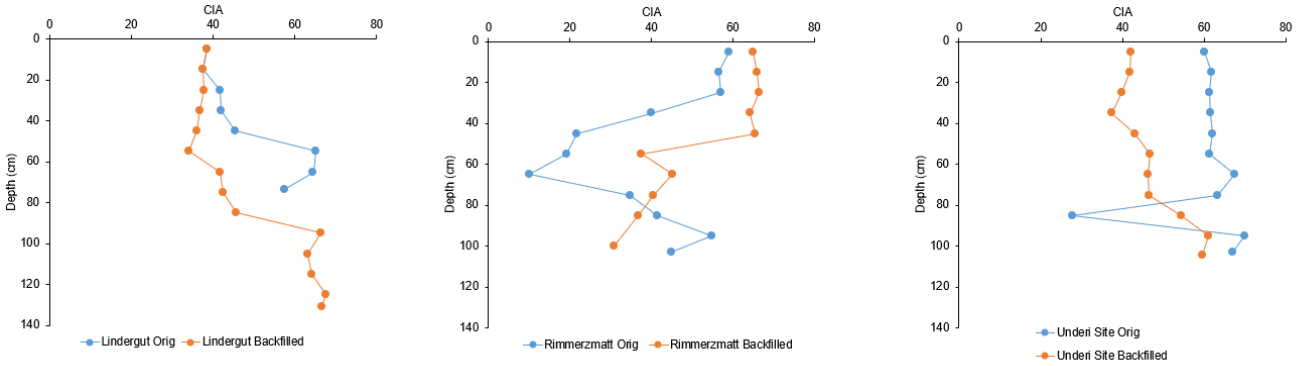

Figure 23: Chemical Index of Alteration (CIA): Lindergut, Rimmerzmatt, Underi Site

Across all study sites, the lines in the topsoil sometimes run close together or a temporary parallelism is discernible. With increasing depth, the divergence increases, and the curves occasionally intersect.

At the Lindergut site, the original soil exhibits higher CIA values throughout the entire depth range. From the surface down to approximately 60 cm, both lines follow a similar trend; subsequently, they diverge more significantly. While the original soil varies moderately, the backfilled sample shows an increase in weathering and reaches its highest values between approximately 90 and 130 cm.

For Rimmerzmatt, both curves show the highest overall weathering levels of the three sites. In the upper 0–40 cm range, the trends are close together. Below approximately 60–70 cm, the CIA values for the original soil increase. The backfilled sample follows the same trend but exhibits lower values at depth than the original soil.

At the Underi Site, a greater divergence between the curves is observed in the topsoil compared to the other two study sites. Between approximately 70 and 90 cm, the curves intersect. The original soil shows a clear minimum at a depth of 80 centimeters, whereas the backfilled soil has its minimum at a depth of 40 cm.

In summary, the trends of the two series at each site are similar in the topsoil, whereas clear and site-specific differences occur at depth. Rimmerzmatt shows the highest CIA values; at Lindergut, the original values are consistently higher than the backfilled values, and at the Underi Site, the original series predominates with a distinct intersection in the middle depth range.

5.5.3 Primitive Mantle Ratio

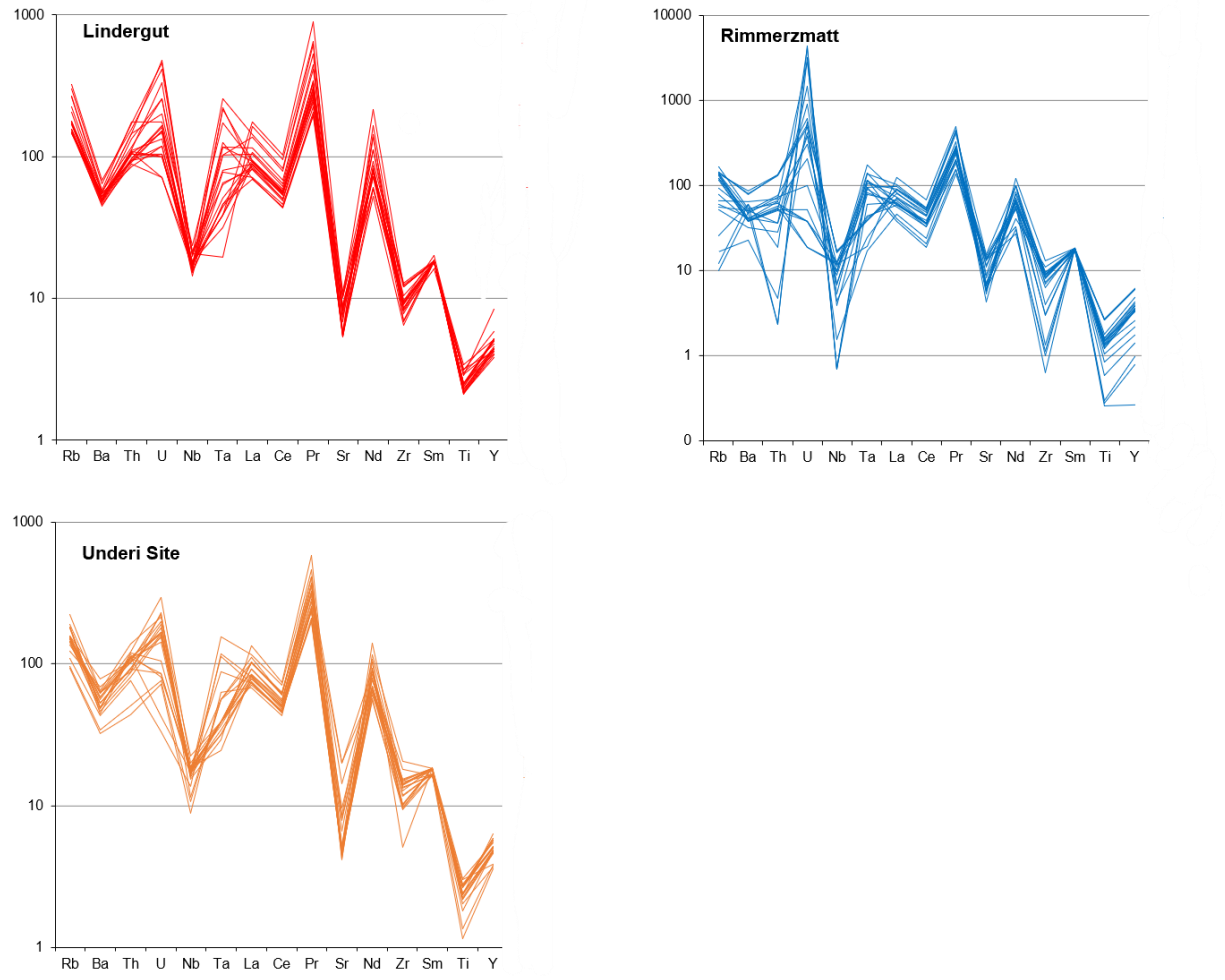

Figure 24: Primitive Mantle Ratios: Lindergut, Rimmerzmatt, Underi Site

The normalization of trace element concentrations was performed based on the primitive mantle values according to (Sun & McDonough, 1989). Figure 24 shows the mean concentration ratios of the investigated soil profiles in comparison to these reference values. The Lindergut (see Figure 24, top left) and Underi Site (see Figure 24, bottom left) locations show nearly identical distribution patterns with pronounced peaks for uranium (U), praseodymium (Pr), and zirconium (Zr); deviations within the profile are minor. In contrast, the Rimmerzmatt profile (see Figure 24, top right) exhibits greater variability with depth as well as individual outliers. While Pr shows the strongest enrichment in all profiles, at Rimmerzmatt the maximum occurs for uranium; at the same time, the Nb contents there are lower. Titanium (Ti) is almost non-detectable in all profiles, which is characteristic of organic peat soils. Overall, similar patterns of enrichment and leaching at all sites indicate that the backfill material is geologically closely related to the autochthonous soil and most likely originates from the immediate regional vicinity.

6 Discussion

6.1 The Altered Soil Profile

The most immediate and consistent effect of anthropogenic fill observed at all three study sites is a fundamental change in the soil profile. This raises the question whether the soils studied can still be defined as pure Histosols at all due to past human intervention.. A Technosol seems rather unlikely due to the absence of clearly recognizable artifacts in the soil. According to IUSS Working Group WRB (2022), the filling transforms the degraded peat soil into an Anthrosol, characterized by a buried organic horizon and resulting in a geochemically inverted profile in which a low-carbon mineral layer overlies a high-carbon organic layer. IUSS Working Group WRB (2022) requires an additional condition for classifying an Anthrosol, namly a history of long and intensive agricultural use. Both WRB criteria apply to the three profiles investigated in this study, which would therefore be classified as Anthrosol. The physical redistribution is reflected in markedly lower concentrations of Soil Organic Carbon (SOC) in the upper 30–50 cm of all backfilled profiles compared to their original counterparts. At the same time, the depth of the SOC maximum is significantly displaced downward: at Lindergut it shifts from 50–60 cm to 70–80 cm, while at both Rimmerzmatt and Underi Site the maximum moves from about 60 cm to near 100 cm.

In response to the first research question the primary effect of the filling is the creation of an Anthrosol that physically covers the original peat horizon. This leads to a distinct vertical decoupling of the new agricultural topsoil from the relict organic horizon below, evident not only in the inverted carbon profile but also in clear changes in biogeochemical indicators such as C/N ratios and stable isotope signatures.

In response to the second research question: the dominant carbon-stabilization mechanism differs fundamentally between these two layers. For the old, buried carbon, which resides in the coarse, chemically labile fraction of POM, preservation is achieved not through chemical alteration but through physical protection, by limiting oxygen supply (Limpens et al., 2008). In contrast, the new mineral topsoil shows evidence of a different process; the generally higher relative proportion of carbon in the fine <63 µm fraction suggests a shift toward the more stable MAOM pathway. Although this mechanism remains a hypothesis pending further methodological refinement, it indicates that the filling could provide the necessary mineral matrix for new, long-term carbon stabilization.

6.2 Carbon Stabilization Mechanisms and the POM Paradox

While the vertical redistribution of carbon is a clear physical consequence of the embankment, the more critical question concerns the stability of this buried carbon. The results reveal an apparent paradox: in the buried peat layers of the backfilled profiles, most of the organic carbon is stored in the coarse >63 µm fraction (see Figures 9, 10, and 11). According to the modern functional framework of SOM, this coarse fraction is analogous to POM (Wander, 2004). This POM pool is considered the labile and active fraction, consisting of less decomposed plant residues that are more easily accessible to microbes and are primarily responsible for short-term nutrient cycling (von Lützow et al., 2007).

This raises the central question of why a supposedly labile carbon pool is being preserved at depth. The most plausible explanation is that the physical protection provided by the embankment material overrides the inherent chemical lability of POM. Acting as a physical barrier, the embankment reduces oxygen diffusion and re-establishes anoxic or semi-anoxic conditions that inhibit microbial decomposition (Limpens et al., 2008).

This indication of physical protection provides a crucial stock-based mechanism that could explain the seemingly contradictory results of recent flux-based studies at similar sites. The findings of this study suggest that the embankment creates a dual system: it physically buries and protects the old, POM-dominated peat, while a new, biologically active topsoil forms at the surface.

This interpretation is supported by the work of Wang et al. (2021), who used radiocarbon analysis to show that CO_2 respired from a mineral-covered peatland originated less from old peat and more from new carbon. The finding of a physically buried POM layer in the present study provides direct physical evidence for this observed source shift. Furthermore, these results explain the findings of Paul et al. (2024), who determined that a embankments did not significantly reduce total CO_2 emissions. The continued emissions likely originate from the new, tilled Ap horizon forming on the embankment, which receives fresh carbon inputs from crop residues, rather than from the protected peat below. Considering that the study sites are still under active agricultural management, Bader et al. (2018) note that around 20% of the organic material can derive from crop residues. These residues could further promote decomposition in a managed topsoil.

In contrast to the physical preservation of old peat at depth, the addition of the embankment is likely to introduce a new dynamic of carbon stabilization in the developing topsoil. A key

finding is as follows: backfilled soils tend to show a higher relative proportion of organic carbon in the fine <63 µm fraction. This suggests that the addition of mineral material promotes a shift away from a POM-dominated system toward one in which the MAOM stabilization pathway is strengthened. This finding is consistent with Kalisz & Urbanowicz (2021), who reported that light siltation can have a protective effect by inhibiting the secondary humification that destabilizes peat after drainage. The observed shift toward a higher proportion of MAOM-proxy in the backfilled soils provides a potential mechanism for this protective effect.

The theoretical basis for this new pathway is well established. The long-term persistence of soil organic matter is primarily controlled by its interaction with the mineral phase, rather than by any inherent resistance to decomposition. The formation of stable MAOM is key to long-term carbon storage. The new mineral surfaces from the embankment material likely provide the necessary binding sites for dissolved organic compounds and enabling the formation of a stable, mineral-associated carbon pool. Although this study did not measure productivity, the new topsoil provides the medium for new carbon inputs from crop residues (Bader et al., 2018). This dynamic reflects the findings of Säurich et al. (2019), who showed that increased productivity and higher carbon inputs following sand addition can more than compensate for simultaneously increased decomposition rates, leading to a net carbon gain. The formation of this new topsoil thus exemplifies the dual role of SOM: it must sustain fertility via a labile POM pool fed by crop residues, while the embankment simultaneously provides the mineral matrix required to build a stable MAOM pool.

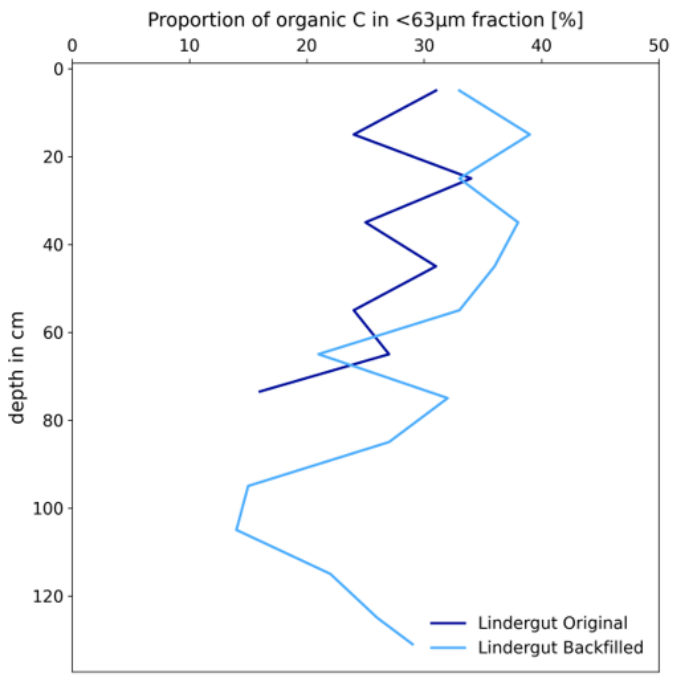

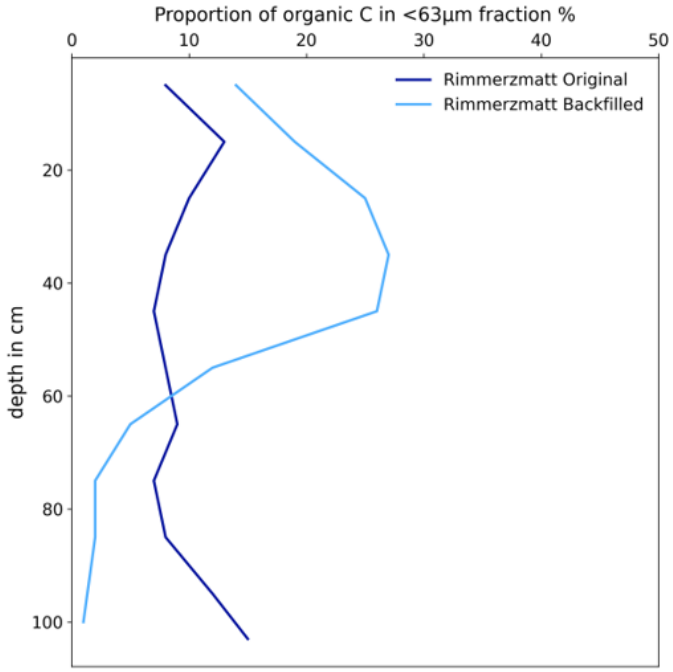

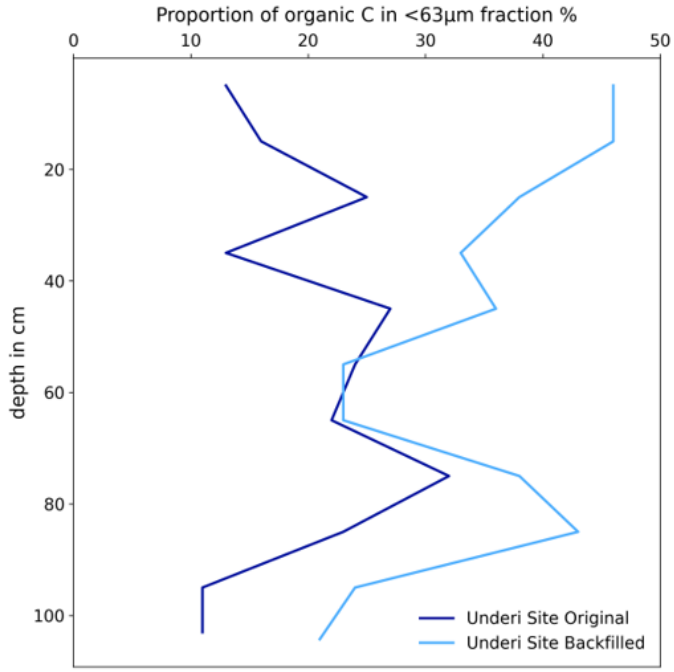

Figure 25: Relative proportions of organic Carbon in the <63µm fraction in %: Lindergut, Rimmerzmatt and Underi Site

6.3 Biogeochemical Indicators

Beyond carbon partitioning, the biogeochemical signatures of the original, uncovered profiles reflect a long history of drainage-induced degradation and mineralization. This is evidenced by a general decline in C/N ratios from the deep, preserved peat horizons toward the surface. The extreme C/N spikes (>90), observed particularly in the deep original peat at the Underi Site, strongly indicate nitrogen-depleted and poorly decomposed organic matter, a classic hallmark of preserved peat.

However, interpreting this trend requires critical nuance, since the C/N ratio does not respond uniformly to mineralization. The C/N ratio is determined by the relative loss rates of carbon and nitrogen. If both elements are mineralized at similar rates, the ratio does not change even as the total SOM stock declines. Therefore, the C/N profiles in the original soils must be read as a complex signature of degradation. The decrease in the ratio toward the surface confirms a history of preferential C loss and shows that along this degradation gradient, the C/N ratio serves more as a qualitative indicator of the state of organic matter than as a direct quantitative measure of the mineralization rate (Ostrowska, 2015).

This divergence highlights the limitations of using the C/N ratio as a standalone quantitative indicator of mineralization. According to Ostrowska (2015), its value lies in its ability to qualitatively characterize the state of organic matter within a specific pedogenic or management context. The findings of this study provide a clear example of how the same indicator can point to opposing system trajectories, degradation versus functional development, depending on the system under consideration.

The C/N structure observed in the backfilled profiles (see Figures 13, 15 and 17) must therefore be interpreted as a composite signal, reflecting both the decomposition state of the organic matter and the superposition of a low-N mineral mantle (Säurich et al., 2019). This points to an important management trade-off. While measures such as sand additions can increase productivity and N cycling, in some contexts such an approach carries a known risk of elevated nitrous oxide (N_2O) emissions. However, this potential risk stands in sharp contrast to the results of Paul et al. (2024), who observed a strong and significant suppression of N_2O emissions under a thick embankment. Mechanistic differences between the interventions may explain this discrepancy.

6.4 Deconstructing the Temporal Variable

While the general effects of embankment are clear, the data of this thesis do not show a simple relationship between the outcome and the age of intervention. The lack of a clear temporal trend in organic carbon stabilization within the topsoil from the mass balance values (0–40 cm) across the sites Rimmerzmatt (1971), Lindergut (1995), and Underi Site (2013) represents a significant negative finding. This strongly suggests that the initial properties of the embankment material and the application method are more influential than the time elapsed. A clear temporal effect also cannot be demonstrated for the proportional distribution of organic carbon in the <63 µm fraction (see Figure 25). A corresponding effect of the embankment cannot be inferred from the available profiles. The oldest embankment, Rimmerzmatt 1971 shows the lowest proportions, the youngest, Underi Site 2013 the highest; and Lindergut 1995 lies in between. This pattern contradicts a simple age gradient and suggests that the embankment mode and material properties, as well as post-depositional processes, dominate the distribution.

This conclusion is supported by the mineralogical control framework for the stabilization of SOM. Fine-textured materials rich in reactive minerals, such as clays and Fe/Al oxides, could have a much higher capacity to form stable MAOM than inert materials like sand. The type of backfill material is a paramount factor in determining the potential for new carbon stabilization. Additionally, the method of application itself can be a dominant variable; the use of heavy machinery, can lead to soil compaction that significantly alters the physical environment and thus the outcome of the intervention, independent of time (Egli et al., 2020a).

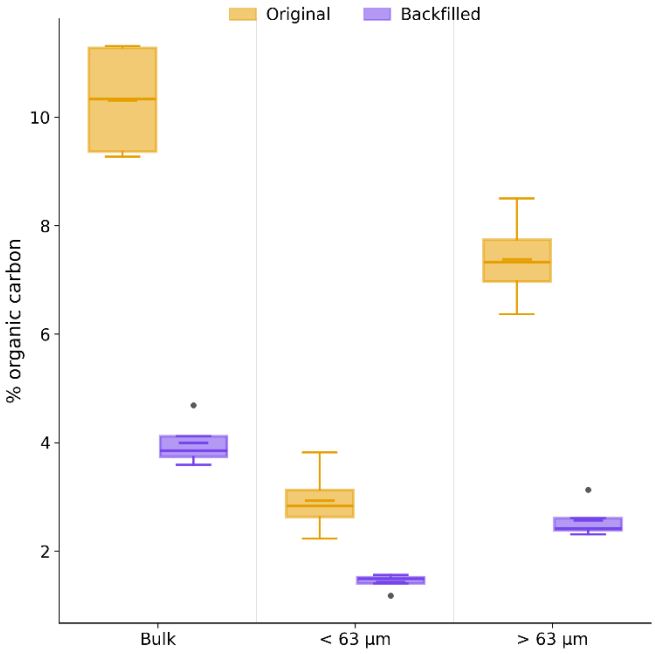

Figure 27: Boxplot Lindergut Topsoil (0–40 cm) from the mass balance divided into fractions and treatment)

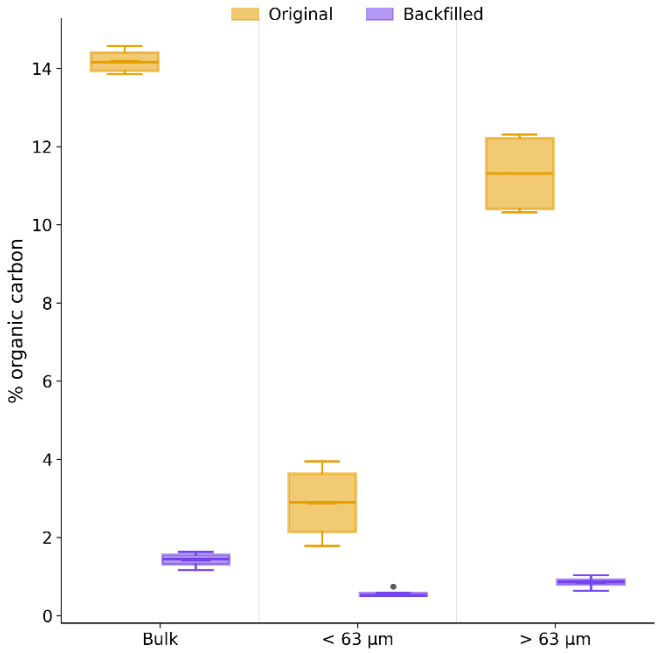

Figure 26: Boxplot Rimmerzmatt Topsoil (0–40 cm) from the mass balance divided into fractions and treatment

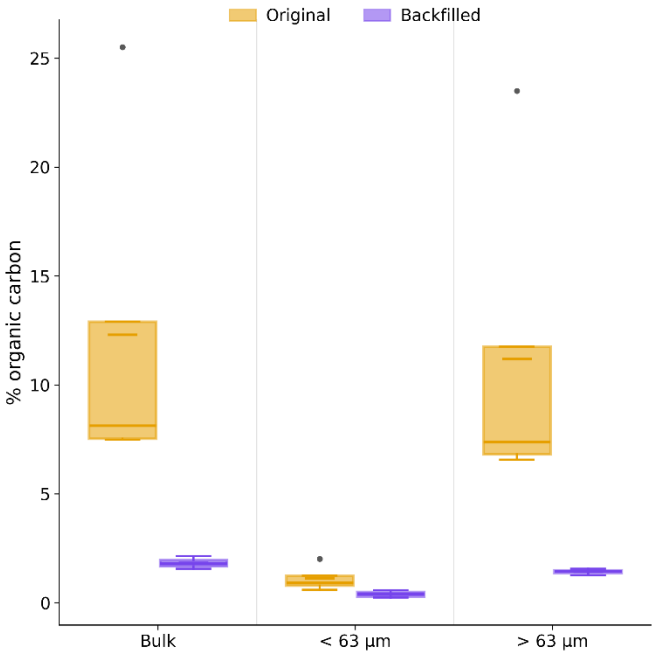

Figure 28: Boxplot Underi Site Topsoil (0–40 cm) from the mass balance divided into fractions and treatment

6.5 Practical Implications for Land Management

These findings can have direct and practical implications for future land management strategies in the Grosses Moos and similar peatland regions. Embankments represent a pragmatic and cost-efficient engineering solution to halt physical subsidence and preserve the remaining peat body, thus addressing the urgent threat of soil exhaustion. While they offer a fresh, stable, and productive agricultural surface, they are not a panacea for halting all greenhouse gas emissions and peat degradation. According to Ferré et al. (2019), the urgency for such interventions is underscored by projections that the peat layer in the region could be exhausted within 66 years. Furthermore, Ferré et al. (2019) have identified embankments as a crucial instrument for mitigating this degradation and safeguarding the soil resource. In the broader context of peat preservation measures in Switzerland, embankments are one of several available options, each offering specific advantages and disadvantages.

This strategy's effectiveness, especially in fostering long-term carbon stabilization in the new topsoil, depends on the material used. The findings lead to a crucial management implication: the type of backfill material is more important than the decision to backfill itself. To effectively boost both productivity and the potential for new carbon stabilization, choosing materials with a high content of reactive minerals over inert sand is essential. This conclusion represents a direct synthesis of the present study's findings with established theoretical frameworks, translating fundamental soil science into an evidence-based management recommendation.

Finally, the embankment strategy must be evaluated against the benchmark of permanent rewetting. While rewetting is the most effective measure for mitigating climate impact, the physical degradation of drained peat is largely irreversible. Embankment serves as a pragmatic alternative that accepts this irreversibility while allowing for continued agricultural land use, thereby addressing a key socioeconomic barrier to full-scale rewetting.

This conclusion is directly supported by the work of Zeitz & Velty (2002), which established that the high bulk density and altered structure of degraded peat are permanent, meaning a rewetted site is a novel ecosystem, not a restored one. Furthermore, the climate benefits of rewetting are subject to complex greenhouse gas trade-offs; for instance, stopping CO_2 loss through rewetting can simultaneously increase emissions of methane (CH_4), further demonstrating that no single solution is perfect.

6.6 Limitations and Future Research

This study provides scientifically grounded evidence for the need to go beyond pure emissions measurements and analyzes internal, process-based changes in carbon pools to understand the effects and implications of land management in the Grossen Moos. However, it is important to acknowledge the limitations of this study. Taking the current scientific literature into account, it represents a snapshot that reflects the present state of knowledge.

As explained in Chapter 4.2, the ≤1 g/cm³ density fractionation yielded only insufficient results. In some cases, the amount of material was so small that a complete evaluation within individual sites was not possible. This fraction was therefore excluded from the analysis. Future investigations should examine whether this fraction is relevant to the research question and, if so, employ alternative fractionation methods for separation.

The analysis in this work is based on carbon concentrations (wt%) rather than stocks (t/ha), as no bulk density data and skeleton content in percent were available to the author. This limitation prevents robust statements about net carbon gains or losses resulting from the embankment. To move from relative concentrations to absolute changes, future studies must include bulk density measurements to calculate carbon stocks.

To infer the temporal effects of embankments on carbon stocks, it is important to document in detail, and accompany scientifically, the type of embankment material, the construction technique used, the machinery, and the weather, since these factors, in addition to the embankment itself, are very likely to have a major impact on the long-term outcome.

Only three sites in a large study area were analyzed, with two in the southern part and only one in the northern part. Given the size of the Grossen Moos, this small number of study sites is not representative, but it does provide important indications. For a more spatially differentiated analysis, additional sites would need to be included to capture a gradient. The present results therefore do not allow statements about long-term effects but merely indicate possible trends.

For future research, establishing a long-term, standardized monitoring program with a larger number of study sites appears advisable to achieve results that are more broadly supported and durably evidence based.

7 Conclusion

This thesis addresses the urgent task of investigating the effects of embankments on carbon inventories in the Grosses Moos. Decades of drainage-induced degradation have transformed the Grosses Moos from a carbon sink into a significant source of greenhouse gases. This thesis closes the gap between flux-based studies and embankment-driven changes in the amount, vertical distribution, and functional stability of soil organic carbon. The results of this investigation provide clear, albeit nuanced, answers to the research questions posed.

About the first research question: the primary effect of embankment is the formation of a geochemically inverted Anthrosol. This practice physically buries the original peat horizon and leads to a pronounced vertical decoupling of the new agricultural topsoil from the older organic horizon beneath.

Regarding the second research question: the dominant mechanism of carbon stabilization differs fundamentally between these two layers. Preservation of the old, buried carbon in the coarse, chemically labile fraction of POM occurs not through chemical alteration but through physical protection. The embankment limits oxygen supply and thereby inhibits microbial decomposition. The embanked soils provide evidence of a different process: the generally higher proportional share of carbon in the fine <63 µm fraction points to a possible shift toward the more stable pathway of the MAOM. This suggests that embankments could provide the mineral matrix required for this new, long-term stabilization mechanism.

This thesis thus offers a crucial, deposit-based link that resolves an important uncertainty in evaluating embankment as a climate mitigation and soil improvement measure. By identifying a dual system, an old carbon stock that is physically protected alongside a newly active, respiring topsoil, this work reconciles the seemingly contradictory findings of earlier emissions-based research. These insights provide a possible explanation for why total CO_2 emissions can persist on embanked soils: the flux most likely originates from the new, active topsoil with fresh carbon inputs, while the old peat carbon is effectively preserved at depth.

Based on the current state of research, embankments are a pragmatic and cost-effective solution to slow peat degradation and preserve the peat resource for continued agricultural use. It is crucial to select and implement the design and material optimally. This study's results, especially the lack of a clear temporal trend in carbon stabilization, highlight the central importance of choosing the right embankment material.

In conclusion, embankments alone cannot halt peat degradation and the associated physical and chemical landscape changes. Nevertheless, embankments are one instrument that can help buy time to develop interdisciplinary, sustainable solutions.

8 Bibliography

Amt für Wasser und Abfall des Kantons Bern. (2024). *Juragewässerkorrektion*. Kanton Bern. https://www.bvd.be.ch/de/start/themen/wasser/gewaesserregulierung/juragewaesserkorrektion.html

Bader, C., Müller, M., Schulin, R., & Leifeld, J. (2018). Peat decomposability in managed organic soils in relation to land use, organic matter composition and temperature. *Biogeosciences*, *15*(3), 703–719. https://doi.org/https://doi.org/10.5194/bg-15-703-2018

Boonman, J., Hefting, M. M., Huissteden, C. J. A. Van, & Berg, M. Van Den. (2022). Cutting peatland CO 2 emissions with water management practices. *Biogeosciences*, *19*, 5707–5727. https://doi.org/doi.org/10.5194/bg-19-5707-2022

Brady, N. C., & Weil, R. R. (2017). *The Nature and Properties of Soils* (15th ed.). Pearson Education, Inc.

Bundesamt für Landestopographie swisstopo. (2025). *Karten der Schweiz*. Schweizerische Eidgenossenschaft. https://map.geo.admin.ch

Cotrufo, M. F., Ranalli, M. G., Haddix, M. L., Six, J., & Lugato, E. (2019). Soil carbon storage informed by particulate and mineral-associated organic matter. *Nature Geoscience*, *12*(12), 989–994. https://doi.org/10.1038/s41561-019-0484-6

Egli, M., & Fitze, P. (2000). Formulation of pedologic mass balance based on immobile elements: A revision. *Soil Science*, *165*(5), 437–443. https://doi.org/10.1097/00010694-200005000-00008

Egli, M., Gärtner, H., Röösli, C., Seibert, J., Wiesenberg, G. L. B., & Wingate, V. (2020). *Landschaftsdynamik im Gebiet des Grossen Mooses - Moorböden, Wassermanagement und landwirtschaftliche Nutzung im Spannungsfeld zwischen Produktivität und Nachhaltigkeit* (Zürich Geographisches Institut der Universität (ed.); 1st ed.). Geographisches Institut der Universität Zürich. https://doi.org/https://doi.org/10.5167/uzh-190633

Egli, M., Plötze, M., Tikhomirov, D., Kraut, T., Wiesenberg, G. L. B., Lauria, G., & Raimondi, S. (2020). Soil development on sediments and evaporites of the Messinian crisis. *Catena*, *187*, 104368. https://doi.org/10.1016/j.catena.2019.104368

Egli, M., Tikhomirov, D., Keller, T., & Brügger, Y. (2025). *Geochronology laboratorty methods Version 2*. https://doi.org/NA

Egli, M., Wiesenberg, G., Leifeld, J., Gärtner, H., Seibert, J., Röösli, C., Wingate, V., Dollenmeier, W., Griffel, P., Suremann, J., Weber, J., Zyberaj, M., & Musso, A. (2021). Formation and decay of peat bogs in the vegetable belt of Switzerland. *Swiss Journal of Geosciences*, *114*(1), 1–16. https://doi.org/10.1186/s00015-020-00376-0

Ferré, M., Muller, A., Leifeld, J., Bader, C., Müller, M., Engel, S., & Wichmann, S. (2019). Land Use Policy Sustainable management of cultivated peatlands in Switzerland :

Insights , challenges , and opportunities. *Land Use Policy*, *87*, 104019. https://doi.org/10.1016/j.landusepol.2019.05.038

Gerke, J. (2022). The Central Role of Soil Organic Matter in Soil Fertility and Carbon Storage. *Soil Systems*, *6*(2), Article 2. https://doi.org/10.3390/soilsystems6020033

Götz, R. (1993). *Eine wirtschaftswissenschaftlicheAnalyse der landwirtschaftlichen Nutzung organischer Böden in der Schweiz*. https://doi.org/https://doi.org/10.3929/ethz-a-000947238

Gross, C. D., & Harrison, R. B. (2019). The case for digging deeper: Soil organic carbon storage, dynamics, and controls in our changing world. *Soil Systems*, *3*(2), 1–24. https://doi.org/10.3390/soilsystems3020028

Guenat, C. (2022). *Aus Flachmooren entstandene entwässerte Torfböden*.

Harrington, C. D., & Whitney, J. W. (1987). Scanning electron microscope method for rock-varnish dating. *Geology*, *15*(10), 967–970.

Hiraishi, T., Krug, T., Tanabe, K., Srivastava, N., Jamsranjav, B., Fukuda, M., & Troxler, T. (2014). *2013 Supplement to the 2006 IPCC Guidelines for National Greenhouse Gas Inventories: Wetlands*.

IUSS Working Group WRB. (2022). *World Reference Base for Soil Resources* (4. Edition). International Union of Soil Sciences.

Jurasinski, G., Ahmad, S., Anadon-rosell, A., Berendt, J., Beyer, F., Bill, R., Blume-werry, G., Couwenberg, J., Günther, A., Joosten, H., Koebsch, F., Köhn, D., Koldrack, N., Kreyling, J., Leinweber, P., Lennartz, B., Liu, H., Michaelis, D., Mrotzek, A., & Smiljani, M. (2020). From Understanding to Sustainable Use of Peatlands : The WETSCAPES Approach. *Soil Systems*, *4*(1), Article 14. https://doi.org/https://doi.org/10.3390/soilsystems4010014

Kalisz, B., & Urbanowicz, P. (2021). Impact of siltation on the stability of organic matter in drained peatlands. *Ecological Indicators*, *130*, Article 108149. https://doi.org/10.1016/j.ecolind.2021.108149

Klingenfuß, C., Roßkopf, N., Walter, J., Heller, C., & Zeitz, J. (2014). Soil organic matter to soil organic carbon ratios of peatland soil substrates. *Geoderma*, *235–236*, 410–417. https://doi.org/10.1016/j.geoderma.2014.07.010

Krüger, J. P., Leifeld, J., Glatzel, S., Szidat, S., & Alewell, C. (2014). Biogeochemical indicators of peatland degradation – a case study of a temperate bog in northern Germany. *Biogeosciences*, *11*, 16825–16854. https://doi.org/10.5194/bgd-11-16825-2014

Lal, R., Kimble, J., Levine, E., & Stewart, B. A. (1995). *SOIL MANAGEMENT AND GREENHOUSE* (1st ed.). CRC Press.

Lavallee, J. M., Soong, J. L., & Cotrufo, M. F. (2020). Conceptualizing soil organic matter into particulate and mineral-associated forms to address global change in the 21st century. *Global Change Biology*, *26*(1), 261–273. https://doi.org/10.1111/gcb.14859

Leifeld, J., & Menichetti, L. (2018). The underappreciated potential of peatlands in global climate change mitigation strategies. *Nature Communications*, *9*(1), 1–7. https://doi.org/10.1038/s41467-018-03406-6

Leifeld, Jens, Müller, T., & Fuhrer, J. (2011). Peatland subsidence and carbon loss from drained temperate fens. *Soil Use and Management*, *27*(2), 170–176. https://doi.org/10.1111/j.1475-2743.2011.00327.x

Leifeld, Jens, Vogel, D., & Bretscher, D. (2019). Treibhausgasemissionen entwässerter Böden. *Agroscope Science*, *1*(74).

Limpens, J., Berendse, F., Blodau, C., Canadell, J. G., Freeman, C., Holden, J., Roulet, N., & Rydin, H. (2008). Peatlands and the carbon cycle : from local processes to global implications – a synthesis. *Biogeosciences*, *5*(5), 1475–1491. https://doi.org/https://doi.org/10.5194/bg-5-1475-2008

Liu, H., Zak, D., Rezanezhad, F., & Lennartz, B. (2019). Soil degradation determines release of nitrous oxide and dissolved organic carbon from peatlands Soil degradation determines release of nitrous oxide and dissolved organic carbon from peatlands. *Environmental Research Letters*, *14*(9), Article 094009. https://doi.org/10.1088/1748-9326/ab3947

Meteoswiss. (2025). *No Title*. Federal Office of Meteorology and Climatology. https://www.meteoswiss.admin.ch

Mohammadi, M., McMackin, C., & Egli, M. (2024). Source identification of morainic materials in soils of the Three Lakes region (Switzerland) using the fingerprinting technique. *Catena*, *234*, Article 107619. https://doi.org/10.1016/j.catena.2023.107619

Nesbit, H. W., & Young, G. M. (1989). Formation and Diagenesis of Weathering Profiles. *The Journal of Geology*, *97*(2), 129–147. https://doi.org/https://doi.org/10.1086/629290

Ostrowska, A. (2015). Assessment of the C / N ratio as an indicator of the decomposability of organic matter in forest soils. *Ecological Indicators*, *49*, 104–109. https://doi.org/http://dx.doi.org/10.1016/j.ecolind.2014.09.044

Otremba, K., Kozłowski, M., Tatuśko, N., & Mariusz, K. (2024). Long - term agricultural reclamation on the chemical properties of Technosols at lignite postmining site – efficiency of winter wheat and winter rape. *Plant and Soil*, *511*, 223–244. https://doi.org/10.1007/s11104-024-06983-2

Paul, S., Ammann, C., Alewell, C., & Leifeld, J. (2021). Carbon budget response of an agriculturally used fen to different soil moisture conditions. *Agricultural and Forest Meteorology*, *300*(2), Article 108319. https://doi.org/10.1016/j.agrformet.2021.108319

Paul, S., Ammann, C., Wang, Y., Alewell, C., & Leifeld, J. (2024). Can mineral soil coverage be a suitable option to mitigate greenhouse gas emissions from agriculturally managed peatlands? *Agriculture, Ecosystems and Environment*, *375*, 1–11. https://doi.org/10.1016/j.agee.2024.109197

Reichstein, M., Bahn, M., Ciais, P., Frank, D., Mahecha, M. D., Seneviratne, S. I., Zscheischler, J., Beer, C., Buchmann, N., Frank, D. C., Papale, D., Rammig, A., & Smith, P. (2013). Climate extremes and the carbon cycle. *Nature*, *500*, 287–295. https://doi.org/10.1038/nature12350

Roeoesli, C., & Egli, M. (2024). Using historical data to access the surface subsidence in the vegetable belt of the Three Lakes Region, Switzerland. *Swiss Journal of Geosciences*, *117*(9), 1–18. https://doi.org/10.1186/s00015-024-00452-9

Säurich, A., Tiemeyer, B., Dettmann, U., & Don, A. (2019). How do sand addition , soil moisture and nutrient status influence greenhouse gas fluxes from drained organic soils ? *Soil Biology and Biochemistry*, *135*(4), 71–84. https://doi.org/10.1016/j.soilbio.2019.04.013

Sun, S. -s., & McDonough, W. F. (1989). Chemical and isotopic systematics of oceanic basalts: implications for mantle composition and processes. *Geological Society, London, Special Publications*, *42*, 313–345. https://doi.org/https://doi.org/10.1144/GSL.SP.1989.042.01.1

Thomet, P., Lehmann, D., Marti, A., Ménétrey, F., & Schwab, A. (2018). *Dritte Juragewässerkorrektion Dritte als Beitrag zur nationalen Ernährungssicherung*.

Tiessen, H., Cuevast, E., & Chacon, P. (1994). The role of soil organic matter in sustaining soil fertility. *Nature*, *371*(6), 783–785. https://doi.org/https://doi.org/10.1038/371783a0

United Nations Environment Programme (UNEP). (2022). *Global Peatlands Assessment – The State of the World's Peatlands: Evidence for action toward the conservation, restoration, and sustainable management of peatlands. Main Report. Global Peatlands Initiative.*

Vincevica-Gaile, Z., Teppand, T., Kriipsalu, M., Krievans, M., Jani, Y., Klavins, M., Setyobudi, R. H., Grinfelde, I., Rudovica, V., Tamm, T., Shanskiy, M., Saaremae, E., Zekker, I., & Burlakovs, J. (2021). Towards Sustainable Soil Stabilization in Peatlands : Secondary Raw Materials as an Alternative. *Sustainability*, *12*(13), 1–26. https://doi.org/https://doi.org/10.3390/su13126726

von Lützow, M., Kögel-Knabner, I., Ekschmitt, K., Flessa, H., Guggenberger, G., Matzner, E., & Marschner, B. (2007). SOM fractionation methods: Relevance to functional pools and to stabilization mechanisms. *Soil Biology and Biochemistry*, *39*(9), 2183–2207. https://doi.org/10.1016/j.soilbio.2007.03.007

Wallimann, L. (2023). *Impacts of Reconstructed Soils on CO2 Emissions in the Bernese Three Lakes Region*. Zurich.

Wander, M. (2004). Soil Organic Matter Fractions and Their Relevance to Soil Function. In F. Magdoff & R. Weil (Eds.), *Soil Organic Matter in Sustainable Agriculture* (pp. 67–102). CRC Press. https://doi.org/10.1201/9780203496374.ch3

Wang, Y., Paul, S. M., Jocher, M., Alewell, C., & Leifeld, J. (2022). Reduced Nitrous Oxide Emissions From Drained Temperate Agricultural Peatland After Coverage With Mineral Soil. *Frontiers in Environmental Science*, *10*, 1–13. https://doi.org/10.3389/fenvs.2022.856599

Wang, Y., Paul, S. M., Jocher, M., Espic, C., Alewell, C., Szidat, S., & Leifeld, J. (2021). Soil carbon loss from drained agricultural peatland after coverage with mineral soil. *Science of the Total Environment*, *800*, Article 149498. https://doi.org/10.1016/j.scitotenv.2021.149498

Wiesmeier, M., Urbanski, L., Hobley, E., Lang, B., Lützow, M. Von, Marin-spiotta, E., Wesemael, B. Van, Rabot, E., Ließ, M., Garcia-franco, N., Wollschläger, U., Vogel, H., & Kögel-knabner, I. (2019). Soil organic carbon storage as a key function of soils - A review of drivers and indicators at various scales. *Geoderma*, *333*, 149–162. https://doi.org/10.1016/j.geoderma.2018.07.026

Wüst-Galley, C., Grünig, A., & Leifeld, J. (2020). Land use-driven historical soil carbon

losses in Swiss peatlands. *Landscape Ecology*, *35*(1), 173–187. https://doi.org/10.1007/s10980-019-00941-5

Yost, J. L., & Hartemink, A. E. (2019). Soil organic carbon in sandy soils: A review. In D. L. Sparks (Ed.), *Advances in Agronomy* (Vol. 158, pp. 217–310). Academic Press. https://doi.org/https://doi.org/10.1016/bs.agron.2019.07.004.

Yu, W., Huang, W., Weintraub-Leff, S. R., & Hall, S. J. (2022). Where and why do particulate organic matter (POM) and mineral-associated organic matter (MAOM) differ among diverse soils? *Soil Biology and Biochemistry*, *172*, 108756. https://doi.org/10.1016/j.soilbio.2022.108756

Yu, Z. (2011). Peatlands and Their Role in the Global Carbon Cycle. *EOS, Transactions, American Geophysical Union*, *92*(12), 97–108. https://doi.org/doi/10.1029/2011EO120001

Zeitz, J., & Velty, S. (2002). Soil properties of drained and rewetted fen soils. *Journal of Plant Nutrition and Soil Science*, *165*(5), 618–626. https://doi.org/10.1002/1522-2624(200210)165:5<618::AID-JPLN618>3.0.CO;2-W

Zimmermann, M., Leifeld, J., Schmidt, M. W. I., Smith, P., & Fuhrer, J. (2007). Measured soil organic matter fractions can be related to pools in the RothC model. *European Journal of Soil Science*, *58*(3), 658–667. https://doi.org/10.1111/j.1365-2389.2006.00855.x

9 Appendix

The appendix presents the raw data or results that were collected by the author during the writing process or in the laboratory as part of this work but were not used.

9.1 Codes samples combined and divided

Lindergut
Bottom and top tube

Combined 65 Samples			Divided 52 Samples		
C24CM101	0	10	C24CM101	0	10
C24CM102	10	20	C24CM102	10	20
C24CM103	20	26	C24CM103	20	30
C24CM104	26	30	C24CM104	30	40
C24CM105	30	40	C24CM105	40	50
C24CM106	40	48	C24CM106	50	60
C24CM107	48	50	C24CM107	60	70
C24CM108	50	60	C24CM108	70	77
C24CM109	60	70	C24CM111	0	10
C24CM110	70	77	C24CM112	0	10
C24CM111	0	10	C24CM121	0	10
C24CM112	0	10	C24CM122	10	20
C24CM121	0	10	C24CM123	20	30
C24CM122	10	20	C24CM124	30	40
C24CM123	20	27	C24CM125	40	50
C24CM124	27	30	C24CM126	50	60
C24CM125	30	40	C24CM127	60	70
C24CM126	40	50	C24CM128	70	80
C24CM127	50	52	C24CM129	80	90
C24CM128	52	60	C24CM130	90	100
C24CM129	60	70	C24CM131	100	110
C24CM130	70	72	C24CM132	110	120
C24CM131	72	80	C24CM133	120	130
C24CM132	80	90	C24CM134	130	132
C24CM133	90	100	C24CM141	0	10
C24CM134	100	107	C24CM142	10	20
C24CM135	107	110	C24CM143	20	30
C24CM136	110	120	C24CM144	30	40
C24CM137	120	130	C24CM145	40	50
C24CM138	130	132	C24CM146	50	60
C24CM141	0	10	C24CM147	60	70
C24CM142	10	20	C24CM148	70	78
C24CM143	20	27	C24CM149	78	78+
C24CM144	27	30	C24CM161	0	10
C24CM145	30	40	C24CM162	10	20
C24CM146	40	50	C24CM163	20	30
C24CM147	50	53	C24CM164	30	40
C24CM148	53	60	C24CM165	40	50
C24CM149	60	70	C24CM166	50	60
C24CM150	70	73	C24CM167	60	70
C24CM151	73	78	C24CM168	70	78
C24CM152	78	78+	C24CM181	0	10
C24CM161	0	10	C24CM182	10	20
C24CM162	10	20	C24CM183	20	30
C24CM163	20	26	C24CM184	30	40
C24CM164	26	30	C24CM185	40	50
C24CM165	30	40	C24CM186	50	60
C24CM166	40	50	C24CM187	60	70
C24CM167	50	52	C24CM188	70	80
C24CM168	52	60	C24CM189	80	90
C24CM169	60	70	C24CM190	90	100
C24CM170	70	78	C24CM191	100	105
C24CM181	0	10			
C24CM182	10	20			
C24CM183	20	26			
C24CM184	26	30			
C24CM185	30	40			
C24CM186	40	50			
C24CM187	50	53			
C24CM188	53	60			
C24CM189	60	70			
C24CM190	70	80			
C24CM191	80	90			
C24CM192	90	100			
C24CM193	100	105			

Rimmerzmatt
Bottom and top tube

Combined 54 Samples			Divided 45 Samples		
C24CM201	0	10	C24CM201	0	10
C24CM202	10	20	C24CM202	10	20
C24CM203	20	26	C24CM203	20	30
C24CM204	26	30	C24CM204	30	40
C24CM205	30	40	C24CM205	40	50
C24CM206	40	50	C24CM206	50	60
C24CM207	50	53	C24CM207	60	70
C24CM208	53	60	C24CM208	70	80
C24CM209	60	70	C24CM209	80	90
C24CM210	70	80	C24CM210	90	100
C24CM211	80	90	C24CM211	100	106
C24CM212	90	100	C24CM212	0	10
C24CM213	100	106	C24CM213	0	10
C24CM221	0	10	C24CM221	0	10
C24CM222	0	10	C24CM222	10	20
C24CM231	0	10	C24CM231	20	30
C24CM232	10	20	C24CM232	30	40
C24CM233	20	27	C24CM233	40	50
C24CM234	27	30	C24CM234	50	60
C24CM235	30	40	C24CM235	60	70
C24CM236	40	50	C24CM236	70	80
C24CM237	50	53	C24CM237	80	90
C24CM238	53	60	C24CM238	90	95
C24CM239	60	70	C24CM239	95	100+
C24CM240	70	80	C24CM240	0	10
C24CM241	80	90	C24CM241	10	20
C24CM242	90	95	C24CM242	20	30
C24CM243	95	100+	C24CM243	30	40
C24CM251	0	10	C24CM251	40	50
C24CM252	10	20	C24CM252	50	60
C24CM253	20	30	C24CM253	60	70
C24CM254	30	40	C24CM254	70	80
C24CM255	40	46	C24CM255	80	90
C24CM256	46	50	C24CM256	90	100
C24CM257	50	60	C24CM257	0	10
C24CM258	60	70	C24CM258	10	20
C24CM259	70	73	C24CM259	20	30
C24CM260	70	73	C24CM260	30	40
C24CM261	73	80	C24CM261	40	50
C24CM262	80	90	C24CM262	50	60
C24CM263	90	100	C24CM263	60	70
C24CM271	0	10	C24CM271	70	80
C24CM272	10	20	C24CM272	80	90
C24CM273	20	26	C24CM273	90	95
C24CM274	26	30	C24CM274	95	105
C24CM275	30	40	C24CM275		
C24CM276	40	50	C24CM276		
C24CM277	50	53	C24CM277		
C24CM278	53	60	C24CM278		
C24CM279	60	70	C24CM279		
C24CM280	70	80	C24CM280		
C24CM281	80	90	C24CM281		
C24CM282	90	95	C24CM282		
C24CM283	95	105	C24CM283		

9. 2 Concentrations table

Site	Treatment	Tube	Depth_Min	Depth_Max	Bulk Soil							Fraction <63um							Fraktion > 63µm			
					Tot_C (%)	Inorg. C (%)	org. C (%)	Tot_N	d13C	d15N	C/N	Tot_C	Inorg. C (%)	%_Corg	Tot_N	d13C	d15N	C/N	Inorg C %	org C %	N	C/N
Lindergut	Original	1	0	10	10.65	1.38	9.27	0.61	-23.94	3.92	15.10	12.06	1.46	10.60	0.84	-24.68	4.53	12.68	1.35	8.77	0.530	16.53
Lindergut	Original	1	10	20	10.77	1.37	9.40	0.62	-23.82	3.93	15.28	11.34	1.17	10.17	0.79	-24.74	4.45	12.96	1.43	9.18	0.568	16.18
Lindergut	Original	1-2	20	30	12.54	1.23	11.31	0.71	-25.00	3.32	15.90	13.21	1.13	12.08	0.85	-25.29	3.50	14.28	1.28	10.95	0.649	16.88
Lindergut	Original	2	30	40	12.51	1.24	11.27	0.72	-25.44	3.22	15.64	14.70	2.03	12.67	0.93	-25.75	3.27	13.56	1.02	10.88	0.660	16.47
Lindergut	Original	2-3	40	50	17.13	0.82	16.31	0.98	-26.53	2.62	16.58	16.85	1.06	15.79	1.07	-26.43	3.08	14.70	0.71	16.56	0.942	17.57
Lindergut	Original	3	50	60	16.83	0.40	16.43	0.93	-27.34	1.72	17.75	14.44	0.37	14.07	0.88	-26.77	2.15	15.98	0.41	17.37	0.944	18.41
Lindergut	Original	3	60	70	10.86	0.22	10.64	0.63	-27.48	1.66	16.84	8.18	0.26	7.92	0.56	-26.90	2.52	14.16	0.20	12.19	0.673	18.10
Lindergut	Original	3	70	77	17.55	0.39	17.16	0.99	-27.32	1.05	17.39	11.54	0.60	10.94	0.70	-26.80	1.44	15.69	0.32	19.23	1.083	17.76
Lindergut	Backfilled	1	0	10	6.26	1.58	4.69	0.39	-20.16	7.99	11.96	6.26	1.79	4.48	0.34	-18.93	3.74	12.98	1.46	4.80	0.417	11.51
Lindergut	Backfilled	1	10	20	5.42	1.63	3.79	0.32	-18.91	8.20	11.80	5.70	1.83	3.87	0.28	-17.51	3.38	13.77	1.50	3.75	0.347	10.80
Lindergut	Backfilled	1-2	20	30	5.17	1.58	3.59	0.32	-18.65	8.69	11.29	5.40	1.87	3.54	0.28	-17.35	4.20	12.42	1.43	3.61	0.335	10.80
Lindergut	Backfilled	2	30	40	5.51	1.57	3.93	0.34	-19.11	8.67	11.46	5.70	1.72	3.98	0.30	-17.79	4.00	13.32	1.48	3.91	0.371	10.54
Lindergut	Backfilled	2	40	50	5.32	1.80	3.52	0.29	-17.49	7.37	12.09	5.30	1.93	3.37	0.23	-15.33	3.52	14.50	1.73	3.60	0.326	11.05
Lindergut	Backfilled	2-3	50	60	8.99	1.91	7.08	0.53	-21.71	6.98	13.43	8.90	1.50	7.40	0.49	-22.02	2.93	15.01	2.10	6.93	0.543	12.76
Lindergut	Backfilled	3	60	70	12.47	1.02	11.45	0.82	-24.88	6.06	13.99	8.37	0.36	8.02	0.51	-25.56	2.98	15.64	1.31	12.92	0.950	13.60
Lindergut	Backfilled	3	70	80	12.31	1.13	11.19	0.81	-24.82	6.62	13.87	12.73	0.84	11.90	0.78	-25.62	3.16	15.20	1.25	10.88	0.817	13.32
Lindergut	Backfilled	4	80	90	11.91	1.21	10.70	0.78	-25.13	5.89	15.25	12.05	1.35	10.69	0.70	-25.83	2.22	17.11	1.16	10.70	0.810	13.22
Lindergut	Backfilled	4	90	100	6.49	0.16	6.33	0.50	-26.81	6.36	13.09	5.65	0.40	5.25	0.39	-26.63	1.96	14.46	0.11	6.56	0.518	12.65
Lindergut	Backfilled	4-5	100	110	13.02	0.23	12.78	0.78	-27.20	3.67	16.61	7.22	0.52	6.70	0.40	-26.91	0.37	18.26	0.13	15.01	0.926	16.22
Lindergut	Backfilled	5	110	120	12.57	0.23	12.34	0.80	-27.29	3.21	15.80	11.18	0.62	10.56	0.62	-27.27	-0.01	17.94	0.10	12.96	0.856	15.15
Lindergut	Backfilled	5	120	130	9.68	0.24	9.43	0.67	-27.24	3.95	14.37	8.92	0.78	8.13	0.58	-26.96	0.61	15.31	0.01	9.98	0.712	14.03
Lindergut	Backfilled	5	130	132	8.35	0.15	8.20	0.56	-26.75	4.99	14.98	8.93	0.47	8.46	0.51	-26.52	1.00	17.46	0.03	8.09	0.575	14.07
Rimmerzmatt	Original	1	0	10	8.09	0.61	7.48	0.68	-26.67	5.75	11.95	7.84	1.48	6.36	0.65	-27.39	4.65	12.04	0.52	7.60	0.680	11.17
Rimmerzmatt	Original	1	10	20	8.04	0.49	7.55	0.60	-27.00	4.37	13.42	8.84	0.85	7.99	0.69	-28.41	4.96	12.89	0.44	7.48	0.587	12.75
Rimmerzmatt	Original	1-2	20	30	9.15	0.46	8.70	0.65	-27.35	4.00	14.15	8.21	0.72	7.50	0.62	-27.64	4.41	13.14	0.42	8.85	0.649	13.63
Rimmerzmatt	Original	2	30	40	26.38	0.88	25.50	1.67	-27.86	3.23	15.79	25.55	0.97	24.57	1.49	-28.24	3.03	17.10	0.88	25.58	1.687	15.16
Rimmerzmatt	Original	2	40	50	36.15	1.30	34.86	2.15	-27.76	1.85	16.83	35.87	1.02	34.85	1.98	-28.14	1.82	18.08	1.32	34.86	2.161	16.13
Rimmerzmatt	Original	2-3	50	60	38.33	1.47	36.86	2.00	-28.13	1.68	19.20	36.89	1.24	35.65	1.82	-28.34	1.51	20.22	1.49	36.96	2.011	18.38
Rimmerzmatt	Original	3	60	70	33.16	1.20	31.95	1.87	-27.73	1.27	17.75	39.25	0.00	39.25	1.99	-28.03	1.17	19.71	1.47	31.41	1.859	16.90
Rimmerzmatt	Original	3	70	80	26.14	0.65	25.48	1.26	-27.07	0.55	20.78	20.97	0.00	20.97	0.75	-27.63	-0.45	27.97	0.83	25.93	1.309	19.81
Rimmerzmatt	Original	4	80	90	23.40	0.42	22.98	0.94	-27.33	-0.45	24.95	16.42	0.00	16.42	0.64	-27.85	-0.67	25.65	0.50	23.83	0.976	24.41
Rimmerzmatt	Original	4	90	100	13.15	0.19	12.96	0.55	-27.58	0.34	23.71	10.19	0.51	9.69	0.47	-27.88	0.22	21.81	0.13	13.59	0.572	23.78
Rimmerzmatt	Original	4	100	106	2.94	0.00	2.94	0.15	-27.44	0.33	20.22	4.64	0.00	4.64	0.26	-27.63	0.73	17.96	0.00	2.77	0.134	20.67
Rimmerzmatt	Backfilled	1	0	10	4.41	2.70	1.71	0.14	-12.26	4.57	30.73	5.47	3.51	1.95	0.30	-18.59	4.56	18.31	2.59	1.68	0.122	13.78
Rimmerzmatt	Backfilled	1	10	20	4.15	2.60	1.55	0.13	-11.75	4.15	31.78	5.34	3.13	2.22	0.28	-18.35	3.86	19.15	2.52	1.44	0.107	13.44
Rimmerzmatt	Backfilled	1-2	20	30	4.48	2.58	1.90	0.13	-11.40	3.98	34.17	6.17	1.09	5.08	0.33	-18.62	4.24	18.47	2.74	1.57	0.110	14.24
Rimmerzmatt	Backfilled	2	30	40	4.99	2.86	2.14	0.15	-12.09	3.28	33.92	7.13	2.16	4.97	0.42	-20.00	3.93	17.16	2.95	1.76	0.112	15.75
Rimmerzmatt	Backfilled	2	40	50	5.10	2.97	2.13	0.17	-11.29	4.21	30.71	7.29	1.93	5.36	0.42	-20.14	3.81	17.33	3.09	1.76	0.137	12.83
Rimmerzmatt	Backfilled	2-3	50	60	8.03	1.89	6.14	0.45	-21.34	2.88	17.94	9.05	1.28	7.77	0.62	-24.00	3.63	14.62	1.95	5.97	0.430	13.89
Rimmerzmatt	Backfilled	3	60	70	17.93	1.16	16.77	1.14	-26.36	2.45	15.72	16.90	2.08	14.82	1.06	-26.74	2.28	15.88	1.10	16.90	1.146	14.75
Rimmerzmatt	Backfilled	4	70	80	25.83	1.10	24.74	1.53	-26.84	1.85	16.90	23.28	4.38	18.90	1.26	-27.21	1.77	18.49	0.99	24.93	1.538	16.21
Rimmerzmatt	Backfilled	4	80	90	31.51	1.12	30.40	1.93	-26.85	1.44	16.34	26.08	4.80	21.28	1.51	-27.28	1.47	17.26	1.01	30.67	1.941	15.80
Rimmerzmatt	Backfilled	4	90	100+	41.09	1.15	39.94	2.29	-27.52	0.60	17.96	30.76	11.18	19.59	1.58	-27.97	0.17	19.47	0.97	40.31	2.301	17.52
Underi Site	Original	1	0	10	14.75	0.10	14.65	1.22	-27.43	5.54	12.10	12.96	0.65	12.31	0.93	-27.20	2.41	13.88	0.00	15.07	1.271	11.86
Underi Site	Original	1	10	20	14.62	0.06	14.57	1.21	-27.35	5.53	12.10	12.94	0.31	12.63	0.93	-27.26	2.34	13.86	0.00	14.99	1.269	11.82
Underi Site	Original	1-2	20	30	13.99	0.14	13.85	1.15	-27.37	5.21	12.19	13.05	0.51	12.54	0.94	-27.21	2.33	13.94	0.00	14.36	1.231	11.67
Underi Site	Original	2	30	40	14.14	0.17	13.97	1.17	-27.40	5.42	12.06	12.76	1.11	11.65	0.94	-27.17	2.60	13.64	0.00	14.39	1.216	11.84
Underi Site	Original	2	40	50	14.36	0.00	14.36	1.19	-27.68	5.19	12.05	12.44	0.00	12.44	0.95	-27.46	2.93	13.05	0.00	15.25	1.302	11.71
Underi Site	Original	2-3	50	60	26.43	0.01	26.42	2.13	-27.61	3.87	12.40	22.71	0.03	22.68	1.60	-27.84	1.18	14.16	0.00	27.89	2.338	11.93
Underi Site	Original	3	60	70	12.99	0.00	12.99	1.10	-27.60	4.08	11.81	11.40	0.00	11.40	0.83	-27.54	0.57	13.79	0.00	13.53	1.192	11.35
Underi Site	Original	3	70	80	3.85	0.00	3.85	0.35	-27.80	6.03	11.02	4.12	0.00	4.12	0.31	-27.57	1.20	13.25	0.00	3.74	0.366	10.22
Underi Site	Original	4	80	90	3.56	2.18	1.38	0.11	-10.14	9.54	32.48	4.35	3.31	1.04	0.11	-10.04	1.30	41.02	1.68	1.53	0.111	13.77
Underi Site	Original	4	90	100	4.21	3.48	0.73	0.05	-4.68	10.20	92.63	5.60	5.30	0.29	0.07	-4.79	1.61	77.87	2.80	0.90	0.036	25.18
Underi Site	Original	4	100	106	5.07	3.41	1.66	0.06	-4.90	10.36	91.31	6.04	5.43	0.61	0.05	-4.54	1.79	129.49	2.58	2.09	0.059	35.33
Underi Site	Backfilled	1	0	10	2.77	1.14	1.63	0.17	-16.63	11.64	16.37	3.14	1.15	1.99	0.15	-15.95	4.26	21.16	1.14	1.42	0.182	7.80
Underi Site	Backfilled	1	10	20	2.44	1.28	1.16	0.14	-15.80	11.37	17.71	3.01	1.56	1.46	0.13	-15.49	3.69	23.17	1.11	0.99	0.142	6.98
Underi Site	Backfilled	1-2	20	30	2.72	1.36	1.36	0.13	-14.18	11.23	20.26	2.77	1.50	1.26	0.10	-13.72	4.02	26.68	1.27	1.42	0.155	9.18
Underi Site	Backfilled	2	30	40	3.15	1.62	1.53	0.15	-13.82	10.60	21.55	3.37	1.66	1.70	0.11	-12.61	3.49	30.80	1.60	1.46	0.162	9.03
Underi Site	Backfilled	2	40	50	5.66	0.87	4.79	0.43	-23.41	8.19	13.19	6.03	0.97	5.06	0.38	-23.02	3.22	15.88	0.82	4.64	0.454	10.23
Underi Site	Backfilled	2-3	50	60	7.03	0.33	6.70	0.57	-26.00	7.02	12.38	8.53	-0.28	8.81	0.63	-26.44	3.02	13.65	0.46	6.26	0.556	11.27
Underi Site	Backfilled	3	60	70	7.02	0.44	6.58	0.57	-25.77	7.45	12.33	8.52	0.12	8.40	0.63	-26.49	3.09	13.54	0.51	6.17	0.556	11.10
Underi Site	Backfilled	3	70	80	7.12	0.39	6.74	0.58	-26.03	6.73	12.36	8.23	0.24	7.99	0.60	-26.45	2.94	13.82	0.45	6.16	0.568	10.84
Underi Site	Backfilled	4	80	90	7.50	0.10	7.40	0.61	-27.17	5.88	12.26	8.14	0.10	8.04	0.61	-27.30	2.65	13.40	0.10	6.98	0.615	11.36
Underi Site	Backfilled	4	90	100	8.59	0.04	8.55	0.71	-27.46	5.55	12.17	6.08	0.01	6.07	0.48	-27.34	2.63	12.76	0.05	9.85	0.826	11.93
Underi Site	Backfilled	4	100	108.5	11.67	0.00	11.67	0.88	-27.78	4.61	13.28	8.48	0.00	8.48	0.56	-27.60	1.52	15.18	0.00	12.98	1.011	12.84

9.3 Table Mass Balance

			Total C (= Corg + Cinorg)					Org. C in bulk soil and fractions				N in bulk soil and fractions			
Site	Treatment	Depth cm	Ctot bulk Weight-%	Ctot < 63µm, Konz. Weight-%	Mass Proportion < 63 µm	Ctot bulk <63µm Weight-%	Ctot bulk >63µm Weight-%	Corg bulk Weight-%	C bulk <63µm Weight-%	C bulk >63µm Weight-%	Relative proportion of org C in the < 63µm fraction	N bulk Weight-%	N bulk <63µm Weight-%	N bulk >63µm Weight-%	Relative proportion of N in the < 63µm fraction
Lindergut	Original	5	10.65	12.06	27.4%	3.30	7.35	9.27	2.90	6.37	31.3%	0.61	0.23	0.39	37.3%
Lindergut	Original	15	10.77	11.34	21.9%	2.48	8.29	9.40	2.23	7.17	23.7%	0.62	0.17	0.44	27.9%
Lindergut	Original	25	12.54	13.21	31.6%	4.17	8.36	11.31	3.82	7.49	33.7%	0.71	0.27	0.44	37.6%
Lindergut	Original	35	12.51	14.70	21.9%	3.22	9.29	11.27	2.77	8.50	24.6%	0.72	0.20	0.52	28.4%
Lindergut	Original	45	17.13	16.85	31.6%	5.32	11.81	16.31	4.99	11.33	30.6%	0.98	0.34	0.64	34.5%
Lindergut	Original	55	16.83	14.44	28.4%	4.10	12.73	16.43	4.00	12.43	24.3%	0.93	0.25	0.68	27.0%
Lindergut	Original	65	10.86	8.18	36.2%	2.96	7.90	10.64	2.87	7.78	26.9%	0.63	0.20	0.43	32.0%
Lindergut	Original	74	17.55	11.54	25.0%	2.88	14.66	17.16	2.73	14.42	15.9%	0.99	0.17	0.81	17.7%
Lindergut	Backfilled	5	6.26	6.26	34.7%	2.18	4.09	4.69	1.56	3.13	33.2%	0.39	0.12	0.27	30.6%
Lindergut	Backfilled	15	5.42	5.70	38.3%	2.18	3.24	3.79	1.48	2.31	39.0%	0.32	0.11	0.21	33.4%
Lindergut	Backfilled	25	5.17	5.40	33.3%	1.80	3.37	3.59	1.18	2.41	32.8%	0.32	0.09	0.22	29.9%
Lindergut	Backfilled	35	5.51	5.70	37.9%	2.16	3.35	3.93	1.51	2.43	38.3%	0.34	0.11	0.23	33.0%
Lindergut	Backfilled	45	5.32	5.30	37.8%	2.00	3.32	3.52	1.27	2.24	36.2%	0.29	0.09	0.20	30.2%
Lindergut	Backfilled	55	8.99	8.90	32.0%	2.84	6.14	7.08	2.36	4.71	33.4%	0.53	0.16	0.37	29.9%
Lindergut	Backfilled	65	12.47	8.37	30.1%	2.52	9.95	11.45	2.41	9.03	21.1%	0.82	0.15	0.66	18.9%
Lindergut	Backfilled	75	12.31	12.73	29.8%	3.79	8.52	11.19	3.54	7.64	31.7%	0.81	0.23	0.57	28.9%
Lindergut	Backfilled	85	11.91	12.05	27.1%	3.26	8.65	10.70	2.90	7.80	27.1%	0.78	0.19	0.59	24.4%
Lindergut	Backfilled	95	6.49	5.65	17.7%	1.00	5.49	6.33	0.93	5.40	14.7%	0.50	0.07	0.43	14.0%
Lindergut	Backfilled	105	13.02	7.22	26.8%	1.94	11.08	12.78	1.79	10.99	14.0%	0.78	0.11	0.68	13.5%
Lindergut	Backfilled	115	12.57	11.18	25.8%	2.88	9.69	12.34	2.72	9.62	22.0%	0.80	0.16	0.64	20.2%
Lindergut	Backfilled	125	9.68	8.92	29.8%	2.66	7.02	9.43	2.42	7.01	25.7%	0.67	0.17	0.50	25.8%
Lindergut	Backfilled	131	8.35	8.93	28.3%	2.52	5.82	8.20	2.39	5.80	29.2%	0.56	0.14	0.41	25.9%
Rimmerzmatt	Original	5	8.09	7.84	9.3%	0.73	7.37	7.48	0.59	6.89	7.9%	0.68	0.06	0.62	8.9%
Rimmerzmatt	Original	15	8.04	8.84	12.4%	1.09	6.94	7.55	0.99	6.56	13.1%	0.60	0.08	0.51	14.2%
Rimmerzmatt	Original	25	9.15	8.21	11.3%	0.93	8.22	8.70	0.85	7.85	9.8%	0.65	0.07	0.58	11.0%
Rimmerzmatt	Original	35	26.38	25.55	8.2%	2.09	24.30	25.50	2.01	23.49	7.9%	1.67	0.12	1.55	7.3%
Rimmerzmatt	Original	45	36.15	35.87	6.9%	2.46	33.69	34.86	2.39	32.46	6.9%	2.15	0.14	2.01	6.3%
Rimmerzmatt	Original	55	38.33	36.89	7.8%	2.89	35.43	36.86	2.80	34.06	7.6%	2.00	0.14	1.85	7.2%
Rimmerzmatt	Original	65	33.16	39.25	6.9%	2.73	30.43	31.95	2.73	29.23	8.5%	1.87	0.14	1.73	7.4%
Rimmerzmatt	Original	75	26.14	20.97	9.1%	1.91	24.23	25.48	1.91	23.58	7.5%	1.26	0.07	1.19	5.4%
Rimmerzmatt	Original	85	23.40	16.42	11.5%	1.88	21.52	22.98	1.88	21.10	8.2%	0.94	0.07	0.86	7.8%
Rimmerzmatt	Original	95	13.15	10.19	16.3%	1.66	11.49	12.96	1.58	11.37	12.2%	0.55	0.08	0.48	13.8%
Rimmerzmatt	Original	103	2.94	4.64	9.3%	0.43	2.51	2.94	0.43	2.51	14.6%	0.15	0.02	0.12	16.5%
Rimmerzmatt	Backfilled	5	4.41	5.47	12.4%	0.68	3.73	1.71	0.24	1.47	14.1%	0.14	0.04	0.11	25.7%
Rimmerzmatt	Backfilled	15	4.15	5.34	13.5%	0.72	3.43	1.55	0.30	1.25	19.4%	0.13	0.04	0.09	28.9%
Rimmerzmatt	Backfilled	25	4.48	6.17	9.4%	0.58	3.90	1.90	0.48	1.42	25.1%	0.13	0.03	0.10	23.9%
Rimmerzmatt	Backfilled	35	4.99	7.13	11.6%	0.83	4.17	2.14	0.58	1.56	26.9%	0.15	0.05	0.10	32.7%
Rimmerzmatt	Backfilled	45	5.10	7.29	10.3%	0.75	4.35	2.13	0.55	1.57	26.0%	0.17	0.04	0.12	26.1%
Rimmerzmatt	Backfilled	55	8.03	9.05	9.4%	0.85	7.18	6.14	0.73	5.41	11.9%	0.45	0.06	0.39	13.0%
Rimmerzmatt	Backfilled	65	17.93	16.90	6.1%	1.03	16.90	16.77	0.91	15.86	5.4%	1.14	0.07	1.08	5.7%
Rimmerzmatt	Backfilled	75	25.83	23.28	3.2%	0.75	25.08	24.74	0.61	24.13	2.5%	1.53	0.04	1.49	2.7%
Rimmerzmatt	Backfilled	85	31.51	26.08	2.9%	0.76	30.75	30.40	0.62	29.78	2.0%	1.93	0.04	1.88	2.3%
Rimmerzmatt	Backfilled	100	41.09	30.76	1.8%	0.55	40.53	39.94	0.35	39.58	0.9%	2.29	0.03	2.26	1.2%
Underi Site	Original	5	14.75	12.96	15.2%	1.97	12.78	14.65	1.87	12.78	12.8%	1.22	0.14	1.08	11.6%
Underi Site	Original	15	14.62	12.94	17.9%	2.32	12.31	14.57	2.26	12.31	15.5%	1.21	0.17	1.04	13.8%
Underi Site	Original	25	13.99	13.05	28.1%	3.67	10.32	13.85	3.53	10.32	25.5%	1.15	0.26	0.88	22.9%
Underi Site	Original	35	14.14	12.76	15.3%	1.95	12.19	13.97	1.78	12.19	12.8%	1.17	0.14	1.03	12.2%
Underi Site	Original	45	14.36	12.44	31.6%	3.94	10.43	14.36	3.94	10.43	27.4%	1.19	0.30	0.89	25.3%
Underi Site	Original	55	26.43	22.71	28.3%	6.42	20.00	26.42	6.41	20.00	24.3%	2.13	0.45	1.68	21.3%
Underi Site	Original	65	12.99	11.40	25.3%	2.88	10.11	12.99	2.88	10.11	22.2%	1.10	0.21	0.89	19.0%
Underi Site	Original	75	3.85	4.12	29.9%	1.23	2.62	3.85	1.23	2.62	32.0%	0.35	0.09	0.26	26.6%
Underi Site	Original	85	3.56	4.35	30.9%	1.35	2.22	1.38	0.32	1.06	23.3%	0.11	0.03	0.08	29.9%
Underi Site	Original	95	4.21	5.60	27.1%	1.52	2.70	0.73	0.08	0.65	10.9%	0.05	0.02	0.03	42.8%
Underi Site	Original	103	5.07	6.04	29.2%	1.76	3.31	1.66	0.18	1.48	10.7%	0.06	0.01	0.04	24.5%
Underi Site	Backfilled	5	2.77	3.14	37.4%	1.17	1.60	1.63	0.74	0.89	45.6%	0.17	0.06	0.11	32.7%
Underi Site	Backfilled	15	2.44	3.01	36.6%	1.10	1.33	1.16	0.53	0.63	45.9%	0.14	0.05	0.09	34.6%
Underi Site	Backfilled	25	2.72	2.77	40.4%	1.12	1.60	1.36	0.51	0.85	37.5%	0.13	0.04	0.09	31.2%
Underi Site	Backfilled	35	3.15	3.37	29.9%	1.01	2.15	1.53	0.51	1.03	33.2%	0.15	0.03	0.11	22.3%
Underi Site	Backfilled	45	5.66	6.03	34.0%	2.05	3.60	4.79	1.72	3.06	36.0%	0.43	0.13	0.30	30.1%
Underi Site	Backfilled	55	7.03	8.53	17.2%	1.47	5.56	6.70	1.51	5.18	22.6%	0.57	0.11	0.46	18.9%
Underi Site	Backfilled	65	7.02	8.52	18.4%	1.56	5.45	6.58	1.54	5.04	23.4%	0.57	0.12	0.45	20.3%
Underi Site	Backfilled	75	7.12	8.23	31.6%	2.60	4.52	6.74	2.53	4.21	37.5%	0.58	0.19	0.39	32.7%
Underi Site	Backfilled	85	7.50	8.14	39.6%	3.22	4.28	7.40	3.18	4.22	43.0%	0.61	0.24	0.37	39.3%
Underi Site	Backfilled	95	8.59	6.08	34.4%	2.09	6.50	8.55	2.09	6.47	24.4%	0.71	0.16	0.54	23.2%
Underi Site	Backfilled	104	11.67	8.48	29.2%	2.47	9.19	11.67	2.47	9.19	21.2%	0.88	0.16	0.72	18.5%

9.4 DRIFT relative Concentrations

Site	Treatment	Tube	Depth_Min	Depth_Max	Band 2	Band 3	Band 4	Band 5	Band 6	Band 7	Band 8	Band 9	Band 10	Band 11	Band 12	Amides	Aromates	Aromaticity	Hydrophobicity
					C=O stretchi	C=O stretchi	Aromatic C=	Aromatic rin	N-H stretchir	Aliphatic C-H	OH deformat	C-O stretchir	C-OH stretch	Secondary al	C-O stretching of polysacc	%	%	ratio	ratio
Lindergut	Original	1	0	10	1.87%	8.67%	0.75%	4.78%	1.27%	4.35%	26.96%	7.14%	36.23%	0.17%	7.81%	9.94%	5.53%	4.97	0.036
Lindergut	Original	1	10	20	0.87%	2.45%	1.89%	0.50%	0.59%	4.10%	18.57%	9.47%	46.40%	0.28%	14.88%	3.04%	2.39%	13.29	0.036
Lindergut	Original	1-2	20	30	2.04%	5.40%	0.77%	3.43%	0.56%	4.67%	31.66%	12.11%	32.58%	-0.09%	6.88%	5.97%	4.19%	7.90	0.020
Lindergut	Original	2	30	40	1.90%	8.22%	1.33%	4.12%	0.71%	5.78%	32.70%	9.50%	23.15%	0.09%	12.49%	8.93%	5.45%	5.48	0.032
Lindergut	Original	2-3	40	50	3.72%	7.46%	3.19%	8.23%	1.38%	5.68%	19.20%	6.51%	36.09%	-0.12%	8.66%	8.85%	11.43%	6.47	0.049
Lindergut	Original	3	50	60	3.36%	9.65%	1.54%	7.47%	0.56%	6.47%	15.58%	21.40%	25.69%	0.28%	8.01%	10.21%	9.01%	5.55	0.026
Lindergut	Original	3	60	70	3.45%	10.59%	1.66%	7.76%	1.40%	6.28%	18.67%	12.16%	28.78%	0.26%	8.99%	11.99%	9.42%	4.40	0.044
Lindergut	Original	3	70	77	3.70%	9.76%	1.65%	8.55%	1.07%	5.59%	18.65%	10.23%	32.60%	-0.19%	8.39%	10.83%	10.20%	5.72	0.031
Lindergut	Backfilled	1	0	10	2.65%	8.73%	1.62%	8.54%	1.35%	5.49%	22.48%	10.28%	35.10%	0.13%	3.64%	10.07%	10.16%	1.60	0.142
Lindergut	Backfilled	1	10	20	2.70%	9.62%	1.82%	9.89%	3.39%	6.96%	16.34%	12.89%	25.61%	0.00%	10.78%	13.01%	11.72%	1.29	0.285
Lindergut	Backfilled	1-2	20	30	2.85%	9.68%	0.98%	7.81%	1.96%	5.22%	32.08%	15.97%	20.59%	0.15%	2.73%	11.64%	8.78%	1.25	0.173
Lindergut	Backfilled	2	30	40	3.26%	11.20%	2.18%	13.93%	5.59%	4.59%	20.42%	5.56%	27.64%	0.15%	5.49%	16.79%	16.11%	1.58	0.296
Lindergut	Backfilled	2	40	50	2.90%	10.89%	1.82%	9.58%	2.94%	5.88%	27.25%	11.04%	22.93%	0.04%	4.72%	13.84%	11.40%	0.78	0.393
Lindergut	Backfilled	2-3	50	60	2.80%	9.11%	2.17%	5.97%	3.94%	6.21%	22.31%	8.83%	24.14%	0.18%	14.35%	13.05%	8.14%	2.29	0.189
Lindergut	Backfilled	3	60	70	2.89%	9.19%	1.25%	6.28%	1.72%	7.05%	26.80%	10.06%	26.65%	0.17%	7.95%	10.91%	7.52%	4.49	0.050
Lindergut	Backfilled	3	70	80	3.98%	10.14%	1.35%	7.35%	1.46%	5.47%	24.00%	13.14%	26.36%	0.13%	6.61%	11.61%	8.70%	3.47	0.052
Lindergut	Backfilled	4	80	90	3.33%	10.26%	1.65%	6.91%	1.54%	6.50%	23.76%	10.02%	29.35%	-0.04%	6.72%	11.80%	8.57%	3.43	0.061
Lindergut	Backfilled	4	90	100	3.83%	11.99%	0.88%	8.76%	2.07%	6.44%	14.89%	22.41%	25.23%	-0.18%	3.70%	14.06%	9.64%	2.43	0.073
Lindergut	Backfilled	4-5	100	110	3.78%	11.73%	0.77%	11.26%	1.73%	6.67%	14.11%	18.85%	27.50%	0.17%	3.43%	13.46%	12.03%	4.35	0.035
Lindergut	Backfilled	5	110	120	4.36%	14.27%	0.91%	11.72%	1.49%	5.75%	16.55%	16.19%	28.49%	0.22%	0.05%	15.76%	12.63%	2.93	0.042
Lindergut	Backfilled	5	120	130	4.79%	14.11%	1.13%	12.02%	2.56%	5.86%	19.88%	13.04%	23.05%	0.39%	3.19%	16.67%	13.15%	2.53	0.073
Lindergut	Backfilled	5	130	132	4.71%	14.80%	1.67%	6.38%	2.07%	7.66%	18.35%	11.26%	29.92%	0.11%	3.06%	16.87%	8.05%	2.88	0.061
Rimmerzmatt	Original	1	0	10	3.02%	8.84%	0.47%	6.86%	1.41%	6.70%	19.11%	13.76%	33.94%	0.29%	5.60%	10.25%	7.33%	4.26	0.036
Rimmerzmatt	Original	1	10	20	3.70%	13.41%	0.62%	8.76%	2.43%	7.34%	20.26%	11.86%	28.91%	0.13%	2.58%	15.84%	9.38%	3.16	0.054
Rimmerzmatt	Original	1-2	20	30	4.27%	13.75%	0.70%	9.55%	1.11%	6.66%	20.92%	11.44%	29.34%	0.13%	2.14%	14.86%	10.26%	2.84	0.034
Rimmerzmatt	Original	2	30	40	5.26%	20.39%	1.06%	12.91%	1.26%	10.65%	16.59%	4.55%	8.00%	0.29%	19.04%	21.65%	13.97%	4.09	0.021
Rimmerzmatt	Original	2	40	50	5.13%	17.15%	1.41%	14.36%	1.56%	10.39%	19.47%	10.15%	5.20%	0.40%	14.79%	18.70%	15.77%	4.40	0.028
Rimmerzmatt	Original	2-3	50	60	6.35%	17.32%	1.30%	15.78%	2.77%	13.34%	16.22%	10.46%	3.54%	0.33%	12.57%	20.09%	17.08%	4.02	0.041
Rimmerzmatt	Original	3	60	70	6.53%	18.18%	1.36%	16.72%	2.55%	11.31%	17.66%	13.26%	4.78%	0.66%	6.98%	20.73%	18.08%	4.36	0.034
Rimmerzmatt	Original	3	70	80	4.01%	9.89%	0.93%	13.88%	1.83%	7.34%	17.52%	4.91%	17.17%	0.15%	22.37%	11.72%	14.81%	7.51	0.025
Rimmerzmatt	Original	4	80	90	3.34%	9.58%	1.37%	14.35%	1.06%	7.06%	11.42%	11.53%	22.52%	0.27%	17.51%	10.64%	15.72%	6.07	0.028
Rimmerzmatt	Original	4	90	100	2.64%	7.90%	1.37%	15.42%	0.96%	6.89%	12.63%	14.33%	24.66%	0.10%	13.09%	8.86%	16.79%	6.04	0.032
Rimmerzmatt	Original	4	100	106	2.63%	6.02%	1.75%	11.56%	0.91%	3.98%	43.04%	8.65%	15.18%	-0.02%	6.31%	6.93%	13.30%	3.71	0.069
Rimmerzmatt	Backfilled	1	0	10	2.65%	7.89%	1.83%	14.07%	2.63%	3.34%	19.88%	13.05%	24.69%	-0.12%	10.10%	10.52%	15.89%	0.55	0.656
Rimmerzmatt	Backfilled	1	10	20	2.89%	9.32%	1.43%	11.89%	2.66%	4.97%	32.18%	10.35%	19.15%	0.02%	5.13%	11.98%	13.32%	0.46	0.646
Rimmerzmatt	Backfilled	1-2	20	30	2.90%	8.51%	2.16%	15.36%	2.12%	3.14%	20.40%	9.94%	24.71%	-0.02%	10.78%	10.63%	17.52%	0.54	0.579
Rimmerzmatt	Backfilled	2	30	40	2.62%	7.79%	2.03%	11.59%	2.54%	3.69%	22.59%	9.21%	24.60%	0.03%	13.30%	10.33%	13.61%	0.59	0.621
Rimmerzmatt	Backfilled	2	40	50	2.50%	7.06%	2.03%	12.95%	3.38%	4.32%	15.52%	9.59%	25.91%	0.02%	16.72%	10.45%	14.98%	0.77	0.608
Rimmerzmatt	Backfilled	2-3	50	60	3.24%	9.75%	1.84%	8.49%	2.44%	5.93%	27.90%	8.74%	23.85%	0.14%	7.69%	12.19%	10.33%	1.56	0.186
Rimmerzmatt	Backfilled	3	60	70	4.49%	12.73%	1.20%	10.44%	2.40%	6.75%	19.05%	6.87%	22.04%	0.07%	13.95%	15.13%	11.64%	3.17	0.062
Rimmerzmatt	Backfilled	4	70	80	4.63%	14.04%	0.31%	11.58%	2.23%	8.70%	19.77%	6.78%	16.36%	0.14%	15.45%	16.27%	11.89%	4.17	0.032
Rimmerzmatt	Backfilled	4	80	90	4.06%	11.39%	1.93%	12.75%	1.79%	9.96%	17.57%	7.04%	13.51%	0.33%	19.65%	13.18%	14.68%	4.31	0.050
Rimmerzmatt	Backfilled	4	90	100+	3.98%	12.65%	1.16%	15.18%	1.52%	10.28%	11.16%	16.84%	14.80%	0.19%	12.25%	14.16%	16.34%	4.55	0.033
Underi Site	Original	1	0	10	2.92%	8.39%	0.41%	8.45%	0.22%	7.39%	21.26%	5.09%	37.18%	-0.24%	8.94%	8.61%	8.85%	6.45	0.008
Underi Site	Original	1	10	20	3.62%	10.25%	1.87%	9.16%	1.22%	8.15%	16.88%	9.88%	33.20%	0.25%	5.53%	11.47%	11.03%	4.22	0.046
Underi Site	Original	1-2	20	30	2.94%	8.77%	1.20%	9.46%	1.12%	6.52%	16.19%	6.80%	35.42%	0.14%	11.43%	9.89%	10.66%	4.53	0.040
Underi Site	Original	2	30	40	4.05%	11.41%	1.32%	12.58%	1.52%	6.51%	15.59%	9.59%	32.56%	0.00%	4.87%	12.93%	13.90%	4.47	0.038
Underi Site	Original	2	40	50	3.76%	9.27%	0.54%	10.28%	1.50%	7.01%	15.07%	11.73%	33.31%	-0.07%	7.61%	10.77%	10.81%	4.84	0.031
Underi Site	Original	2-3	50	60	4.75%	10.78%	1.10%	12.05%	2.07%	7.42%	13.14%	5.50%	31.26%	0.47%	11.47%	12.84%	13.14%	5.34	0.036
Underi Site	Original	3	60	70	3.53%	9.62%	0.37%	11.32%	1.88%	7.11%	19.41%	5.88%	29.36%	0.08%	11.42%	11.50%	11.69%	4.39	0.038
Underi Site	Original	3	70	80	2.88%	8.85%	0.81%	10.82%	1.21%	4.47%	34.85%	12.51%	18.89%	-0.09%	4.81%	10.06%	11.63%	2.27	0.071
Underi Site	Original	4	80	90	2.45%	6.57%	2.20%	12.53%	1.86%	3.78%	29.25%	9.82%	20.67%	-0.03%	10.89%	8.43%	14.74%	0.54	0.666
Underi Site	Original	4	90	100	2.16%	5.44%	2.64%	8.74%	1.65%	3.44%	24.22%	14.46%	22.57%	0.03%	14.65%	7.09%	11.39%	0.15	2.838
Underi Site	Original	4	100	106	1.82%	3.96%	2.58%	8.90%	1.19%	2.77%	29.41%	11.43%	21.20%	-0.09%	16.81%	5.15%	11.49%	0.17	2.712
Underi Site	Backfilled	1	0	10	2.93%	9.42%	1.39%	11.99%	1.77%	5.59%	17.33%	21.43%	24.07%	0.04%	4.05%	11.18%	13.38%	0.54	0.426
Underi Site	Backfilled	1	10	20	2.87%	10.53%	1.93%	12.37%	4.48%	5.72%	15.50%	15.03%	27.37%	-0.30%	4.50%	15.01%	14.30%	0.44	0.940
Underi Site	Backfilled	1-2	20	30	3.12%	10.62%	1.57%	11.19%	2.46%	5.93%	24.68%	12.95%	24.12%	-0.08%	3.45%	13.07%	12.76%	0.33	0.802
Underi Site	Backfilled	2	30	40	3.11%	10.63%	1.37%	14.22%	2.47%	6.83%	22.79%	10.00%	24.12%	-0.08%	4.55%	13.10%	15.59%	0.33	0.777
Underi Site	Backfilled	2	40	50	3.26%	10.60%	1.98%	10.00%	2.53%	7.63%	12.48%	12.58%	31.96%	0.05%	6.93%	13.13%	11.98%	1.95	0.146
Underi Site	Backfilled	2-3	50	60	3.23%	9.42%	1.42%	9.42%	2.01%	7.88%	3.92%	23.46%	27.59%	0.07%	11.59%	11.42%	10.83%	3.36	0.072
Underi Site	Backfilled	3	60	70	3.36%	9.87%	1.14%	9.32%	2.54%	5.92%	12.11%	15.40%	29.25%	-0.20%	11.28%	12.42%	10.47%	2.93	0.087
Underi Site	Backfilled	3	70	80	4.32%	12.14%	1.39%	8.91%	2.42%	6.57%	10.30%	10.94%	32.60%	0.03%	10.38%	14.56%	10.30%	2.93	0.073
Underi Site	Backfilled	4	80	90	3.77%	10.42%	1.64%	11.48%	1.88%	7.03%	21.90%	8.27%	25.91%	-0.18%	7.89%	12.30%	13.12%	3.13	0.071
Underi Site	Backfilled	4	90	100	3.72%	10.76%	1.42%	10.85%	1.40%	6.11%	20.53%	19.07%	23.10%	0.02%	3.01%	12.16%	12.27%	2.49	0.071
Underi Site	Backfilled	4	100	108.5	4.25%	11.46%	1.44%	12.80%	1.51%	7.21%	14.44%	13.12%	29.73%	-0.34%	4.40%	12.97%	14.24%	3.10	0.056

9.5 DRIFT Data Bands

Site	Treatment	Tube	Depth_Min	Depth_Max	Band1: Aliphatic C-H stretching			Band2: C=O stretching of COOH,			Band3: C=O stretching of amide			Band4: Aromatic C=C, strongly H-			Band5: Aromtatic rings, amide II			Band6: N-H stretching of proteic amides		
					Results	Band_Start	Band_End	Results	Band_Start	Band_End	Results	Band_Start	Band_End	Results	Band_Start	Band_End	Results	Band_Start	Band_End	Results	Band_Start	Band_End
Lindergut	Original	1	0	10	1.95	2980	2886	0.07	1725	1710	0.30	1658	1631	0.03	1620	1600	0.17	1529	1502	0.04	1481	1470
Lindergut	Original	1	10	20	2.23	2980	2880	0.03	1716	1708	0.08	1660	1636	0.06	1620	1600	0.02	1520	1506	0.02	1487	1474
Lindergut	Original	1-2	20	30	2.20	2980	2887	0.07	1725	1710	0.18	1658	1631	0.03	1620	1600	0.12	1530	1503	0.02	1480	1470
Lindergut	Original	2	30	40	2.65	2980	2886	0.08	1725	1710	0.35	1659	1630	0.06	1620	1600	0.17	1530	1503	0.03	1494	1484
Lindergut	Original	2-3	40	50	3.03	2980	2880	0.12	1725	1710	0.24	1659	1632	0.10	1622	1592	0.27	1530	1503	0.05	1495	1486
Lindergut	Original	3	50	60	3.15	2980	2880	0.13	1725	1710	0.38	1659	1631	0.06	1620	1594	0.29	1530	1503	0.02	1493	1486
Lindergut	Original	3	60	70	2.42	2980	2880	0.12	1725	1710	0.37	1658	1632	0.06	1621	1602	0.27	1529	1503	0.05	1495	1484
Lindergut	Original	3	70	77	3.15	2980	2880	0.14	1725	1710	0.36	1659	1631	0.06	1620	1595	0.31	1531	1502	0.04	1493	1485
Lindergut	Backfilled	1	0	10	0.99	2974	2898	0.13	1725	1710	0.42	1658	1631	0.08	1620	1600	0.41	1529	1500	0.06	1493	1484
Lindergut	Backfilled	1	10	20	0.93	2968	2897	0.14	1723	1710	0.49	1659	1631	0.09	1620	1600	0.51	1529	1502	0.17	1495	1469
Lindergut	Backfilled	1-2	20	30	0.81	2972	2892	0.14	1725	1710	0.47	1659	1632	0.05	1620	1600	0.38	1530	1503	0.09	1481	1470
Lindergut	Backfilled	2	30	40	1.05	2980	2890	0.13	1725	1710	0.45	1659	1631	0.09	1620	1600	0.56	1529	1500	0.22	1494	1468
Lindergut	Backfilled	2	40	50	0.57	2962	2900	0.14	1722	1710	0.52	1658	1631	0.09	1620	1599	0.45	1530	1502	0.14	1494	1470
Lindergut	Backfilled	2-3	50	60	1.64	2980	2888	0.14	1725	1710	0.46	1658	1631	0.11	1620	1598	0.30	1530	1503	0.20	1495	1468
Lindergut	Backfilled	3	60	70	2.40	2980	2887	0.12	1725	1710	0.37	1658	1632	0.05	1620	1600	0.25	1529	1503	0.07	1481	1470
Lindergut	Backfilled	3	70	80	2.39	2980	2885	0.18	1725	1710	0.45	1659	1631	0.06	1620	1600	0.33	1530	1502	0.07	1482	1470
Lindergut	Backfilled	4	80	90	2.38	2980	2886	0.15	1725	1710	0.47	1658	1631	0.08	1621	1599	0.31	1529	1502	0.07	1481	1470
Lindergut	Backfilled	4	90	100	1.57	2980	2880	0.15	1725	1710	0.46	1659	1632	0.03	1620	1598	0.34	1530	1502	0.08	1479	1470
Lindergut	Backfilled	4-5	100	110	2.87	2980	2880	0.15	1725	1710	0.48	1658	1631	0.03	1620	1598	0.46	1530	1502	0.07	1479	1470
Lindergut	Backfilled	5	110	120	2.38	2980	2880	0.18	1725	1710	0.59	1659	1631	0.04	1620	1600	0.49	1529	1503	0.06	1478	1470
Lindergut	Backfilled	5	120	130	1.84	2980	2880	0.17	1725	1710	0.51	1659	1631	0.04	1620	1599	0.44	1529	1503	0.09	1479	1468
Lindergut	Backfilled	5	130	132	2.15	2980	2880	0.17	1725	1710	0.52	1658	1631	0.06	1621	1602	0.23	1532	1503	0.07	1480	1469
Rimmerzmatt	Original	1	0	10	2.01	2980	2880	0.12	1722	1710	0.34	1659	1631	0.02	1620	1605	0.26	1529	1503	0.05	1479	1471
Rimmerzmatt	Original	1	10	20	2.17	2980	2880	0.14	1725	1710	0.52	1658	1631	0.02	1620	1598	0.34	1530	1503	0.09	1480	1470
Rimmerzmatt	Original	1-2	20	30	2.11	2980	2880	0.17	1722	1710	0.55	1659	1631	0.03	1621	1602	0.38	1530	1502	0.04	1480	1470
Rimmerzmatt	Original	2	30	40	3.39	2980	2885	0.16	1725	1710	0.63	1660	1631	0.03	1620	1600	0.40	1530	1502	0.04	1478	1470
Rimmerzmatt	Original	2	40	50	3.41	2980	2880	0.17	1725	1710	0.56	1658	1632	0.05	1620	1605	0.47	1529	1503	0.05	1480	1470
Rimmerzmatt	Original	2-3	50	60	3.00	2980	2880	0.19	1725	1710	0.52	1658	1632	0.04	1621	1598	0.47	1530	1503	0.08	1480	1469
Rimmerzmatt	Original	3	60	70	3.26	2980	2886	0.19	1725	1710	0.52	1659	1630	0.04	1620	1605	0.48	1530	1503	0.07	1480	1470
Rimmerzmatt	Original	3	70	80	5.06	2980	2880	0.18	1725	1710	0.45	1659	1631	0.04	1620	1605	0.63	1530	1503	0.08	1479	1470
Rimmerzmatt	Original	4	80	90	4.50	2980	2880	0.17	1725	1710	0.50	1658	1631	0.07	1620	1599	0.74	1529	1500	0.06	1480	1470
Rimmerzmatt	Original	4	90	100	4.35	2980	2880	0.16	1725	1710	0.48	1658	1631	0.08	1621	1600	0.93	1530	1500	0.06	1479	1470
Rimmerzmatt	Original	4	100	106	2.50	2980	2880	0.17	1725	1710	0.39	1659	1632	0.11	1620	1600	0.75	1535	1503	0.06	1480	1470
Rimmerzmatt	Backfilled	1	0	10	0.39	2961	2901	0.15	1725	1710	0.45	1659	1631	0.10	1620	1600	0.80	1534	1502	0.15	1495	1470
Rimmerzmatt	Backfilled	1	10	20	0.35	2967	2901	0.16	1725	1710	0.52	1659	1631	0.08	1620	1600	0.66	1535	1500	0.15	1495	1470
Rimmerzmatt	Backfilled	1-2	20	30	0.40	2966	2906	0.16	1725	1710	0.47	1659	1633	0.12	1620	1600	0.84	1535	1500	0.12	1495	1470
Rimmerzmatt	Backfilled	2	30	40	0.45	2968	2900	0.16	1725	1710	0.47	1659	1632	0.12	1620	1600	0.70	1535	1503	0.15	1494	1470
Rimmerzmatt	Backfilled	2	40	50	0.57	2969	2898	0.16	1725	1710	0.46	1659	1630	0.13	1620	1600	0.83	1535	1502	0.22	1495	1468
Rimmerzmatt	Backfilled	2-3	50	60	1.19	2974	2893	0.17	1725	1710	0.50	1659	1632	0.10	1620	1600	0.44	1530	1502	0.13	1493	1468
Rimmerzmatt	Backfilled	3	60	70	2.48	2980	2880	0.19	1725	1710	0.54	1659	1632	0.05	1620	1600	0.44	1530	1503	0.10	1481	1470
Rimmerzmatt	Backfilled	4	70	80	2.80	2980	2880	0.16	1725	1710	0.50	1659	1631	0.01	1620	1600	0.41	1529	1503	0.08	1480	1470
Rimmerzmatt	Backfilled	4	80	90	3.14	2980	2880	0.17	1725	1710	0.48	1658	1630	0.08	1620	1599	0.53	1530	1502	0.08	1480	1470
Rimmerzmatt	Backfilled	4	90	100+	3.42	2980	2880	0.17	1725	1710	0.53	1659	1631	0.05	1619	1599	0.64	1531	1502	0.06	1480	1470
Underi Site	Original	1	0	10	2.80	2980	2880	0.11	1725	1710	0.31	1658	1631	0.02	1620	1600	0.31	1530	1503	0.01	1478	1470
Underi Site	Original	1	10	20	2.89	2980	2880	0.16	1725	1710	0.45	1659	1632	0.08	1620	1599	0.40	1531	1503	0.05	1480	1470
Underi Site	Original	1-2	20	30	2.88	2980	2882	0.15	1725	1710	0.43	1659	1632	0.06	1620	1599	0.47	1529	1503	0.06	1480	1470
Underi Site	Original	2	30	40	3.02	2980	2880	0.16	1725	1710	0.46	1659	1630	0.05	1620	1600	0.51	1529	1503	0.06	1480	1470
Underi Site	Original	2	40	50	2.94	2980	2880	0.17	1725	1710	0.41	1658	1631	0.02	1620	1599	0.46	1530	1503	0.07	1480	1470
Underi Site	Original	2-3	50	60	3.57	2987	2880	0.19	1725	1710	0.43	1659	1631	0.04	1620	1599	0.48	1529	1503	0.08	1479	1470
Underi Site	Original	3	60	70	2.91	2980	2880	0.17	1725	1710	0.47	1659	1632	0.02	1620	1604	0.55	1529	1503	0.09	1480	1470
Underi Site	Original	3	70	80	1.65	2980	2880	0.17	1725	1710	0.51	1659	1631	0.05	1620	1600	0.63	1535	1503	0.07	1480	1470
Underi Site	Original	4	80	90	0.38	2966	2898	0.15	1725	1710	0.41	1659	1632	0.14	1620	1600	0.77	1535	1500	0.12	1483	1470
Underi Site	Original	4	90	100	0.10	2963	2914	0.14	1725	1710	0.36	1659	1632	0.17	1620	1600	0.57	1535	1502	0.11	1483	1471
Underi Site	Original	4	100	106	0.10	2963	2913	0.14	1725	1710	0.30	1659	1632	0.19	1620	1600	0.67	1535	1502	0.09	1483	1470
Underi Site	Backfilled	1	0	10	0.33	2957	2899	0.13	1725	1710	0.42	1659	1631	0.06	1620	1600	0.54	1535	1502	0.08	1483	1470
Underi Site	Backfilled	1	10	20	0.32	2959	2899	0.13	1725	1710	0.49	1658	1631	0.09	1620	1600	0.58	1529	1502	0.21	1495	1470
Underi Site	Backfilled	1-2	20	30	0.24	2970	2898	0.15	1725	1710	0.51	1659	1631	0.08	1620	1600	0.54	1531	1503	0.12	1483	1470
Underi Site	Backfilled	2	30	40	0.24	2964	2902	0.15	1725	1710	0.51	1659	1632	0.07	1620	1600	0.69	1535	1502	0.12	1483	1470
Underi Site	Backfilled	2	40	50	1.19	2969	2894	0.13	1725	1710	0.41	1659	1632	0.08	1620	1600	0.38	1529	1503	0.10	1482	1470
Underi Site	Backfilled	2-3	50	60	2.00	2980	2883	0.14	1723	1710	0.40	1659	1631	0.06	1620	1600	0.40	1530	1503	0.09	1483	1470
Underi Site	Backfilled	3	60	70	1.92	2980	2880	0.15	1725	1710	0.45	1659	1631	0.05	1620	1600	0.43	1529	1503	0.12	1483	1470
Underi Site	Backfilled	3	70	80	1.88	2980	2880	0.16	1725	1710	0.44	1659	1631	0.05	1620	1600	0.32	1529	1504	0.09	1483	1470
Underi Site	Backfilled	4	80	90	2.23	2980	2880	0.17	1725	1710	0.47	1659	1631	0.07	1619	1600	0.52	1529	1503	0.09	1480	1470
Underi Site	Backfilled	4	90	100	1.79	2980	2880	0.17	1725	1710	0.49	1659	1632	0.06	1620	1599	0.49	1530	1502	0.06	1477	1470
Underi Site	Backfilled	4	100	108.5	2.17	2980	2880	0.17	1725	1710	0.47	1659	1631	0.06	1620	1599	0.52	1529	1503	0.06	1480	1470

Band7: Aliphatic C-H stretching			Band8: OH deformation & C-O			Band9: C-O stretching & OH			Band10: C-OH stretching of aliphatic,			Band11: Secondary alcohols			Band12: C-O stretching of		
Results	Band_Start	Band_End	Results	Band_Start	Band_End	Results	Band_Start	Band_End	Results	Band_Start	Band_End	Results	Band_Start	Band_End	Results	Band_Start	Band_End
0.15	1468	1442	0.94	1413	1359	0.25	1280	1225	1.26	1190	1127	0.01	1110	1120	0.27	1080	1044
0.13	1470	1440	0.60	1413	1363	0.31	1284	1224	1.49	1190	1129	0.01	1114	1125	0.48	1080	1037
0.16	1468	1440	1.07	1413	1349	0.41	1287	1227	1.10	1190	1135	0.00	1116	1127	0.23	1077	1043
0.24	1467	1440	1.38	1437	1357	0.40	1287	1228	0.98	1190	1141	0.00	1114	1125	0.53	1080	1040
0.19	1470	1442	0.63	1413	1348	0.21	1280	1226	1.18	1190	1133	0.00	1114	1125	0.28	1080	1041
0.25	1467	1444	0.61	1413	1348	0.83	1292	1226	1.00	1190	1142	0.01	1111	1122	0.31	1080	1044
0.22	1467	1443	0.65	1413	1347	0.43	1280	1226	1.01	1190	1139	0.01	1116	1127	0.32	1080	1040
0.20	1467	1441	0.68	1413	1347	0.37	1280	1223	1.19	1190	1132	-0.01	1113	1124	0.31	1080	1045
0.26	1470	1440	1.07	1413	1358	0.49	1286	1226	1.67	1201	1137	0.01	1118	1129	0.17	1077	1043
0.36	1468	1444	0.83	1413	1370	0.66	1293	1227	1.31	1190	1138	0.00	1122	1133	0.55	1078	1035
0.25	1470	1440	1.54	1413	1357	0.77	1295	1225	0.99	1190	1136	0.01	1116	1127	0.13	1077	1048
0.18	1467	1443	0.82	1413	1370	0.22	1280	1226	1.10	1190	1135	0.01	1123	1114	0.22	1073	1042
0.28	1470	1444	1.29	1413	1357	0.52	1299	1225	1.08	1190	1138	0.00	1116	1127	0.22	1079	1044
0.32	1467	1441	1.13	1413	1360	0.45	1291	1227	1.23	1189	1133	0.01	1128	1120	0.73	1075	1030
0.28	1470	1440	1.08	1413	1350	0.40	1284	1230	1.07	1190	1132	0.01	1110	1118	0.32	1080	1042
0.24	1470	1442	1.07	1413	1356	0.58	1290	1227	1.17	1190	1132	0.01	1110	1119	0.29	1080	1042
0.30	1470	1443	1.08	1413	1358	0.46	1287	1227	1.33	1190	1127	0.00	1116	1127	0.31	1080	1046
0.25	1467	1443	0.58	1413	1345	0.87	1280	1227	0.98	1190	1142	-0.01	1116	1127	0.14	1080	1049
0.27	1470	1443	0.57	1413	1347	0.76	1280	1224	1.11	1190	1135	0.01	1116	1127	0.14	1082	1053
0.24	1468	1445	0.69	1413	1347	0.67	1280	1226	1.18	1190	1137	0.01	1113	1120	0.00	1042	1035
0.21	1465	1445	0.72	1413	1349	0.47	1280	1226	0.84	1190	1148	0.01	1110	1121	0.12	1072	1051
0.27	1467	1444	0.65	1413	1352	0.40	1280	1227	1.06	1190	1142	0.00	1109	1120	0.11	1076	1051
0.26	1470	1440	0.73	1413	1348	0.53	1292	1231	1.30	1190	1132	0.01	1110	1120	0.22	1074	1046
0.28	1468	1443	0.78	1413	1352	0.46	1286	1230	1.12	1190	1136	0.01	1116	1127	0.10	1077	1050
0.27	1467	1445	0.83	1413	1350	0.46	1288	1226	1.17	1190	1135	0.01	1116	1125	0.09	1075	1049
0.33	1470	1440	0.51	1413	1357	0.14	1281	1227	0.25	1176	1147	0.01	1116	1127	0.59	1076	1033
0.34	1468	1440	0.64	1413	1349	0.33	1280	1200	0.17	1177	1145	0.01	1116	1127	0.48	1073	1030
0.40	1467	1442	0.49	1410	1354	0.31	1280	1208	0.11	1190	1145	0.01	1116	1127	0.38	1080	1030
0.32	1470	1445	0.51	1413	1354	0.38	1280	1200	0.14	1175	1142	0.02	1111	1120	0.20	1071	1030
0.33	1470	1444	0.80	1413	1351	0.22	1280	1227	0.78	1190	1143	0.01	1116	1124	1.02	1079	1029
0.37	1470	1440	0.59	1408	1333	0.60	1291	1229	1.17	1190	1132	0.01	1105	1116	0.91	1072	1030
0.42	1470	1443	0.76	1409	1333	0.87	1291	1227	1.49	1190	1127	0.01	1116	1127	0.79	1077	1030
0.26	1468	1443	2.78	1413	1333	0.56	1292	1255	0.98	1175	1135	0.00	1116	1127	0.41	1073	1033
0.19	1470	1445	1.13	1413	1368	0.74	1287	1227	1.41	1190	1127	-0.01	1116	1127	0.58	1080	1030
0.28	1468	1443	1.78	1413	1358	0.57	1290	1227	1.06	1190	1131	0.00	1116	1127	0.28	1080	1046
0.17	1470	1443	1.12	1413	1370	0.54	1285	1229	1.35	1190	1126	0.00	1116	1125	0.59	1080	1040
0.22	1470	1443	1.37	1413	1360	0.56	1297	1230	1.49	1190	1127	0.00	1116	1127	0.81	1073	1034
0.28	1468	1442	1.00	1415	1383	0.62	1289	1227	1.67	1190	1127	0.00	1110	1117	1.08	1072	1030
0.31	1468	1443	1.44	1413	1358	0.45	1293	1225	1.23	1190	1130	0.01	1116	1127	0.40	1074	1040
0.29	1468	1443	0.81	1413	1356	0.29	1284	1227	0.94	1190	1135	0.00	1116	1127	0.59	1074	1030
0.31	1468	1442	0.70	1413	1351	0.24	1280	1224	0.58	1185	1140	0.01	1116	1127	0.55	1074	1030
0.42	1470	1440	0.74	1413	1350	0.30	1280	1221	0.57	1184	1141	0.01	1116	1127	0.82	1079	1030
0.43	1470	1443	0.47	1412	1354	0.71	1280	1206	0.63	1189	1139	0.01	1116	1127	0.52	1078	1030
0.27	1470	1440	0.79	1413	1333	0.19	1280	1225	1.37	1190	1127	-0.01	1116	1127	0.33	1080	1042
0.35	1468	1442	0.73	1413	1333	0.43	1283	1228	1.44	1190	1130	0.01	1104	1115	0.24	1076	1048
0.32	1468	1440	0.80	1413	1333	0.34	1280	1226	1.74	1193	1130	0.01	1106	1117	0.56	1075	1034
0.26	1468	1445	0.63	1411	1333	0.39	1280	1226	1.31	1190	1132	0.00	1116	1127	0.20	1076	1042
0.31	1468	1440	0.67	1410	1333	0.52	1281	1224	1.49	1190	1127	0.00	1116	1127	0.34	1080	1045
0.30	1470	1443	0.53	1413	1346	0.22	1281	1226	1.26	1191	1129	0.02	1116	1127	0.46	1080	1040
0.35	1468	1442	0.95	1411	1333	0.29	1286	1253	1.44	1191	1130	0.00	1116	1127	0.56	1074	1036
0.26	1468	1444	2.02	1413	1333	0.73	1287	1231	1.10	1190	1136	-0.01	1116	1127	0.28	1080	1038
0.23	1468	1443	1.80	1413	1358	0.61	1288	1227	1.28	1190	1127	0.00	1116	1127	0.67	1074	1030
0.23	1468	1443	1.58	1413	1360	0.95	1294	1227	1.48	1190	1127	0.00	1110	1120	0.96	1077	1032
0.21	1468	1443	2.20	1413	1358	0.85	1295	1227	1.58	1190	1127	-0.01	1116	1127	1.26	1075	1030
0.25	1468	1443	0.78	1413	1371	0.96	1289	1226	1.08	1190	1131	0.00	1116	1120	0.18	1080	1049
0.27	1468	1442	0.72	1411	1381	0.70	1287	1227	1.28	1190	1132	-0.01	1116	1127	0.21	1080	1046
0.29	1468	1443	1.20	1413	1369	0.63	1288	1226	1.17	1190	1127	0.00	1116	1127	0.17	1080	1049
0.33	1468	1444	1.10	1413	1368	0.48	1286	1231	1.16	1190	1127	0.00	1116	1127	0.22	1080	1047
0.29	1468	1444	0.48	1413	1383	0.48	1284	1226	1.23	1190	1132	0.00	1116	1127	0.27	1080	1048
0.33	1468	1440	0.17	1410	1384	0.99	1292	1228	1.17	1190	1127	0.00	1116	1127	0.49	1080	1030
0.27	1468	1444	0.55	1413	1356	0.70	1294	1226	1.33	1190	1127	-0.01	1116	1127	0.51	1076	1030
0.24	1468	1444	0.37	1413	1355	0.39	1292	1239	1.17	1190	1130	0.00	1116	1120	0.37	1076	1038
0.32	1468	1443	0.99	1413	1333	0.37	1286	1226	1.17	1190	1132	-0.01	1116	1127	0.36	1074	1035
0.28	1468	1444	0.93	1413	1333	0.86	1290	1228	1.04	1190	1137	0.00	1116	1127	0.14	1076	1046
0.30	1468	1442	0.59	1410	1333	0.54	1280	1223	1.22	1190	1135	-0.01	1116	1127	0.18	1080	1047

9.6 Weathering indices

Profile	Type	Depth_Min	Depth_Max	Depth (cm)			Weathering Indices					
							(Ca+K)/Ti	A Index	B Index	CIA	WIP	(Na+K)/Ti
Lindergut	Original	0	10	5	1	C24JO101	32.7	0.898	0.615	38.5	54.4	15.2
Lindergut	Original	10	20	15	2	C24JO102	34.8	0.902	0.624	37.6	52.1	13.7
Lindergut	Original	20	30	25	3	C24JO103	29.0	0.892	0.583	41.7	49.6	14.5
Lindergut	Original	30	40	35	4	C24JO104	29.2	0.889	0.580	42.0	44.6	13.6
Lindergut	Original	40	50	45	5	C24JO105	25.4	0.878	0.546	45.4	43.6	13.3
Lindergut	Original	50	60	55	6	C24JO106	11.2	0.860	0.349	65.1	39.1	13.5
Lindergut	Original	60	70	65	7	C24JO107	11.5	0.867	0.355	64.5	41.2	11.6
Lindergut	Original	70	77	74	8	C24JO108	15.2	0.866	0.425	57.5	38.4	12.2
Lindergut	Backfilled	0	10	5	9	C24JO121	31.3	0.903	0.614	38.6	57.5	13.6
Lindergut	Backfilled	10	20	15	10	C24JO122	31.8	0.906	0.624	37.6	59.4	14.2
Lindergut	Backfilled	20	30	25	11	C24JO123	31.9	0.907	0.622	37.8	59.1	14.4
Lindergut	Backfilled	30	40	35	12	C24JO124	33.3	0.909	0.632	36.8	60.0	15.6
Lindergut	Backfilled	40	50	45	13	C24JO125	33.9	0.905	0.639	36.1	60.0	13.0
Lindergut	Backfilled	50	60	55	14	C24JO126	38.6	0.906	0.660	34.0	54.9	12.2
Lindergut	Backfilled	60	70	65	15	C24JO127	28.2	0.888	0.582	41.8	50.6	13.7
Lindergut	Backfilled	70	80	75	16	C24JO128	28.5	0.887	0.574	42.6	47.9	12.4
Lindergut	Backfilled	80	90	85	17	C24JO129	24.9	0.882	0.543	45.7	47.9	12.7
Lindergut	Backfilled	90	100	95	18	C24JO130	11.1	0.866	0.337	66.3	44.4	11.7
Lindergut	Backfilled	100	110	105	19	C24JO131	11.3	0.869	0.367	63.3	40.3	11.6
Lindergut	Backfilled	110	120	115	20	C24JO132	12.8	0.859	0.358	64.2	41.7	12.5
Lindergut	Backfilled	120	130	125	21	C24JO133	11.8	0.855	0.325	67.5	41.0	11.5
Lindergut	Backfilled	130	132	131	22	C24JO134	13.0	0.858	0.334	66.6	43.2	13.4
Rimmerzmatt	Original	0	10	5	23	C24CM201	13.0	0.872	0.409	59.1	42.2	13.1
Rimmerzmatt	Original	10	20	15	24	C24CM202	14.9	0.871	0.435	56.5	46.4	14.7
Rimmerzmatt	Original	20	30	25	25	C24CM203	14.1	0.863	0.430	57.0	44.1	12.9
Rimmerzmatt	Original	30	40	35	26	C24CM204	30.2	0.858	0.599	40.1	32.7	12.0
Rimmerzmatt	Original	40	50	45	27	C24CM205	79.2	0.884	0.783	21.7	24.1	11.8
Rimmerzmatt	Original	50	60	55	28	C24CM206	103.3	0.886	0.809	19.1	13.5	7.3
Rimmerzmatt	Original	60	70	65	29	C24CM207	189.6	0.924	0.900	10.0	25.7	16.7
Rimmerzmatt	Original	70	80	75	30	C24CM208	32.7	0.901	0.652	34.8	33.0	16.1
Rimmerzmatt	Original	80	90	85	31	C24CM209	26.0	0.910	0.587	41.3	33.7	18.8
Rimmerzmatt	Original	90	100	95	32	C24CM210	16.9	0.908	0.452	54.8	40.6	21.6
Rimmerzmatt	Original	100	106	103	33	C24CM211	32.4	0.937	0.550	45.0	53.0	42.2
Rimmerzmatt	Backfilled	0	10	5	34	C24CM231	11.3	0.920	0.350	65.0	44.3	25.4
Rimmerzmatt	Backfilled	10	20	15	35	C24CM232	10.7	0.914	0.341	65.9	46.1	24.5
Rimmerzmatt	Backfilled	20	30	25	36	C24CM233	11.7	0.922	0.336	66.4	41.1	24.7
Rimmerzmatt	Backfilled	30	40	35	37	C24CM234	12.1	0.925	0.358	64.2	42.4	28.6
Rimmerzmatt	Backfilled	40	50	45	38	C24CM235	12.1	0.928	0.346	65.4	39.4	27.1
Rimmerzmatt	Backfilled	50	60	55	39	C24CM236	37.5	0.912	0.624	37.6	50.0	20.3
Rimmerzmatt	Backfilled	60	70	65	40	C24CM237	24.1	0.890	0.549	45.1	38.1	19.0
Rimmerzmatt	Backfilled	70	80	75	41	C24CM238	28.2	0.879	0.595	40.5	31.0	22.4
Rimmerzmatt	Backfilled	80	90	85	42	C24CM239	34.0	0.890	0.632	36.8	27.1	22.5
Rimmerzmatt	Backfilled	90	100+	100	43	C24CM240	41.3	0.885	0.691	30.9	13.2	41.4
Underi Site	Original	0	10	5	44	C24CM301	10.7	0.885	0.400	60.0	36.8	12.8
Underi Site	Original	10	20	15	45	C24CM302	10.5	0.884	0.383	61.7	34.4	11.8
Underi Site	Original	20	30	25	46	C24CM303	10.7	0.884	0.387	61.3	35.6	12.2
Underi Site	Original	30	40	35	47	C24CM304	10.5	0.882	0.385	61.5	35.0	11.7
Underi Site	Original	40	50	45	48	C24CM305	10.1	0.881	0.380	62.0	36.1	12.1
Underi Site	Original	50	60	55	49	C24CM306	11.4	0.860	0.386	61.4	27.7	12.4
Underi Site	Original	60	70	65	50	C24CM307	8.3	0.893	0.326	67.4	31.7	13.1
Underi Site	Original	70	80	75	51	C24CM308	8.6	0.924	0.366	63.4	35.5	16.4
Underi Site	Original	80	90	85	52	C24CM309	47.5	0.939	0.722	27.8	54.7	14.7
Underi Site	Original	90	100	95	53	C24CM310	8.5	0.940	0.300	70.0	29.7	16.4
Underi Site	Original	100	106	103	54	C24CM311	9.8	0.941	0.330	67.0	32.1	21.6
Underi Site	Backfilled	0	10	5	55	C24CM341	25.3	0.908	0.580	42.0	61.8	17.5
Underi Site	Backfilled	10	20	15	56	C24CM342	25.7	0.907	0.581	41.9	61.4	16.8
Underi Site	Backfilled	20	30	25	57	C24CM343	29.1	0.907	0.602	39.8	63.5	16.5
Underi Site	Backfilled	30	40	35	58	C24CM344	32.2	0.904	0.626	37.4	66.3	15.2
Underi Site	Backfilled	40	50	45	59	C24CM345	23.3	0.914	0.570	43.0	51.3	16.8
Underi Site	Backfilled	50	60	55	60	C24CM346	19.0	0.918	0.532	46.8	46.9	18.6
Underi Site	Backfilled	60	70	65	61	C24CM347	20.7	0.918	0.537	46.3	44.8	17.1
Underi Site	Backfilled	70	80	75	62	C24CM348	20.4	0.917	0.534	46.6	44.2	16.8
Underi Site	Backfilled	80	90	85	63	C24CM349	12.8	0.914	0.455	54.5	42.8	18.0
Underi Site	Backfilled	90	100	95	64	C24CM350	10.2	0.893	0.390	61.0	40.3	13.3
Underi Site	Backfilled	100	108.5	104	65	C24CM351	10.0	0.882	0.405	59.5	43.6	13.7

9.7 XRF

Site	Treatment	Tube	Depth_Min	Depth_Max	Na	Mg	Al	Si	P	S	Cl	K	Ca	Ti	V	Cr	Mn	Fe	Co	Ni	Cu	Zn	Ga	Ge	As
					%	%	%	%	%	%	%	%	%	%	%	%	%	%	%	%	%	%	%	%	%
Lindergut	Original	1	0	10	1.00	1.07	6.61	24.86	0.16	0.21	0.00	1.88	6.15	0.29	0.01	0.01	0.04	2.13	0.00	0.00	0.01	0.01	0.00	0.00	0.00
Lindergut	Original	1	10	20	0.75	1.05	6.32	24.70	0.15	0.20	0.00	1.80	6.32	0.28	0.01	0.01	0.04	2.06	0.00	0.00	0.01	0.01	0.00	0.00	0.00
Lindergut	Original	1-2	20	30	0.89	0.98	6.47	23.10	0.18	0.23	0.00	1.81	5.43	0.28	0.01	0.01	0.04	2.09	0.00	0.00	0.01	0.01	0.00	0.00	0.00
Lindergut	Original	2	30	40	0.77	0.97	6.42	22.21	0.18	0.25	0.01	1.78	5.10	0.28	0.01	0.01	0.04	2.09	0.00	0.00	0.01	0.01	0.00	0.00	0.00
Lindergut	Original	2-3	40	50	0.78	0.91	6.44	20.01	0.16	0.29	0.01	1.71	4.39	0.28	0.01	0.01	0.04	2.14	0.00	0.00	0.01	0.01	0.00	0.00	0.00
Lindergut	Original	3	50	60	0.94	0.98	7.13	20.76	0.13	0.27	0.01	1.99	2.74	0.32	0.01	0.01	0.04	2.29	0.00	0.00	0.01	0.01	0.00	0.00	0.00
Lindergut	Original	3	60	70	0.88	1.21	8.58	26.61	0.08	0.18	0.00	2.42	1.77	0.41	0.02	0.01	0.02	2.54	0.00	0.00	0.00	0.01	0.00	0.00	0.00
Lindergut	Original	3	70	77	0.80	1.02	7.05	20.96	0.07	0.38	0.01	1.92	2.44	0.33	0.01	0.01	0.02	2.42	0.00	0.00	0.00	0.01	0.00	0.00	0.00
Lindergut	Backfilled	1	0	10	0.96	1.31	7.06	28.36	0.07	0.11	0.01	1.98	6.77	0.33	0.01	0.01	0.04	2.42	0.00	0.00	0.00	0.01	0.00	0.00	0.00
Lindergut	Backfilled	1	10	20	1.05	1.28	6.91	28.52	0.06	0.09	0.00	1.95	6.80	0.32	0.01	0.01	0.04	2.43	0.00	0.00	0.00	0.01	0.00	0.00	0.00
Lindergut	Backfilled	1-2	20	30	1.07	1.23	7.00	29.37	0.06	0.09	0.00	1.99	6.76	0.32	0.01	0.01	0.04	2.40	0.00	0.00	0.00	0.01	0.00	0.00	0.00
Lindergut	Backfilled	2	30	40	1.17	1.25	6.77	29.11	0.07	0.10	0.02	1.96	6.73	0.31	0.01	0.01	0.04	2.39	0.00	0.00	0.00	0.01	0.00	0.00	0.00
Lindergut	Backfilled	2	40	50	0.91	1.29	6.91	28.08	0.06	0.09	0.00	1.92	7.69	0.33	0.01	0.01	0.04	2.55	0.00	0.00	0.00	0.01	0.00	0.00	0.00
Lindergut	Backfilled	2-3	50	60	0.71	1.06	6.22	24.88	0.06	0.14	0.00	1.64	8.17	0.28	0.01	0.01	0.04	2.32	0.00	0.00	0.00	0.01	0.00	0.00	0.00
Lindergut	Backfilled	3	60	70	0.95	1.06	6.79	23.16	0.11	0.21	0.00	1.71	5.32	0.30	0.01	0.01	0.04	2.20	0.00	0.00	0.00	0.01	0.00	0.00	0.00
Lindergut	Backfilled	3	70	80	0.75	1.07	6.82	23.16	0.10	0.21	0.00	1.71	5.46	0.30	0.01	0.01	0.04	2.18	0.00	0.00	0.01	0.01	0.00	0.00	0.00
Lindergut	Backfilled	4	80	90	0.85	1.09	7.22	23.60	0.08	0.20	0.00	1.81	4.86	0.31	0.01	0.01	0.04	2.32	0.00	0.00	0.00	0.01	0.00	0.00	0.00
Lindergut	Backfilled	4	90	100	0.94	1.33	9.50	29.40	0.05	0.12	0.00	2.68	1.54	0.45	0.02	0.01	0.02	2.68	0.00	0.00	0.00	0.01	0.00	0.00	0.00
Lindergut	Backfilled	4-5	100	110	0.91	1.20	7.87	24.72	0.04	0.39	0.01	2.15	1.93	0.39	0.01	0.01	0.01	2.55	0.00	0.00	0.00	0.01	0.00	0.00	0.00
Lindergut	Backfilled	5	110	120	0.80	1.15	8.43	24.31	0.04	0.35	0.00	2.52	1.79	0.38	0.01	0.01	0.01	2.86	0.00	0.00	0.00	0.01	0.00	0.00	0.00
Lindergut	Backfilled	5	120	130	0.75	1.22	9.40	26.39	0.03	0.25	0.00	2.55	1.58	0.41	0.02	0.01	0.01	2.72	0.00	0.01	0.01	0.01	0.00	0.00	0.00
Lindergut	Backfilled	5	130	132	0.86	1.24	9.31	26.96	0.03	0.19	0.00	2.58	1.57	0.37	0.02	0.01	0.01	2.39	0.00	0.00	0.01	0.01	0.00	0.00	0.00
Rimmerzmatt	Original	1	0	10	1.16	1.16	7.50	23.86	0.11	0.17	0.00	1.65	2.85	0.34	0.01	0.01	0.07	3.38	0.00	0.00	0.01	0.01	0.00	0.00	0.00
Rimmerzmatt	Original	1	10	20	1.42	1.25	8.05	25.18	0.11	0.18	0.00	1.71	2.81	0.34	0.01	0.01	0.07	3.44	0.00	0.00	0.01	0.01	0.00	0.00	0.00
Rimmerzmatt	Original	1-2	20	30	1.29	1.25	8.03	23.26	0.09	0.19	0.00	1.52	2.75	0.35	0.01	0.01	0.06	3.64	0.00	0.00	0.01	0.01	0.00	0.00	0.00
Rimmerzmatt	Original	2	30	40	0.72	0.77	4.66	11.03	0.05	0.50	0.01	0.68	4.50	0.19	0.01	0.01	0.04	2.46	0.00	0.00	0.01	0.00	0.00	0.00	0.00
Rimmerzmatt	Original	2	40	50	0.31	0.43	1.93	3.99	0.01	0.76	0.01	0.21	6.49	0.08	0.01	0.00	0.04	1.54	0.00	0.00	0.00	0.00	0.00	0.00	0.00
Rimmerzmatt	Original	2-3	50	60	0.08	0.36	0.99	1.81	0.00	0.74	0.01	0.07	7.44	0.04	0.00	0.00	0.06	1.45	0.00	0.00	0.00	0.00	0.00	0.00	0.00
Rimmerzmatt	Original	3	60	70	0.27	0.33	0.94	1.51	0.01	0.70	0.01	0.06	7.30	0.04	0.00	0.00	0.04	1.31	0.00	0.00	0.00	0.00	0.00	0.00	0.00
Rimmerzmatt	Original	3	70	80	0.90	0.48	3.72	14.01	0.01	0.58	0.01	0.78	4.12	0.18	0.00	0.00	0.01	0.97	0.00	0.00	0.00	0.00	0.00	0.00	0.00
Rimmerzmatt	Original	4	80	90	0.99	0.57	3.99	18.04	0.02	0.47	0.01	1.04	2.90	0.18	0.00	0.01	0.01	1.08	0.00	0.00	0.00	0.00	0.00	0.00	0.00
Rimmerzmatt	Original	4	90	100	1.38	0.86	5.87	27.62	0.03	0.27	0.01	1.74	1.56	0.23	0.01	0.01	0.02	1.53	0.00	0.00	0.00	0.00	0.00	0.00	0.00
Rimmerzmatt	Original	4	100	106	2.00	0.47	5.57	39.64	0.03	0.09	0.01	2.39	0.67	0.17	0.00	0.00	0.01	1.13	0.00	0.00	0.00	0.00	0.00	0.00	0.00
Rimmerzmatt	Backfilled	1	0	10	1.33	1.03	5.21	29.91	0.05	0.05	0.01	1.79	0.01	0.20	0.01	0.01	0.06	2.04	0.00	0.00	0.00	0.01	0.00	0.00	0.00
Rimmerzmatt	Backfilled	1	10	20	1.39	1.11	5.59	29.53	0.05	0.05	0.00	1.82	0.01	0.21	0.01	0.01	0.07	2.11	0.00	0.00	0.00	0.01	0.00	0.00	0.00
Rimmerzmatt	Backfilled	1-2	20	30	1.15	0.90	5.06	29.92	0.04	0.05	0.00	1.73	0.01	0.18	0.01	0.01	0.06	1.93	0.00	0.00	0.00	0.01	0.00	0.00	0.00
Rimmerzmatt	Backfilled	2	30	40	1.29	0.82	4.70	28.79	0.04	0.06	0.00	1.58	0.01	0.16	0.01	0.01	0.06	1.77	0.00	0.00	0.00	0.01	0.00	0.00	0.00
Rimmerzmatt	Backfilled	2	40	50	1.13	0.80	4.55	29.40	0.02	0.05	0.00	1.53	0.01	0.16	0.00	0.01	0.06	1.74	0.00	0.00	0.00	0.00	0.00	0.00	0.00
Rimmerzmatt	Backfilled	2-3	50	60	1.16	0.97	5.50	24.80	0.04	0.12	0.00	1.49	8.26	0.21	0.01	0.01	0.08	2.42	0.00	0.00	0.00	0.01	0.00	0.00	0.00
Rimmerzmatt	Backfilled	3	60	70	1.13	0.82	4.81	17.10	0.06	0.25	0.01	1.11	5.34	0.20	0.01	0.01	0.10	2.70	0.00	0.00	0.00	0.00	0.00	0.00	0.00
Rimmerzmatt	Backfilled	4	70	80	1.06	0.66	3.45	10.43	0.05	0.32	0.01	0.68	5.19	0.14	0.00	0.00	0.08	2.76	0.00	0.00	0.00	0.00	0.00	0.00	0.00
Rimmerzmatt	Backfilled	4	80	90	0.83	0.57	2.77	9.22	0.04	0.41	0.01	0.61	5.51	0.11	0.00	0.00	0.07	2.49	0.00	0.00	0.00	0.00	0.00	0.00	0.00
Rimmerzmatt	Backfilled	4	90	100+	0.57	0.30	0.95	2.69	0.01	0.40	0.01	0.16	5.41	0.03	0.00	0.00	0.04	1.67	0.00	0.00	0.00	0.00	0.00	0.00	0.00
Underi Site	Original	1	0	10	1.16	0.86	6.63	24.33	0.16	0.43	0.01	1.69	1.51	0.35	0.01	0.01	0.05	3.22	0.00	0.00	0.00	0.01	0.00	0.00	0.00
Underi Site	Original	1	10	20	0.96	0.85	6.50	23.76	0.16	0.43	0.01	1.66	1.48	0.34	0.01	0.01	0.04	3.14	0.00	0.00	0.00	0.01	0.00	0.00	0.00
Underi Site	Original	1-2	20	30	1.05	0.93	6.78	24.68	0.16	0.42	0.01	1.68	1.66	0.35	0.01	0.01	0.05	3.25	0.00	0.00	0.00	0.01	0.00	0.00	0.00
Underi Site	Original	2	30	40	0.99	0.91	6.69	23.83	0.16	0.42	0.01	1.64	1.69	0.35	0.01	0.01	0.05	3.34	0.00	0.00	0.00	0.01	0.00	0.00	0.00
Underi Site	Original	2	40	50	1.10	0.96	6.89	24.24	0.15	0.46	0.01	1.70	1.39	0.36	0.02	0.01	0.04	3.38	0.00	0.00	0.00	0.01	0.00	0.00	0.00
Underi Site	Original	2-3	50	60	0.81	0.61	5.49	15.81	0.08	0.89	0.01	1.27	1.22	0.26	0.01	0.01	0.01	2.68	0.00	0.00	0.00	0.00	0.00	0.00	0.00
Underi Site	Original	3	60	70	1.08	0.78	6.48	26.38	0.07	0.52	0.01	1.54	0.70	0.32	0.01	0.01	0.01	2.52	0.00	0.00	0.00	0.01	0.00	0.00	0.00
Underi Site	Original	3	70	80	1.49	0.76	6.28	37.76	0.04	0.15	0.01	1.56	0.66	0.30	0.01	0.01	0.02	1.88	0.00	0.00	0.00	0.01	0.00	0.00	0.00
Underi Site	Original	4	80	90	0.87	0.84	4.89	32.45	0.00	0.08	0.00	1.35	9.10	0.24	0.01	0.01	0.03	1.69	0.00	0.00	0.00	0.00	0.00	0.00	0.00
Underi Site	Original	4	90	100	0.67	0.75	3.81	30.51	0.00	0.06	0.00	1.20	0.01	0.18	0.00	0.01	0.03	1.36	0.00	0.00	0.00	0.00	0.00	0.00	0.00
Underi Site	Original	4	100	106	0.85	0.70	3.73	30.07	0.00	0.07	0.00	1.19	0.01	0.15	0.00	0.01	0.03	1.42	0.00	0.00	0.00	0.00	0.00	0.00	0.00
Underi Site	Backfilled	1	0	10	1.55	1.42	7.38	32.62	0.08	0.05	0.00	2.39	5.16	0.35	0.01	0.01	0.08	3.07	0.00	0.00	0.00	0.01	0.00	0.00	0.00
Underi Site	Backfilled	1	10	20	1.42	1.44	7.33	32.04	0.07	0.05	0.00	2.38	5.38	0.35	0.01	0.01	0.08	3.11	0.00	0.00	0.00	0.01	0.00	0.00	0.00
Underi Site	Backfilled	1-2	20	30	1.35	1.49	7.46	31.88	0.06	0.05	0.00	2.37	6.14	0.35	0.01	0.01	0.08	3.08	0.00	0.00	0.00	0.01	0.00	0.00	0.00
Underi Site	Backfilled	2	30	40	1.17	1.54	7.42	29.81	0.05	0.05	0.00	2.36	7.14	0.35	0.01	0.01	0.08	3.27	0.00	0.00	0.00	0.01	0.00	0.00	0.00
Underi Site	Backfilled	2	40	50	1.34	1.02	6.26	30.46	0.11	0.16	0.00	1.93	4.37	0.31	0.01	0.01	0.07	3.07	0.00	0.00	0.00	0.01	0.00	0.00	0.00
Underi Site	Backfilled	2-3	50	60	1.56	0.86	6.01	31.26	0.15	0.22	0.01	1.77	2.90	0.29	0.01	0.01	0.07	3.03	0.00	0.00	0.00	0.01	0.00	0.00	0.00
Underi Site	Backfilled	3	60	70	1.29	0.80	5.94	30.84	0.17	0.24	0.01	1.74	3.24	0.28	0.01	0.01	0.07	2.96	0.00	0.00	0.00	0.01	0.00	0.00	0.00
Underi Site	Backfilled	3	70	80	1.28	0.82	6.00	30.98	0.17	0.24	0.01	1.74	3.16	0.29	0.01	0.01	0.07	3.02	0.00	0.00	0.00	0.01	0.00	0.00	0.00
Underi Site	Backfilled	4	80	90	1.63	0.82	6.18	31.30	0.14	0.28	0.01	1.77	1.64	0.31	0.01	0.01	0.06	3.29	0.00	0.00	0.00	0.01	0.00	0.00	0.00
Underi Site	Backfilled	4	90	100	1.28	0.86	7.12	28.59	0.11	0.40	0.01	2.07	1.30	0.39	0.01	0.01	0.04	4.26	0.00	0.00	0.00	0.01	0.00	0.00	0.00
Underi Site	Backfilled	4	100	108.5	1.29	0.59	6.52	22.99	0.06	0.48	0.01	2.28	1.03	0.40	0.01	0.01	0.02	4.01	0.00	0.00	0.00	0.00	0.00	0.00	0.00

Se	Br	Rb	Sr	Y	Zr	Nb	Mo	Ru	Rh	Pd	Ag	Cd	In	Sn	Sb	Te	I	Cs	Ba	La	Ce	Pr	Nd	Sm	Hf	Ta	W	Au	Hg	Tl	Pb	Bi	Th	U
%	%	%	%	%	%	%	%	%	%	%	%	%	%	%	%	%	%	%	%	%	%	%	%	%	%	%	%	%	%	%	%	%	%	%
0.00	0.00	0.01	0.02	0.00	0.01	0.00	0.00	0.00	0.00	0.00	0.00	0.00	0.00	0.00	0.00	0.00	0.00	0.00	0.03	0.00	0.01	0.01	0.01	0.00	0.00	0.00	0.01	0.00	0.00	0.00	0.00	0.00	0.00	0.00
0.00	0.00	0.01	0.02	0.00	0.01	0.00	0.00	0.00	0.00	0.00	0.00	0.00	0.00	0.00	0.00	0.00	0.00	0.00	0.03	0.01	0.01	0.01	0.01	0.00	0.00	0.00	0.01	0.00	0.00	0.00	0.00	0.00	0.00	0.00
0.00	0.00	0.01	0.02	0.00	0.01	0.00	0.00	0.00	0.00	0.00	0.00	0.00	0.00	0.00	0.00	0.00	0.00	0.00	0.04	0.01	0.01	0.01	0.02	0.00	0.00	0.00	0.01	0.00	0.00	0.00	0.00	0.00	0.00	0.00
0.00	0.00	0.01	0.02	0.00	0.01	0.00	0.00	0.00	0.00	0.00	0.00	0.00	0.00	0.00	0.00	0.00	0.00	0.00	0.04	0.01	0.01	0.01	0.01	0.00	0.00	0.00	0.01	0.00	0.00	0.00	0.00	0.00	0.00	0.00
0.00	0.00	0.01	0.01	0.00	0.01	0.00	0.00	0.00	0.00	0.00	0.00	0.00	0.00	0.00	0.00	0.00	0.00	0.00	0.04	0.01	0.01	0.02	0.02	0.00	0.00	0.00	0.00	0.00	0.00	0.00	0.00	0.00	0.00	0.00
0.00	0.00	0.01	0.01	0.00	0.01	0.00	0.00	0.00	0.00	0.00	0.00	0.00	0.00	0.00	0.00	0.00	0.00	0.00	0.04	0.01	0.01	0.01	0.01	0.00	0.00	0.00	0.00	0.00	0.00	0.00	0.00	0.00	0.00	0.00
0.00	0.00	0.01	0.01	0.00	0.01	0.00	0.00	0.00	0.00	0.00	0.00	0.00	0.00	0.00	0.00	0.00	0.00	0.00	0.04	0.01	0.01	0.01	0.01	0.00	0.00	0.00	0.00	0.00	0.00	0.00	0.00	0.00	0.00	0.00
0.00	0.00	0.01	0.01	0.00	0.01	0.00	0.00	0.00	0.00	0.00	0.00	0.00	0.00	0.00	0.00	0.00	0.00	0.00	0.03	0.00	0.01	0.01	0.01	0.00	0.00	0.00	0.00	0.00	0.00	0.00	0.00	0.00	0.00	0.00
0.00	0.00	0.01	0.02	0.00	0.01	0.00	0.00	0.00	0.00	0.00	0.00	0.00	0.00	0.00	0.00	0.00	0.00	0.00	0.04	0.01	0.02	0.02	0.03	0.00	0.00	0.00	0.01	0.00	0.00	0.00	0.00	0.00	0.00	0.00
0.00	0.00	0.01	0.02	0.00	0.01	0.00	0.00	0.00	0.00	0.00	0.00	0.00	0.00	0.00	0.00	0.00	0.00	0.00	0.04	0.01	0.01	0.01	0.01	0.00	0.00	0.00	0.01	0.00	0.00	0.00	0.00	0.00	0.00	0.00
0.00	0.00	0.01	0.02	0.00	0.01	0.00	0.00	0.00	0.00	0.00	0.00	0.00	0.00	0.00	0.00	0.00	0.00	0.00	0.03	0.01	0.01	0.01	0.01	0.00	0.00	0.00	0.01	0.00	0.00	0.00	0.00	0.00	0.00	0.00
0.00	0.00	0.01	0.02	0.00	0.01	0.00	0.00	0.00	0.00	0.00	0.00	0.00	0.00	0.00	0.00	0.00	0.00	0.00	0.03	0.01	0.01	0.01	0.01	0.00	0.00	0.00	0.01	0.00	0.00	0.00	0.00	0.00	0.00	0.00
0.00	0.00	0.01	0.02	0.00	0.01	0.00	0.00	0.00	0.00	0.00	0.00	0.00	0.00	0.00	0.00	0.00	0.00	0.00	0.04	0.01	0.01	0.01	0.02	0.00	0.00	0.00	0.01	0.00	0.00	0.00	0.00	0.00	0.00	0.00
0.00	0.00	0.01	0.02	0.00	0.01	0.00	0.00	0.00	0.00	0.00	0.00	0.00	0.00	0.00	0.00	0.00	0.00	0.00	0.03	0.01	0.01	0.01	0.01	0.00	0.00	0.00	0.01	0.00	0.00	0.00	0.00	0.00	0.00	0.00
0.00	0.00	0.01	0.02	0.00	0.01	0.00	0.00	0.00	0.00	0.00	0.00	0.00	0.00	0.00	0.00	0.00	0.00	0.00	0.04	0.00	0.01	0.01	0.01	0.00	0.00	0.00	0.00	0.00	0.00	0.00	0.00	0.00	0.00	0.00
0.00	0.00	0.01	0.02	0.00	0.01	0.00	0.00	0.00	0.00	0.00	0.00	0.00	0.00	0.00	0.00	0.00	0.00	0.00	0.03	0.01	0.01	0.01	0.01	0.00	0.00	0.00	0.01	0.00	0.00	0.00	0.00	0.00	0.00	0.00
0.00	0.00	0.01	0.02	0.00	0.01	0.00	0.00	0.00	0.00	0.00	0.00	0.00	0.00	0.00	0.00	0.00	0.00	0.00	0.04	0.01	0.01	0.01	0.01	0.00	0.00	0.00	0.00	0.00	0.00	0.00	0.01	0.00	0.00	0.00
0.00	0.00	0.02	0.01	0.00	0.01	0.00	0.00	0.00	0.00	0.00	0.00	0.00	0.00	0.00	0.00	0.00	0.00	0.00	0.04	0.01	0.01	0.01	0.01	0.00	0.00	0.00	0.00	0.00	0.00	0.00	0.00	0.00	0.00	0.00
0.00	0.00	0.01	0.01	0.00	0.01	0.00	0.00	0.00	0.00	0.00	0.00	0.00	0.00	0.00	0.00	0.00	0.00	0.00	0.04	0.01	0.01	0.01	0.01	0.00	0.00	0.00	0.00	0.00	0.00	0.00	0.00	0.00	0.00	0.00
0.00	0.00	0.02	0.01	0.00	0.01	0.00	0.00	0.00	0.00	0.00	0.00	0.00	0.00	0.00	0.00	0.00	0.00	0.00	0.04	0.01	0.01	0.01	0.01	0.00	0.00	0.00	0.00	0.00	0.00	0.00	0.00	0.00	0.00	0.00
0.00	0.00	0.02	0.01	0.00	0.01	0.00	0.00	0.00	0.00	0.00	0.00	0.00	0.00	0.00	0.00	0.00	0.00	0.00	0.05	0.01	0.01	0.01	0.02	0.00	0.00	0.00	0.00	0.00	0.00	0.00	0.00	0.00	0.00	0.00
0.00	0.00	0.02	0.01	0.00	0.01	0.00	0.00	0.00	0.00	0.00	0.00	0.00	0.00	0.00	0.00	0.00	0.00	0.00	0.05	0.01	0.02	0.02	0.02	0.00	0.00	0.00	0.00	0.00	0.00	0.00	0.00	0.00	0.00	0.00
0.00	0.00	0.01	0.01	0.00	0.01	0.00	0.00	0.00	0.00	0.00	0.00	0.00	0.00	0.00	0.00	0.00	0.00	0.00	0.05	0.01	0.01	0.01	0.01	0.00	0.00	0.00	0.00	0.00	0.00	0.00	0.00	0.00	0.00	0.00
0.00	0.00	0.01	0.01	0.00	0.01	0.00	0.00	0.00	0.00	0.00	0.00	0.00	0.00	0.00	0.00	0.00	0.00	0.00	0.06	0.01	0.01	0.01	0.01	0.00	0.00	0.00	0.01	0.00	0.00	0.00	0.00	0.00	0.00	0.00
0.00	0.00	0.01	0.01	0.00	0.01	0.00	0.00	0.00	0.00	0.00	0.00	0.00	0.00	0.00	0.00	0.00	0.00	0.00	0.06	0.01	0.01	0.01	0.01	0.00	0.00	0.00	0.00	0.00	0.00	0.00	0.00	0.00	0.00	0.00
0.00	0.00	0.00	0.02	0.00	0.00	0.00	0.00	0.00	0.00	0.00	0.00	0.00	0.00	0.00	0.00	0.00	0.00	0.00	0.04	0.00	0.01	0.01	0.01	0.00	0.00	0.00	0.00	0.00	0.00	0.00	0.00	0.00	0.00	0.01
0.00	0.00	0.00	0.02	0.00	0.00	0.00	0.00	0.00	0.00	0.00	0.00	0.00	0.00	0.00	0.00	0.00	0.00	0.00	0.04	0.00	0.01	0.01	0.01	0.00	0.00	0.00	0.00	0.00	0.00	0.00	0.00	0.00	0.00	0.01
0.00	0.00	0.00	0.03	0.00	0.00	0.00	0.00	0.00	0.00	0.00	0.00	0.00	0.00	0.00	0.00	0.00	0.00	0.00	0.04	0.00	0.00	0.00	0.00	0.00	0.00	0.00	0.00	0.00	0.00	0.00	0.00	0.00	0.00	0.01
0.00	0.00	0.00	0.03	0.00	0.00	0.00	0.00	0.00	0.00	0.00	0.00	0.00	0.00	0.00	0.00	0.00	0.00	0.00	0.03	0.00	0.00	0.00	0.00	0.00	0.00	0.00	0.00	0.00	0.00	0.00	0.00	0.00	0.00	0.01
0.00	0.00	0.00	0.02	0.00	0.01	0.00	0.00	0.00	0.00	0.00	0.00	0.00	0.00	0.00	0.00	0.00	0.00	0.00	0.04	0.01	0.01	0.01	0.01	0.00	0.00	0.00	0.01	0.00	0.00	0.00	0.00	0.00	0.00	0.00
0.00	0.00	0.00	0.01	0.00	0.01	0.00	0.00	0.00	0.00	0.00	0.00	0.00	0.00	0.00	0.00	0.00	0.00	0.00	0.03	0.00	0.01	0.00	0.01	0.00	0.00	0.00	0.01	0.00	0.00	0.00	0.00	0.00	0.00	0.00
0.00	0.00	0.01	0.01	0.00	0.01	0.00	0.00	0.00	0.00	0.00	0.00	0.00	0.00	0.00	0.00	0.00	0.00	0.00	0.04	0.01	0.01	0.01	0.02	0.00	0.00	0.00	0.02	0.00	0.00	0.00	0.00	0.00	0.00	0.00
0.00	0.00	0.01	0.01	0.00	0.01	0.00	0.00	0.00	0.00	0.00	0.00	0.00	0.00	0.00	0.00	0.00	0.00	0.00	0.04	0.01	0.01	0.01	0.01	0.00	0.00	0.00	0.06	0.00	0.00	0.00	0.00	0.00	0.00	0.00
0.00	0.00	0.01	0.03	0.00	0.01	0.00	0.00	0.00	0.00	0.00	0.00	0.00	0.00	0.00	0.00	0.00	0.00	0.00	0.03	0.00	0.01	0.01	0.01	0.00	0.00	0.00	0.02	0.00	0.00	0.00	0.00	0.00	0.00	0.00
0.00	0.00	0.01	0.03	0.00	0.01	0.00	0.00	0.00	0.00	0.00	0.00	0.00	0.00	0.00	0.00	0.00	0.00	0.00	0.03	0.01	0.01	0.01	0.01	0.00	0.00	0.00	0.02	0.00	0.00	0.00	0.00	0.00	0.00	0.00
0.00	0.00	0.01	0.03	0.00	0.01	0.00	0.00	0.00	0.00	0.00	0.00	0.00	0.00	0.00	0.00	0.00	0.00	0.00	0.03	0.00	0.01	0.01	0.01	0.00	0.00	0.00	0.02	0.00	0.00	0.00	0.00	0.00	0.00	0.00
0.00	0.00	0.01	0.03	0.00	0.01	0.00	0.00	0.00	0.00	0.00	0.00	0.00	0.00	0.00	0.00	0.00	0.00	0.00	0.03	0.00	0.01	0.01	0.01	0.00	0.00	0.00	0.02	0.00	0.00	0.00	0.00	0.00	0.00	0.00
0.00	0.00	0.01	0.03	0.00	0.01	0.00	0.00	0.00	0.00	0.00	0.00	0.00	0.00	0.00	0.00	0.00	0.00	0.00	0.03	0.01	0.01	0.01	0.01	0.00	0.00	0.00	0.02	0.00	0.00	0.00	0.00	0.00	0.00	0.00
0.00	0.00	0.01	0.02	0.00	0.01	0.00	0.00	0.00	0.00	0.00	0.00	0.00	0.00	0.00	0.00	0.00	0.00	0.00	0.03	0.00	0.01	0.01	0.01	0.00	0.00	0.00	0.01	0.00	0.00	0.00	0.00	0.00	0.00	0.00
0.00	0.00	0.01	0.02	0.00	0.01	0.00	0.00	0.00	0.00	0.00	0.00	0.00	0.00	0.00	0.00	0.00	0.00	0.00	0.03	0.00	0.01	0.01	0.01	0.00	0.00	0.00	0.01	0.00	0.00	0.00	0.00	0.00	0.00	0.00
0.00	0.00	0.00	0.01	0.00	0.00	0.00	0.00	0.00	0.00	0.00	0.00	0.00	0.00	0.00	0.00	0.00	0.00	0.00	0.03	0.01	0.01	0.01	0.01	0.00	0.00	0.00	0.00	0.00	0.00	0.00	0.00	0.00	0.00	0.00
0.00	0.00	0.00	0.01	0.00	0.00	0.00	0.00	0.00	0.00	0.00	0.00	0.00	0.00	0.00	0.00	0.00	0.00	0.00	0.02	0.00	0.01	0.01	0.01	0.00	0.00	0.00	0.00	0.00	0.00	0.00	0.00	0.00	0.00	0.00
0.00	0.00	0.00	0.01	0.00	0.00	0.00	0.00	0.00	0.00	0.00	0.00	0.00	0.00	0.00	0.00	0.00	0.00	0.00	0.02	0.00	0.00	0.01	0.00	0.00	0.00	0.00	0.00	0.00	0.00	0.00	0.00	0.00	0.00	0.00
0.00	0.00	0.01	0.01	0.00	0.01	0.00	0.00	0.00	0.00	0.00	0.00	0.00	0.00	0.00	0.00	0.00	0.00	0.00	0.04	0.01	0.01	0.01	0.01	0.00	0.00	0.00	0.00	0.00	0.00	0.00	0.00	0.00	0.00	0.00
0.00	0.00	0.01	0.01	0.00	0.01	0.00	0.00	0.00	0.00	0.00	0.00	0.00	0.00	0.00	0.00	0.00	0.00	0.00	0.04	0.01	0.01	0.01	0.01	0.00	0.00	0.00	0.00	0.00	0.00	0.00	0.00	0.00	0.00	0.00
0.00	0.00	0.01	0.01	0.00	0.01	0.00	0.00	0.00	0.00	0.00	0.00	0.00	0.00	0.00	0.00	0.00	0.00	0.00	0.04	0.01	0.01	0.01	0.01	0.00	0.00	0.00	0.00	0.00	0.00	0.00	0.00	0.00	0.00	0.00
0.00	0.00	0.01	0.01	0.00	0.01	0.00	0.00	0.00	0.00	0.00	0.00	0.00	0.00	0.00	0.00	0.00	0.00	0.00	0.04	0.01	0.01	0.01	0.01	0.00	0.00	0.00	0.00	0.00	0.00	0.00	0.00	0.00	0.00	0.00
0.00	0.00	0.01	0.01	0.00	0.01	0.00	0.00	0.00	0.00	0.00	0.00	0.00	0.00	0.00	0.00	0.00	0.00	0.00	0.04	0.00	0.01	0.01	0.01	0.00	0.00	0.00	0.00	0.00	0.00	0.00	0.00	0.00	0.00	0.00
0.00	0.00	0.01	0.01	0.00	0.01	0.00	0.00	0.00	0.00	0.00	0.00	0.00	0.00	0.00	0.00	0.00	0.00	0.00	0.04	0.01	0.01	0.01	0.01	0.00	0.00	0.00	0.00	0.00	0.00	0.00	0.00	0.00	0.00	0.00
0.00	0.00	0.01	0.01	0.00	0.01	0.00	0.00	0.00	0.00	0.00	0.00	0.00	0.00	0.00	0.00	0.00	0.00	0.00	0.06	0.01	0.01	0.01	0.01	0.00	0.00	0.00	0.01	0.00	0.00	0.00	0.00	0.00	0.00	0.00
0.00	0.00	0.01	0.01	0.00	0.02	0.00	0.00	0.00	0.00	0.00	0.00	0.00	0.00	0.00	0.00	0.00	0.00	0.00	0.05	0.01	0.01	0.01	0.02	0.00	0.00	0.00	0.02	0.00	0.00	0.00	0.00	0.00	0.00	0.00
0.00	0.00	0.01	0.03	0.00	0.02	0.00	0.00	0.00	0.00	0.00	0.00	0.00	0.00	0.00	0.00	0.00	0.00	0.00	0.03	0.01	0.01	0.01	0.01	0.00	0.00	0.00	0.02	0.00	0.00	0.00	0.00	0.00	0.00	0.00
0.00	0.00	0.01	0.04	0.00	0.02	0.00	0.00	0.00	0.00	0.00	0.00	0.00	0.00	0.00	0.00	0.00	0.00	0.00	0.02	0.01	0.01	0.01	0.01	0.00	0.00	0.00	0.02	0.00	0.00	0.00	0.00	0.00	0.00	0.00
0.00	0.00	0.01	0.04	0.00	0.01	0.00	0.00	0.00	0.00	0.00	0.00	0.00	0.00	0.00	0.00	0.00	0.00	0.00	0.02	0.00	0.01	0.01	0.01	0.00	0.00	0.00	0.02	0.00	0.00	0.00	0.00	0.00	0.00	0.00
0.00	0.00	0.01	0.02	0.00	0.02	0.00	0.00	0.00	0.00	0.00	0.00	0.00	0.00	0.00	0.00	0.00	0.00	0.00	0.03	0.01	0.01	0.01	0.01	0.00	0.00	0.00	0.01	0.00	0.00	0.00	0.00	0.00	0.00	0.00
0.00	0.00	0.01	0.02	0.00	0.02	0.00	0.00	0.00	0.00	0.00	0.00	0.00	0.00	0.00	0.00	0.00	0.00	0.00	0.03	0.01	0.01	0.01	0.01	0.00	0.00	0.00	0.01	0.00	0.00	0.00	0.00	0.00	0.00	0.00
0.00	0.00	0.01	0.02	0.00	0.02	0.00	0.00	0.00	0.00	0.00	0.00	0.00	0.00	0.00	0.00	0.00	0.00	0.00	0.03	0.01	0.01	0.01	0.01	0.00	0.00	0.00	0.01	0.00	0.00	0.00	0.00	0.00	0.00	0.00
0.00	0.00	0.01	0.02	0.00	0.01	0.00	0.00	0.00	0.00	0.00	0.00	0.00	0.00	0.00	0.00	0.00	0.00	0.00	0.03	0.01	0.01	0.01	0.01	0.00	0.00	0.00	0.01	0.00	0.00	0.00	0.00	0.00	0.00	0.00
0.00	0.00	0.01	0.01	0.00	0.02	0.00	0.00	0.00	0.00	0.00	0.00	0.00	0.00	0.00	0.00	0.00	0.00	0.00	0.04	0.01	0.01	0.01	0.01	0.00	0.00	0.00	0.01	0.00	0.00	0.00	0.00	0.00	0.00	0.00
0.00	0.00	0.01	0.01	0.00	0.02	0.00	0.00	0.00	0.00	0.00	0.00	0.00	0.00	0.00	0.00	0.00	0.00	0.00	0.03	0.01	0.01	0.01	0.01	0.00	0.00	0.00	0.01	0.00	0.00	0.00	0.00	0.00	0.00	0.00
0.00	0.00	0.01	0.01	0.00	0.02	0.00	0.00	0.00	0.00	0.00	0.00	0.00	0.00	0.00	0.00	0.00	0.00	0.00	0.03	0.00	0.01	0.01	0.01	0.00	0.00	0.00	0.01	0.00	0.00	0.00	0.00	0.00	0.00	0.00
0.00	0.00	0.01	0.01	0.00	0.02	0.00	0.00	0.00	0.00	0.00	0.00	0.00	0.00	0.00	0.00	0.00	0.00	0.00	0.04	0.01	0.01	0.02	0.02	0.00	0.00	0.00	0.01	0.00	0.00	0.00	0.00	0.00	0.00	0.00
0.00	0.00	0.01	0.01	0.00	0.02	0.00	0.00	0.00	0.00	0.00	0.00	0.00	0.00	0.00	0.00	0.00	0.00	0.00	0.04	0.00	0.01	0.01	0.01	0.00	0.00	0.00	0.01	0.00	0.00	0.00	0.00	0.00	0.00	0.00
0.00	0.00	0.01	0.01	0.00	0.01	0.00	0.00	0.00	0.00	0.00	0.00	0.00	0.00	0.00	0.00	0.00	0.00	0.00	0.04	0.01	0.01	0.01	0.01	0.00	0.00	0.00	0.00	0.00	0.00	0.00	0.00	0.00	0.00	0.00
0.00	0.00	0.01	0.01	0.00	0.01	0.00	0.00	0.00	0.00	0.00	0.00	0.00	0.00	0.00	0.00	0.00	0.00	0.00	0.05	0.01	0.01	0.01	0.01	0.00	0.00	0.00	0.00	0.00	0.00	0.00	0.00	0.00	0.00	0.00

9.8 Primitive Mantle ratio

Ratio to primitive mantle

UZH nr	Site	Site	Type	Rb	Ba	Th	U	Nb	Ta	La	Ce	Pr	Sr	Nd	Zr	Sm	Ti	Y
C24JO101	1	Lindergut	Original	153.9	44.7	94.1	119.0	15.3	46.3	69.7	44.5	206.2	8.3	59.1	9.2	18.2	2.2	4.4
C24JO102	2	Lindergut	Original	149.9	47.4	94.1	104.8	15.6	46.3	87.5	53.7	310.9	8.2	79.3	9.7	18.2	2.1	4.2
C24JO103	3	Lindergut	Original	150.9	53.0	84.7	119.0	16.1	117.1	115.7	67.9	447.5	7.8	111.6	9.1	18.2	2.2	4.2
C24JO104	4	Lindergut	Original	148.5	55.0	94.1	152.4	15.7	117.1	92.9	55.4	331.2	7.4	79.6	8.3	18.2	2.1	4.0
C24JO105	5	Lindergut	Original	144.7	55.3	91.8	152.4	14.4	102.4	137.8	78.8	619.6	6.8	142.8	6.8	18.2	2.2	3.8
C24JO106	6	Lindergut	Original	177.5	56.8	116.5	257.1	17.1	217.1	94.3	56.5	307.2	5.8	77.6	7.0	18.2	2.5	4.1
C24JO107	7	Lindergut	Original	224.4	55.8	144.7	200.0	21.6	63.4	85.3	50.6	223.9	5.4	59.8	8.5	18.2	3.2	4.3
C24JO108	8	Lindergut	Original	175.3	49.8	112.9	333.3	17.0	126.8	70.7	43.3	194.2	5.6	52.7	6.5	18.2	2.5	4.5
C24JO121	9	Lindergut	Backfilled	172.6	52.8	104.7	100.0	17.8	39.0	176.0	103.0	900.4	10.3	215.1	12.1	18.2	2.5	5.0
C24JO122	10	Lindergut	Backfilled	174.0	50.3	107.1	71.4	18.2	51.2	94.8	59.4	340.9	10.5	92.7	12.8	18.5	2.5	5.1
C24JO123	11	Lindergut	Backfilled	172.9	49.1	105.9	147.6	18.1	31.7	88.2	54.3	273.6	10.2	80.1	12.1	18.2	2.5	5.2
C24JO124	12	Lindergut	Backfilled	169.3	49.0	103.5	104.8	17.7	43.9	82.4	55.4	282.2	10.3	80.4	12.5	18.2	2.4	5.1
C24JO125	13	Lindergut	Backfilled	172.3	50.7	109.4	100.0	18.2	39.0	107.1	64.7	414.1	11.3	111.5	12.1	18.2	2.5	5.2
C24JO126	14	Lindergut	Backfilled	146.8	46.2	89.4	71.4	16.5	65.9	81.1	48.8	253.6	9.0	72.2	10.5	18.2	2.2	4.4
C24JO127	15	Lindergut	Backfilled	155.7	50.5	96.5	166.7	16.7	78.0	71.8	46.3	198.2	8.7	60.8	9.3	18.2	2.3	4.5
C24JO128	16	Lindergut	Backfilled	156.9	48.5	96.5	161.9	15.8	222.0	80.9	50.3	260.9	8.8	71.4	9.2	18.2	2.3	4.4
C24JO129	17	Lindergut	Backfilled	169.8	52.3	110.6	133.3	17.7	39.0	91.0	56.3	295.3	8.4	82.4	9.2	18.2	2.4	4.5
C24JO130	18	Lindergut	Backfilled	267.1	58.5	175.3	176.2	23.6	173.2	92.9	57.8	243.8	5.5	79.8	9.3	18.2	3.4	5.1
C24JO131	19	Lindergut	Backfilled	207.6	50.1	134.1	257.1	20.5	80.5	89.1	55.3	281.5	5.3	80.3	8.1	16.2	3.0	4.7
C24JO132	20	Lindergut	Backfilled	262.7	55.8	145.9	481.0	19.9	102.4	104.8	61.8	338.0	5.5	86.1	7.9	18.2	2.9	4.4
C24JO133	21	Lindergut	Backfilled	302.8	64.6	171.8	461.9	20.1	258.5	143.5	83.1	534.1	5.6	138.1	8.6	18.7	3.1	5.8
C24JO134	22	Lindergut	Backfilled	324.7	68.7	156.5	414.3	20.6	19.5	164.3	95.2	651.1	5.8	165.5	9.5	20.3	2.8	8.4
C24CM201	23	Rimmerzmat	Original	143.9	77.8	132.9	523.8	16.7	39.0	79.9	48.4	255.8	5.9	67.0	8.4	18.2	2.6	6.0
C24CM202	24	Rimmerzmat	Original	145.2	81.6	131.8	485.7	17.1	39.0	90.7	54.4	284.4	5.8	85.4	9.5	16.9	2.6	6.0
C24CM203	25	Rimmerzmat	Original	137.8	87.2	134.1	619.0	16.3	39.0	88.1	51.0	276.8	6.0	70.9	8.8	17.3	2.7	6.2
C24CM204	26	Rimmerzmat	Original	66.3	64.3	69.4	2861.9	3.9	78.0	65.6	35.7	241.3	8.2	56.6	3.1	18.2	1.5	3.6
C24CM205	27	Rimmerzmat	Original	25.5	60.8	18.8	4200.0	0.7	61.0	63.3	33.1	273.2	11.6	57.1	1.3	18.2	0.6	1.4
C24CM206	28	Rimmerzmat	Original	12.1	60.0	2.4	4428.6	0.7	117.1	41.2	20.9	156.9	13.8	32.7	0.6	18.2	0.3	0.8
C24CM207	29	Rimmerzmat	Original	9.9	48.4	2.4	3228.6	0.7	95.1	38.4	18.7	135.9	13.5	26.8	1.1	18.2	0.3	1.0
C24CM208	30	Rimmerzmat	Original	56.2	50.7	36.5	1471.4	5.3	136.6	102.6	55.0	447.5	8.9	99.6	8.9	18.2	1.3	2.5
C24CM209	31	Rimmerzmat	Original	77.8	38.7	52.9	909.5	7.0	90.2	56.5	33.2	155.1	6.6	40.6	11.2	18.2	1.4	3.3
C24CM210	32	Rimmerzmat	Original	136.4	50.7	77.6	304.8	11.8	19.5	124.0	68.1	497.1	5.3	120.6	13.0	18.2	1.8	4.8
C24CM211	33	Rimmerzmat	Original	166.8	53.6	62.4	38.1	9.8	175.6	83.0	45.2	327.9	4.3	77.9	9.5	18.2	1.3	3.6
C24CM231	34	Rimmerzmat	Backfilled	134.8	41.1	57.6	38.1	12.8	43.9	59.2	39.1	201.4	13.5	61.1	8.9	18.2	1.5	3.8
C24CM232	35	Rimmerzmat	Backfilled	139.8	41.3	64.7	19.0	12.5	112.2	73.2	43.7	260.5	13.2	63.8	9.1	18.2	1.6	4.0
C24CM233	36	Rimmerzmat	Backfilled	130.9	39.0	55.3	19.0	11.8	82.9	60.4	35.7	185.1	14.2	52.6	8.0	18.2	1.4	3.8
C24CM234	37	Rimmerzmat	Backfilled	122.0	38.3	50.6	38.1	9.8	117.1	62.4	36.4	231.2	14.9	62.3	7.3	16.7	1.2	3.4
C24CM235	38	Rimmerzmat	Backfilled	116.7	37.7	51.8	52.4	9.0	104.9	91.7	51.7	412.3	15.5	101.3	6.9	17.1	1.2	3.4
C24CM236	39	Rimmerzmat	Backfilled	123.1	47.1	72.9	100.0	11.2	41.5	69.9	44.1	248.2	11.0	67.8	8.3	18.2	1.6	4.3
C24CM237	40	Rimmerzmat	Backfilled	94.3	49.9	67.1	204.8	9.8	141.5	58.5	36.4	198.9	7.1	55.6	6.3	18.2	1.5	3.3
C24CM238	41	Rimmerzmat	Backfilled	60.6	42.3	36.5	376.2	6.7	95.1	97.2	52.3	442.0	6.6	101.0	4.0	18.2	1.0	2.2
C24CM239	42	Rimmerzmat	Backfilled	52.1	32.3	28.2	414.3	4.3	24.4	70.6	36.1	292.4	7.0	64.6	3.0	18.2	0.8	1.7
C24CM240	43	Rimmerzmat	Backfilled	16.5	22.6	4.7	552.4	1.5	17.1	46.6	24.1	202.9	6.1	30.9	1.0	18.2	0.3	0.3
C24CM301	44	Underi Site	Original	151.3	56.4	109.4	142.9	16.8	31.7	75.0	46.3	204.0	4.7	55.1	9.8	16.4	2.7	5.0
C24CM302	45	Underi Site	Original	150.2	61.7	101.2	166.7	18.1	39.0	83.3	51.4	246.0	4.6	68.1	10.1	18.2	2.6	5.0
C24CM303	46	Underi Site	Original	153.7	61.7	111.8	161.9	18.4	56.1	101.5	62.5	360.1	4.8	90.2	10.0	18.2	2.7	5.1
C24CM304	47	Underi Site	Original	155.0	58.4	103.5	152.4	18.5	24.4	81.8	47.6	243.8	4.8	64.8	10.2	18.2	2.7	5.1
C24CM305	48	Underi Site	Original	157.8	58.1	110.6	166.7	18.2	87.8	72.6	46.0	210.1	4.6	56.8	9.4	16.2	2.8	5.1
C24CM306	49	Underi Site	Original	136.9	62.9	88.2	228.6	11.5	56.1	110.6	60.4	411.2	4.2	103.8	5.1	18.2	2.0	3.7
C24CM307	50	Underi Site	Original	157.6	78.8	103.5	223.8	15.8	39.0	103.2	60.3	369.6	4.2	92.9	12.6	18.2	2.4	4.7
C24CM308	51	Underi Site	Original	123.6	69.3	107.1	200.0	16.4	156.1	116.9	71.1	459.8	4.5	116.1	20.4	18.2	2.3	6.4
C24CM309	52	Underi Site	Original	108.8	43.3	76.5	33.3	13.7	117.1	80.8	49.5	310.9	14.2	77.5	18.1	16.2	1.8	4.8
C24CM310	53	Underi Site	Original	95.7	34.4	50.6	76.2	10.7	56.1	84.9	52.8	355.4	19.9	89.6	14.2	17.8	1.3	3.8
C24CM311	54	Underi Site	Original	93.9	32.1	43.5	71.4	8.8	63.4	68.1	43.1	284.4	19.9	67.9	11.9	16.7	1.2	3.6
C24CM341	55	Underi Site	Backfilled	181.6	49.0	109.4	85.7	17.7	31.7	78.9	50.6	253.3	7.9	69.9	14.7	16.4	2.7	5.9
C24CM342	56	Underi Site	Backfilled	181.7	49.3	116.5	81.0	18.9	36.6	84.9	54.4	272.8	8.1	77.1	15.1	18.2	2.7	5.9
C24CM343	57	Underi Site	Backfilled	179.7	44.3	112.9	42.9	17.3	39.0	102.5	61.6	408.3	8.5	108.0	13.5	16.2	2.7	5.8
C24CM344	58	Underi Site	Backfilled	182.7	48.4	118.8	104.8	18.1	39.0	78.3	50.1	237.7	9.6	69.2	13.4	16.4	2.7	5.6
C24CM345	59	Underi Site	Backfilled	156.9	52.6	91.8	85.7	17.0	39.0	92.0	56.3	315.9	6.6	83.8	14.2	18.2	2.4	4.8
C24CM346	60	Underi Site	Backfilled	144.4	46.3	81.2	157.1	17.0	34.1	74.4	45.4	243.5	5.1	69.1	13.8	18.2	2.2	4.8
C24CM347	61	Underi Site	Backfilled	142.8	48.3	87.1	161.9	16.1	112.2	72.6	46.8	236.2	5.2	63.3	14.9	18.2	2.2	4.6
C24CM348	62	Underi Site	Backfilled	143.8	52.9	92.9	181.0	15.4	29.3	134.2	73.9	584.1	5.1	139.6	14.0	18.2	2.2	4.7
C24CM349	63	Underi Site	Backfilled	149.8	53.2	91.8	190.5	17.7	39.0	70.9	46.3	199.3	4.7	60.2	15.4	18.2	2.4	4.9
C24CM350	64	Underi Site	Backfilled	190.6	62.8	121.2	295.2	19.9	39.0	92.4	54.3	315.9	5.1	79.3	11.7	16.7	3.0	3.8
C24CM351	65	Underi Site	Backfilled	223.5	65.2	138.8	214.3	22.6	39.0	102.6	63.0	327.2	4.7	89.1	9.5	18.7	3.1	5.5

10 Declarations

Hereby declare that the submitted thesis is the result of my own, independent work. All external sources are explicitly acknowledged in the thesis. I have not submitted this thesis, or any part of it, previously to any institution for assessment purposes.

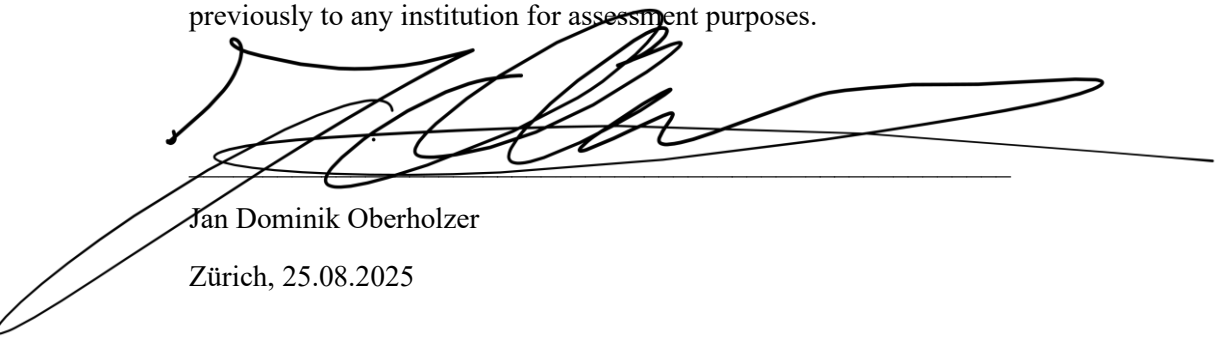

Jan Dominik Oberholzer

Zürich, 25.08.2025